

Studies on Metabolism and Functional Role of Dietary Phospholipids in the Digestive System

2021

BERNARD Ephantus Nguma

**Doctoral Program of
Animal Science and Agriculture
Graduate School of
Animal and Veterinary Sciences and Agriculture
Obihiro University of
Agriculture and Veterinary Medicine**

食餌性リン脂質の消化器官における 代謝並びに機能に関する研究

令和3年
(2021)

帯広畜産大学大学院畜産学研究科

畜産科学専攻 博士後期課程

バーナード エフアンタス グマ

TABLE OF CONTENTS

| | |
|---|------|
| LIST OF TABLES | vii |
| LIST OF FIGURE | viii |
| PREFACE | x |
| 1. CHAPTER 1: Literature Review | 1 |
| 1.1. General introduction to lipids and glycerophospholipids | 1 |
| 1.2. Ethanolamine glycerophospholipids..... | 1 |
| 1.3. Inflammatory bowel disease (IBD) and colon cancer..... | 3 |
| 1.4. Fatty acid composition of dietary fat and IBD/colon cancer | 5 |
| 1.5. Hypothesis and study objectives..... | 5 |
| 1.5.1. Statement of research questions | 5 |
| 1.5.2. Hypothesis and study aims | 6 |
| 2. CHAPTER 2: Dietary ethanolamine plasmalogen ameliorates colon mucosa inflammatory stress and pre-cancerous ACF in 1,2-DMH-induced colon carcinogenesis mice model: protective role of vinyl ether linkage..... | 10 |
| 2.1. Abstract..... | 10 |
| 2.2. Introduction | 10 |
| 2.3. Material and Methods..... | 12 |
| 2.3.1. Materials and Reagents..... | 12 |
| 2.3.2. Preparation of EtnGpl and Experimental Diets | 13 |
| 2.3.3. Animals and Experimental design..... | 18 |
| 2.3.4. Blood, Tissues, and Colon Mucosa Preparation | 20 |
| 2.3.5. Identification of Aberrant Crypt Foci (ACF)..... | 20 |
| 2.3.6. TNF- α and Apoptosis Array Assays..... | 20 |
| 2.3.7. Lipid Extraction and Assay | 21 |
| 2.3.8. Other Assays..... | 23 |

| | |
|--|----|
| 2.3.9. Statistical Analysis | 24 |
| 2.4. Results | 24 |
| 2.4.1. EtnGpl Fractions from Ascidian Muscle and Porcine Liver..... | 24 |
| 2.4.2. Fish and Soy Oil Acyl and Alkenyl Chains..... | 25 |
| 2.4.3. Diet Lipid Composition | 26 |
| 2.4.4. Animal and Tissues Data..... | 27 |
| 2.4.5. Dietary PE Inhibits AC Development and Suppresses ACF Formation..... | 29 |
| 2.4.6. Dietary EtnGpl Reduces the Levels of Apoptosis Related Proteins and TNF- α | 30 |
| 2.4.7. Alteration of Phospholipid Species in the Plasma, Liver, and Colon Mucosa | 32 |
| 2.4.8. Alteration of Acyl and Alkenyl Chains Composition in the Plasma, Liver, and Colon Mucosa..... | 36 |
| 2.5. Discussion..... | 38 |
| 2.6. Conclusion..... | 41 |
| 3. CHAPTER 3: Ethanolamine plasmalogen suppresses apoptosis in human intestinal tract cells <i>in vitro</i> by attenuating induced inflammatory stress | 43 |
| 3.1. Abstract..... | 43 |
| 3.2. Introduction | 43 |
| 3.3. Materials and Methods | 44 |
| 3.3.1. Materials | 44 |
| 3.3.2. Ascidian muscle and porcine liver EtnGpl preparation | 45 |
| 3.3.3. Cell culture | 45 |
| 3.3.4. Cell viability | 45 |
| 3.3.5. Apoptosis detection | 45 |
| 3.3.6. Cytokine array | 46 |
| 3.3.7. TNF- α assay | 47 |
| 3.3.8. Lipid extraction and assay | 47 |
| 3.3.9. Statistical analysis | 48 |

| | |
|--|----|
| 3.4. Results | 48 |
| 3.4.1. EtnGpl Fraction from Ascidian Muscle and Porcine Liver | 48 |
| 3.4.2. Extrinsic EtnGpl Enhances Cell Viability of Differentiated Caco-2 cells under Inflammatory Stress | 48 |
| 3.4.3. Extrinsic EtnGpl Inhibits Apoptosis by Modulating Apoptosis Related Proteins in Inflammatory Stressed Differentiated Caco-2 Cells | 49 |
| 3.4.4. Extrinsic EtnGpl Ameliorates Inflammation in Differentiated Caco-2 Cells by Lowering Cytokine Levels | 53 |
| 3.4.5. Uptake of Extrinsic EtnGpl by Differentiated Caco-2 Cells | 55 |
| 3.4.6. Extrinsic EtnGpl Suppresses TNF- α in Differentiated Caco-2 Cells under Inflammatory Stress | 58 |
| 3.5. Discussion..... | 59 |
| 3.6. Conclusion..... | 62 |
| 4. CHAPTER 4: Dietary ethanolamine plasmalogen ameliorates dextran sulfate sodium-induced colitis in mice | 63 |
| 4.1. Abstract..... | 63 |
| 4.2. Introduction | 63 |
| 4.3. Material and Methods..... | 65 |
| 4.3.1 Materials | 65 |
| 4.3.2. Preparation of purified EtnGpl (ascidian muscle and porcine liver) and experimental diets | 65 |
| 4.3.3. Animals..... | 65 |
| 4.3.4. Experimental design and induction of colitis | 66 |
| 4.3.5. Blood, Tissue and colon mucosa preparation | 67 |
| 4.3.6. Histopathological evaluation | 67 |
| 4.3.7. Myeloperoxidase (MPO) activity in colon mucosa | 67 |
| 4.3.8. Cytokines quantification and apoptosis assay | 68 |
| 4.3.9. Lipid assay in colon mucosa, and plasma..... | 68 |

| | |
|--|----|
| 4.3.10. Other assays..... | 68 |
| 4.3.11. Statistical analysis..... | 68 |
| 4.4. Results | 69 |
| 4.4.1. EtnGpl Fractions from Porcine Liver and Ascidian Muscle..... | 69 |
| 4.4.2. Fish and Soy Oil Acyl and Alkenyl Chains..... | 70 |
| 4.4.3. Diet Lipid Composition | 71 |
| 4.4.4. Dietary EtnGpl suppresses the progression of DSS-induced colitis | 72 |
| 4.4.5. Dietary EtnGpl attenuates inflammatory mediators in the colon mucosa | 74 |
| 4.4.6. Dietary EtnGpl modulates apoptosis-related proteins in the colon mucosa | 75 |
| 4.4.7. Dietary EtnGpl alters tissues lipid composition | 77 |
| 4.5. Discussion..... | 79 |
| 4.6. Conclusion..... | 82 |
| 5. GENERAL DISCUSSION | 83 |
| 6. GENERAL CONCLUSIONS AND FUTURE PERSPECTIVES..... | 85 |
| 7. REFERENCES | 87 |
| 8. ABSTRACT (English)..... | 97 |
| 9. ABSTRACT (Japanese)..... | 99 |

LIST OF TABLES

Chapter 2

| | |
|---|----|
| Table 2.1 Modified AIN-93G diet to form the basal diet, porcine liver and ascidian muscle EtnGpl diets prepared by adding 0.1% of the respective EtnGpl to the basal diet. | 18 |
| Table 2.2 Composition of acyl and alkenyl chains (A), and phospholipid species (B) of prepared EtnGpl (mol%)..... | 25 |
| Table 2.3 Composition of acyl and alkenyl chains (mol%) in fish and soy oil..... | 26 |
| Table 2.4 Composition of acyl and alkenyl chains ($\mu\text{mol}/100\text{g}$) in the experimental diet | 27 |
| Table 2.5 Daily diet intake, body, liver and spleen weights, colon length and TBARS after 10 weeks of the animal experiment | 28 |
| Table 2.6 Phospholipid species level (nmol/mL) in plasma after 10 weeks of treatments | 32 |
| Table 2.7 Phospholipid species level (pmol/mg protein) in liver after 10 weeks of treatments | 33 |
| Table 2.8 Phospholipid species level (pmol/mg protein) in colon mucosa after 10 weeks of treatments..... | 34 |
| Table 2.9 Composition of acyl and alkenyl chains (mol%) in plasma phospholipid fraction after 10 weeks of treatments | 36 |
| Table 2.10 Composition of acyl and alkenyl chains (mol%) in liver phospholipid fraction after 10 weeks of treatments | 37 |
| Table 2.11 Composition of acyl and alkenyl chains (mol%) in colon mucosa phospholipid fraction after 10 weeks of treatments | 38 |

Chapter 4

| | |
|--|----|
| Table 4.1 Composition of acyl and alkenyl chains (A), and phospholipid species (B) of prepared EtnGpl (mol%)..... | 70 |
| Table 4.2 Composition of acyl and alkenyl chains (mol%) in fish and soy oil..... | 71 |
| Table 4.3 Composition of acyl and alkenyl chains ($\mu\text{mol}/100\text{g}$) in the experimental diet | 72 |
| Table 4.4 Composition of acyl and alkenyl chains (mol%) in colon mucosa phospholipid fraction after 16 days of DSS-induced colitis (early/middle stage of inflammation)..... | 78 |
| Table 4.5 Composition of acyl and alkenyl chains (mol%) in plasma phospholipid fraction after 16 days of DSS-induced colitis (early/middle stage of inflammation) | 79 |

LIST OF FIGURE

Chapter 1

| | |
|---|---|
| Figure 1.1 Structures of acyl, alkyl, and alkenyl EtnGpl. | 3 |
| Figure 1.2 Colon cancer incidences, and mortality in both sexes, globally | 5 |
| Figure 1.3 Colon carcinogenesis model..... | 7 |

Chapter 2

| | |
|---|----|
| Figure 2.1 Preparation and purification of ascidian muscle EtnGpl | 14 |
| Figure 2.2 Preparation and purification of porcine liver EtnGpl | 16 |
| Figure 2.3 Experimental design of i.p. DMH-induced colon carcinogenesis in mice for 10 weeks..... | 19 |
| Figure 2.4 Effect of dietary EtnGpl on ACF formation in 1,2-DMH-treated mice. | 30 |
| Figure 2.5 Dietary EtnGpl suppresses the induction of apoptosis and related downstream death signaling cascade in colon epithelial cells of 1,2-DMH-treated mice (fold change vs. blank). | 31 |

Chapter 3

| | |
|---|----|
| Figure 3.1 Cell viability during LPS induced inflammatory stress in differentiated Caco-2 cells. | 49 |
| Figure 3.2 Apoptotic cells during LPS induced inflammatory stress in differentiated Caco-2 cells. | 50 |
| Figure 3.3 Relative levels of apoptosis-related proteins (fold change vs. blank) during LPS induced inflammatory stress in differentiated Caco-2 cells. | 53 |
| Figure 3.4 Relative levels of cytokine (fold change vs. blank group = 1.0) during LPS induced inflammatory stress in differentiated Caco-2 cells. | 54 |
| Figure 3.5 Time-dependent changes of various phospholipids in differentiated Caco-2 cells. | 57 |
| Figure 3.6 Time-dependent changes of phospholipid carbon chain composition in differentiated Caco-2 cells after treatment with 50 μ M porcine liver and ascidian muscle EtnGpl. | 57 |
| Figure 3.7 Time-dependent changes of phospholipid carbon chain composition in differentiated Caco-2 cells after treatment with LPS + 50 μ M porcine liver and ascidian muscle EtnGpl. | 58 |
| Figure 3.8 TNF- α levels during LPS induced inflammatory stress in differentiated Caco-2 cells | 59 |
| Figure 3.9 Schematic illustration of antiapoptotic effect of PlsEtn in differentiated Caco-2 cells under LPS- treatment | 62 |

Chapter 4

| | |
|--|----|
| Figure 4.1 Experimental design of DSS-induced colitis in mice. | 67 |
| Figure 4.2 General evaluation of effects of dietary EtnGpl on DSS-induced colitis in mice | 73 |
| Figure 4.3 Dietary EtnGpl is associated with decreased inflammatory mediators in the colon tissue of DSS- induced colitis in mice | 74 |

Figure 4.4 Effect of dietary EtnGpl on pro-inflammatory mediators in the colon tissue and plasma of DSS-induced colitis in mice75

Figure 4.5 Effect of dietary EtnGpl on relative levels of apoptosis-related proteins (fold change vs. blank) in DSS-induced colitis in mice.77

General conclusion

Figure 6.1 Schematic illustration of anti-carcinogenic, anti-apoptotic and anti-colitis effect of dietary PlsEtn. 85

PREFACE

This doctoral (PhD) thesis is based on food biochemistry and functionality of complex phospholipids in the intestines and aims at contributing to the currently increasing research interest on the health benefits of ethanolamine plasmalogen, a subclass of glycerophospholipids. It has been written to fulfill the graduation requirements of the Doctoral Program of Animal Science and Agriculture of Obihiro University of Agriculture and Veterinary Medicine. Harmonious with the mission of Obihiro University of Agriculture and Veterinary Medicine, it is my hope that the findings from this research will advance our knowledge on dietary lipids (functional role and metabolism) and health. In addition, it is my hope that in future, the findings of this thesis will contribute to the development of products that will improve human health.

I would like to thank my supervisors, Prof. Mikio Kinoshita and Assistant Prof. Shinji Yamashita for accepting me into their Laboratory and most importantly for their excellent guidance, support, and kindness during my entire doctoral program. I also wish to thank them for playing a critical role in conceptualizing and actualization of my research questions. Despite of the challenges I faced while undertaking the research, not to mention the devastating effects and disruptions from COVID-19 pandemic, I have been able to answer a larger part of the research questions. Importantly, I thank Prof. Hiroshi Koaze in a special way, first for recommending me to Prof. Mikio Kinoshita Laboratory and secondly for his continued support and encouragement throughout my doctoral research, I shall always be indebted to you.

I thank Prof. Michihiro Fukushima, my co-supervisor and Prof. Kenichiro Shimada, member of my PhD examination committee, for their invaluable feedback and words of encouragement.

I thank Prof. Teruo Miyazawa, Prof. Kiyotaka Nakagawa, Associate Prof. Takahiro Eitsuka and Assistant Prof. Yurika Otoki in Tohoku University for helping me to analyze my samples with LC-MS/MS and conducting data curation. I also thank them for reviewing abstracts and presentations slides for the conferences that I participated.

To the current and former members of the Food Biochemistry and Functionality Laboratory, I thank them for their support and making the laboratory space conducive for conducting experiments as well as enjoyable. Particularly, I am grateful to Mr. Yuki Tominaga, for his immense support and teamwork he embraced during the DMH mice experiment in my first year research. Special thanks to Miss Wakaba Yutani and Miss Chisato Higaki for helping me to translate my abstract from English to Japanese.

I thank Obihiro University of Agriculture and Veterinary Medicine for giving me the opportunity to be part of the Institution as a doctoral student, secondly for funding my PhD scholarship during my first year and thirdly

for wavering my tuition fee. I also wish to thank the Rotary Yoneyama Scholarship Foundation for funding my scholarship during my second and third year and in a special way thank the Obihiro South Rotary Club for being very kind and supportive to me. Without your support, it would have been impossible to accomplish what I have done so far.

I wish to acknowledge the international students in Obihiro University, particularly the African Obihiro Research Network (AORNet) for their input to improve my research during the organization's research sessions. Over and above this, I participated in quite a number of events organized by the University international students, which always reminded me that there is more to life than doing a PhD.

Most importantly, I acknowledge the incredible support and unconditional love from my wife, Roselyne Mwende and my daughter Hannah Koki as well as my mother, Stephana Koki, my sisters Clarine Koki and Pascalia Munugwa, and my brothers Ignatius Maundi and Augustine Muisyo. I will be forever grateful to them for believing in me, their prayers, and for encouraging and inspiring me to give my best.

1. CHAPTER 1: LITERATURE REVIEW

1.1. GENERAL INTRODUCTION TO LIPIDS AND GLYCEROPHOSPHOLIPIDS

Lipid are polar small molecules widely known as components of cell membranes and play essential roles in all cellular processes. Recent literature has established lipids as modulators of different biological functions (Cas et al., 2020). Alteration of lipid metabolism is associated with cellular membrane composition, which influences cellular functions such as homeostasis, cell adhesion and migration, neurotransmission, signal transduction, post-translational modification, apoptosis, cell proliferation, immunity and inflammation (Messias et al., 2018). Further to these, alteration of lipid metabolism has been linked to several diseases such as inflammation, diabetes, neurological disorders, and cancer (Huang and Freter, 2015). Generally lipids are classified into; fatty acids, glycerolipids, glycerophospholipids, sphingolipids, sterol lipids, prenol lipids, saccharolipids, and polyketides - International Lipids Classification and Nomenclature Committee (Huang and Freter, 2015).

Glycerophospholipids (Gpl) are the main component of biological membranes. Gpl contains either an acyl, alkyl or alkenyl residue at the *sn*-1 position of the glycerol moiety and the head group (either choline, ethanolamine, serine, inositol, and glycerol) attached to the phosphate allows for many different Gpls. During metabolism of Gpl, many different bioactive lipids are generated, which are involved in different cellular biochemical cascades. (Huang and Freter, 2015). Gpl extracted from food sources and marine organisms are referred to as dietary Gpl. It is assumed that 20% of intestinal phospholipids are absorbed passively without hydrolysis and incorporated into high density lipoproteins, where the Gpl are transferred into the plasma membranes of numerous cells (liver, lung, tumor cells) and alter the membrane fatty acid (FA) composition of the cells (Taylor et al., 2010). Therefore, selection of dietary Gpl with specific lipid composition have the potential to alter cellular membrane composition, consequently modulating the activity of membrane bound enzymes and cells functionality like signaling, transport and adaption to cellular environmental factors like oxidative stress (Küllenberg et al., 2012).

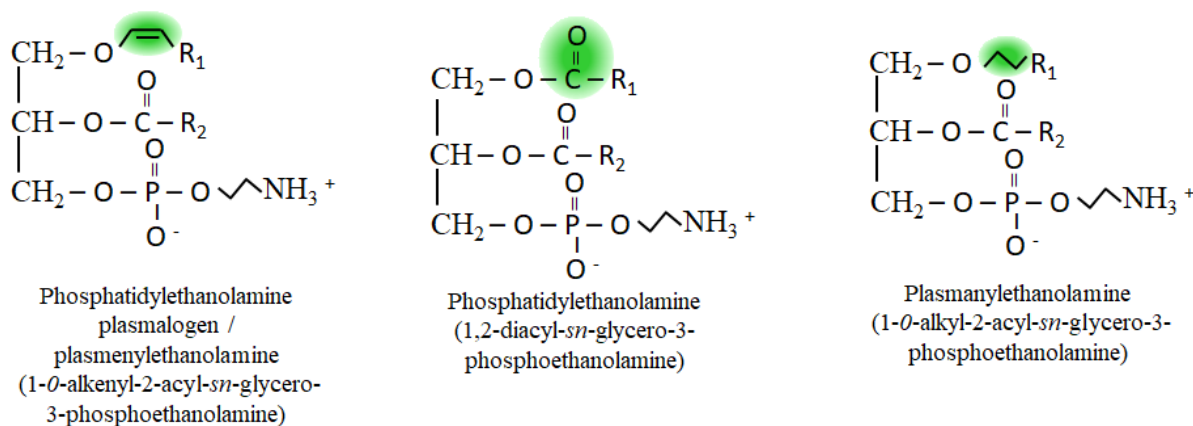
1.2. ETHANOLAMINE GLYCEROPHOSPHOLIPIDS

Ethanolamine glycerophospholipids (EtnGpl) are a major subclass of Gpl in biological membranes and exists in three forms depending on the ether linkage at the *sn*-1 position of the glycerol moiety, that is alkenyl, acyl or alkyl linkages (1-*O*-alkenyl-2-acyl-*sn*-glycerol-3-phosphoethanolamine, PlsEtn; 1,2-diacyl-*sn*-glycerol-3-phosphoethanolamine, PtdEtn; and 1-*O*-alkyl-2-acyl-*sn*-glycerol-3-phosphoethanolamine, PakEtn, respectively as shown in Figure 1.1. The alkenylacyl form is referred to as plasmalogen (Pls) (Braverman and Moser, 2012). PlsEtn has a unique property of a vinyl-ether (-O-CH = CH-)-linkage at the *sn*-1 position, which

is linked to a fatty alcohol. The fatty alcohol consists of C16:0 (palmitic acid), C18:0 (stearic acid) or C18:1 (oleic acid) carbon chains (Brites et al., 2004). At the *sn*-2 position of the glycerol moiety, PlsEtn are enriched with polyunsaturated fatty acids (PUFA) such as 22:6n-3 (DHA), 20:5n-3 (EPA), and 20:4n-6 (ARA), which plays an important role in the structural and functional role of membranes. The PUFA at the *sn*-2 position have been shown to depend on the food source of PlsEtn. Marine food sources such as sea squirt muscle, mussel muscle, scallop, sea cucumber, and sea snail are enriched with EPA and DHA. The high EPA and DHA in marine sources is thought to be from marine animals' diets because they consist of marine bacteria and algae, which synthesis these PUFA (Yamashita et al., 2016a; Zhang et al., 2019). Land food sources such as pig, chicken and cattle leg muscle are enriched with ARA (Yamashita et al., 2016a).

In addition of being components of membrane structures, PlsEtn are critical for human health and have established roles such as reservoirs of second messengers, involved in membrane fusion, ion transport, cholesterol efflux, neuronal development, the immune response, and as endogenous antioxidants. (Lohner, 1996; Braverman and Moser, 2012; Paul et al., 2019; Ding et al., 2020). The vinyl-ether linkage at the *sn*-1 position makes PlsEtn susceptible to oxidative stress compared to ester bond in PtdEtn, which acts as an antioxidant and protects cells from oxidative stress (Yavin and Gatt, 1972; Maeba and Ueta, 2003). One vinyl ether double bond in Pls has been shown to scavenge two peroxy radicals (Hahnel et al., 1999). The anti-oxidant effect of PlsEtn has been shown to degrade the vinyl ether linkage rapidly with a considerable delay in oxidation of PUFA double bonds at the *sn*-2 position (Reiss et al., 1997). Dysregulation of PlsEtn or low levels have been associated with several diseases such as peroxisomal diseases (Zellweger syndrome spectrum disorders and rhizomelic chondridysplasia punctate type 1) (Steinberg et al., 2006) neurodegenerative diseases (Alzheimer's disease and parkinson's disease) (Ginsberg et al., 1995; Dragonas et al., 2009), and metabolic diseases (type 2 diabetes, cardiovascular disease, and certain forms of cancer) (Paul et al., 2019). Yamashita et al. demonstrated that PlsEtn suppresses the activities of caspases 3, 8, and, 9 in serum-starved neuronal cells, which inhibited neuronal apoptosis (Yamashita et al., 2015). PlsEtn has been shown to improve learning ability and memory function of high-fat diet fed SAMP8 mice (Che et al., 2018b). Ifuku et al. demonstrated that Pls with 47.6% PlsEtn could significantly suppress LPS-induced neuro-inflammation and reduce the accumulation of amyloid β protein in mice brains (Ifuku et al., 2012). In addition, oral administration of EtnGpl with high PlsEtn level has been shown to improve memory impairment in amyloid β -infused rats (Yamashita et al., 2017). Moreover, PlsEtn enriched with EPA alleviated amyloid β -induced neurotoxicity by inhibiting oxidative stress, neuronal injury, apoptosis, and neuro-inflammation, which depended on the vinyl ether linkage at the *sn*-1 position (Che et al., 2018a). Despite of these functional roles, biological functions and the underlying mechanistic bases of PlsEtn in colonic health are not well defined.

PlsEtn content in mammalian species varies considerably depending on the tissue. In human tissues, PlsEtn levels in EtnGpl differ significantly; the brain and nervous system contain 60-90%, the plasma and red blood cells, 50-60%, the heart, about 53%, the kidney, 20-45%, the skeletal muscle, 10-25%, while the liver contains the lowest levels, at about 2-5% (Braverman and Moser, 2012). In the colon, PlsEtn accounts for approximately 35% of EtnGpl (Dueck et al., 1996). PlsEtn levels in plasma and organs are maintained by a combination of the regulation in its biosynthesis and degradation (Honsho and Fujiki, 2017; Honsho et al., 2017). Degradation of dietary PlsEtn by pancreatic phospholipase A₂ leads to the release of the fatty acids in the *sn*-2 position and yields lysoPlsEtn (Cohn et al., 2010). The hydrolyzed products are taken up into the enterocytes. Some of released fatty acids are metabolized into eicosanoids and docosanoids, which serve as anti- or pro-inflammatory mediators (Küllenberg et al., 2012). Some of the yielded lyoPlsEtn are re-esterified via the Land's cycle into preferentially PlsEtn bearing ARA (Nishimukai et al., 2011; Takahashi et al., 2020; Yamashita et al., 2020b). The re-esterified PlsEtn, fatty acids and lyoPlsEtn form chylomicrons, which are secreted into the lymphatic system and enter circulation (Zhang et al., 2019). These biologically active lipid molecules contribute to different functionalities and can remarkably offer protective role during colon inflammation and carcinogenesis.



Adopted from Braverman *et al.*, *Biochim. Biophys. Acta* (2012)

Figure 1.1 Structures of acyl, alkyl, and alkenyl EtnGpl.

R1 denotes fatty alcohols at *sn*-1 position and R2 polyunsaturated fatty acids at *sn*-2 position.

1.3. INFLAMMATORY BOWEL DISEASE (IBD) AND COLON CANCER

Inflammatory bowel disease (IBD), which includes Crohn's disease (CD) and Ulcerative colitis (UC), represents a group of chronic disorders with poorly understood etiology and is characterized by chronic inflammation of the gastrointestinal tract (Axelrad et al., 2016). It is generally recognized that patients with IBD have significant increased risk of developing colon cancer and extra-intestinal malignancies, which are primarily

a result of chronic intestinal inflammation (Nadeem et al., 2019). The inflammatory microenvironment of IBD has many similarities to the microenvironment of cancers like immune response and oxidative stress. Activated macrophages and monocytes are thought to be major mediators to the production of inflammatory cytokines in the gut, and imbalance of the cytokines contributes to the pathogenesis of IBD (Sanchez-muñoz et al., 2008).

Currently, colon cancer is increasingly becoming a devastating disease posing a great threat to mortality of both sexes in the entire world despite of the progressive steps made toward its diagnosis and treatment. According to GLOBOCAN, colon cancer ranks third among all cancer related diseases in terms of incidences and second with respect to mortality as shown in Figure 1.2. Incidences of colon cancer are closely related to lifestyle with higher incidence rates (3-fold higher) being reported in transitioned countries in Europe (Norway, Netherlands, Hungary), Australia/New Zealand, USA/Canada and Eastern Asia (Japan and Korea) compared to transitioning countries (Bray et al., 2018). To further support this, Bray *et al.* (2018) has shown that incidences of colon cancer tends to increase uniformly with increasing human development index in countries undergoing major development transition. Colon cancer is caused by multiple factors; however, environmental factors such as smoking, lack of physical activities, old age, and eating habits contribute to about 75% of incidences while about 25% of incidences are due to hereditary factors. Diet is considered the major exogenous factor in the etiology of colon cancer (Labianca et al., 2010). For instance, high fat intake has been demonstrated to be strongly associated with the likelihood of colon cancer development, especially the quantity and type of fatty acid consumed (Dwivedi et al., 2003).

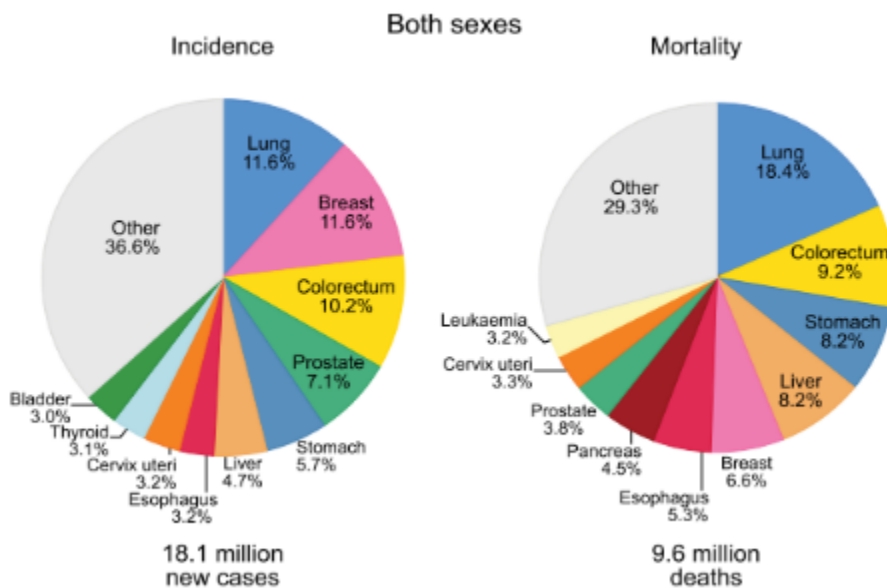


Figure 1.2 Colon cancer incidences, and mortality in both sexes, globally

Proportion of the total number of cases and deaths of 10 most common cancer cases in 2018 for both sexes.

Source: Bray et al., 2018.

1.4. FATTY ACID COMPOSITION OF DIETARY FAT AND IBD/COLON CANCER

Mammals cannot synthesize essential PUFA (n-3 and n-6); therefore, the PUFA have to be provided from external dietary sources. The dietary qualitative and quantitative content of these essential PUFA play an important role in colon health and disease. Linoleic acid (18:2, n-6) present in many plants is mainly a precursor for AA (20:4, n-6), while α -linoleic acid (18:3, n-3) present in fish oil is a precursor for EPA (20:5, n-3) and DHA (22:6, n-3) (Hofmanová et al., 2014). Excessive amounts of n-6 PUFA, which is typical “*Western diet*” is known to promote the pathogenesis of IBD and colon carcinogenesis through the elevation of inflammation (Kim et al., 2010). In contrast, epidemiological studies have demonstrated that intake of diets with high n-3 PUFA significantly lowers incidence of colon cancer (Byers, 1996; Calviello et al., 2007).

EPA and DHA are metabolized into anti-inflammatory mediators (docosanoids and eicosanoids such as prostaglandin (PG) E₃, leukotriene (LT) B₅, LTC₅, LTD₅ resolvins, protectins, and maserins). On the other hand, ARA is metabolized into pro-inflammatory mediators (eicosanoids such as PGE₂, LTB₄, LTC₄, and LTD₄) (Gil, 2002; Calder, 2015; Lee et al., 2017). EPA and DHA compete with ARA for fatty acid metabolism enzymes (cyclooxygenase (COX), lipoxygenase (LOX), and cytochrome P450), thus the presence of EPA and DHA (n-3) reduces the availability of ARA (n-6) to form pro-inflammatory eicosanoids (Hofmanová et al., 2014). This indicates that the balance between n-3 and n-6 PUFA has a direct effect on cellular inflammation metabolites, which ultimately influence cell proliferation, differentiation, and apoptosis (Hofmanová et al., 2014). Therefore, n-3/n-6 ratio in a diet is critical in determining the risk of IBD and colon cancer development. The 2.5:1 ratio of fish oil (n-3 PUFA) to corn oil (n-6 PUFA) demonstrated better inhibition of dihydrochloride-induced colon carcinogenesis by suppressing cell cycle progression compared to 1:1 ratio (Sarotra et al., 2012). Importantly, the current recommended ratio of n-3/n-6 PUFA is 2:1 to 5:1 (Zhang et al., 2019), while the World Health Organization (WHO) recommended level is at 5:1 to 10:1 (World Health Organization Fat and Oils in human Nutrition, 1994).

1.5. HYPOTHESIS AND STUDY OBJECTIVES

1.5.1. Statement of research questions

PlsEtn metabolism has been reported to be profoundly dysregulated in dedifferentiated colon mucosa. This indicates that PlsEtn may play a key role in protecting normal colon mucosa from transition to hyper-proliferative

(pre-cancerous state) due to several factors like cell injury or mutation originating from inflammatory or oxidative stresses. While some studies have identified the functional role of PlsEtn in diseases such as AD, Parkinson's, and atherosclerosis, the functional role and metabolism of PlsEtn, its metabolites, and molecular species in colon health and disease is still not fully understood. As highlighted before, PlsEtn makes about 35% of EtnGpl in colon mucosa, and therefore might play a critical role during colon pathophysiological state (colon inflammation, injury, or cancer initiation). Therefore our main question in this study was what is the functional role of dietary PlsEtn during colon inflammation and cancer development? and secondly, how is it metabolized?

My PhD study focused on addressing these research questions using comprehensive experimental designs, suitable mice models, and cell culture, combined with liquid chromatography with tandem mass spectrometry (LC-MS/MS). Elucidating the effect of PlsEtn and its metabolites and molecular species will provide insights on the potential benefits of PlsEtn with abundant vinyl ether linkages as a dietary therapy for pathological colon conditions such as IBD and colon cancer.

1.5.2. Hypothesis and study aims

Our first hypothesis was that dietary PlsEtn may suppress colon inflammatory stress and subsequent formation of colon precancerous lesions (aberrant crypt foci – ACF) due to the abundance of vinyl ether linkages at the *sn-1* position. Here we investigated the effect of diets containing 0.1% purified EtnGpl from ascidian muscle with high PlsEtn (87.3 mol% PlsEtn in EtnGpl) and from porcine liver with low PlsEtn (7.2 mol% PlsEtn in EtnGpl) levels and consisting of relatively similar n-3/n-6 ratio by supplementing with 1% fish oil on the formation of ACF using 1,2-dimethylhydrazine (DMH)-induced colon carcinogenesis mice model.

1.5.2.1. 1,2-dimethylhydrazine (DMH)-induces ACF formation in vivo

Development of colon cancer is a multistep process, mainly involving three stages: initiation, promotion, and progression. Initiation stage involves exposure of normal colon crypt epithelial cells to carcinogenic agents or chemicals that causes changes at genomic level, altering the normal proliferation of colon mucosal cells. Evidence shows that 1,2-dimethylhydrazine (DMH) is a colon carcinogen and induces aberrant crypt foci (ACF) formation, which are described as precursor lesion of chemically induced colon cancer in mice and rats models in a dose-dependent manner (McLellan et al., 1991). In addition, sequential injection of DMH at an interval to mice or rats results in higher ACF formation and foci multiplicity compared to one or two injections (Bird, 1995). DMH induced carcinogenesis mice and rats exclusively occurs in the colon and since tumors in humans and mice or rats share many histological and genetic characteristics, this serves as a good predictor of diets with colon cancer efficacy in humans (Femia et al., 2010).

Aberrant crypt foci (ACF) are described as putative precursors of colon cancer and considered as the earliest identifiable morphological changes in normal colon crypts (Corpet et al., 2009). ACF are about 2-3 fold larger than normal surrounding crypts, elevated, have an elliptical luminal opening as opposed to circular in normal crypts and have a thick epithelial lining that stains darker than normal crypts with a large space between neighboring crypts (pericryptal zone) (Orlando et al., 2008). Under a microscope, ACF appear as single or cluster of large atypia colon crypts after staining with methylene blue making it easy to identify and count from the mounted colon (Cheng and Lai, 2003; Corpet et al., 2009). Evaluation of ACF is based on density, which is the number of ACF per square centimeter of mucosa surface (Cheng and Lai, 2003). Based on cellular, molecular, morphologic and growth behavior of precancerous lesions, ACF shows similar dysplasia characteristics, indicative that ACF are preneoplastic lesions (Bird, 1995). As preneoplastic lesions, ACF appears during the initiation stage of colon cancer, enabling their use in the identification of colon cancer modulators (Orlando et al., 2008). This makes ACF biomarkers of both colorectal cancer risk and chemopreventive response diet. Indeed, tumor incidences and large number of ACF have been shown to have a positive correlation ($r = 0.76$, $p < 0.01$, $n = 36$) (Corpet et al., 2009). Typically, some of the formed ACF go through the multistep process of malignancy to form microadenoma. Subsequently, some microadenomas mutate and develop into adenomas and finally progress to adenocarcinoma prior to metastasis as shown in Figure 1.3. Therefore, identification of ACF as preinvasive lesions in carcinogen-treated mice makes it possible to study colon cancer at its precancerous stage.

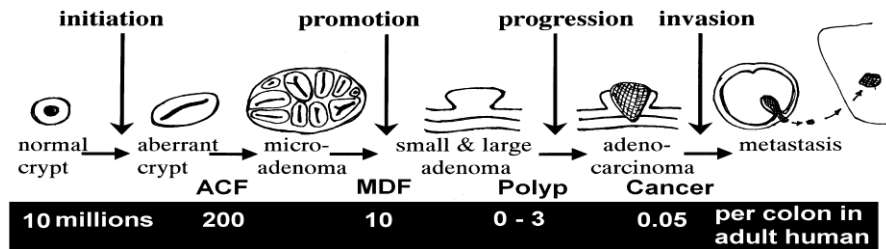


Figure 1.3 Colon carcinogenesis model

Schematic representation of the pathological steps involved in the development of colon cancer, from normal crypt to aberrant crypt, aberrant crypt foci, adenoma, and adenocarcinoma.

Source: Bruce and Corpet, 1996.

Our second hypothesis was that extrinsic PlsEtn may inhibit apoptosis in human intestinal tract cells under lipopolysaccharide (LPS)-induced inflammatory stress. Here we clarified that PlsEtn with abundant vinyl ether linkages has the potential to reduce the degree of LPS-induced apoptotic cells using differentiated Caco-2 cells as an *in vitro* model.

1.5.2.3. Lipopolysaccharide (LPS)-induces apoptosis of cells in vitro

LPS is a main constituent of Gram-negative bacterial membrane and specifically activates Toll-like receptor 4 (TLR4), therefore acts as a potent activator of the innate immune system (Beutler et al., 2001; Rhee, 2014). It has been well established in many studies that LPS induces apoptosis by activating the caspase-3 signal pathways in various cells. It is worth noting that IBD patients are suggested to have increased expression of TLR4 (Cario and Podolsky, 2000) as well as increased intestinal epithelial cells apoptosis (Blander, 2016). Yang et al. have shown that LPS induces apoptosis of intestinal epithelial cells as a result of cell injury from up regulation of pro-inflammatory mediators (Yang et al., 2016). In addition, Liu et al. have shown that LPS induces apoptosis of enterocytes *in vitro* in IPEC-J2 cells and *in vivo* in mice (Liu et al., 2019). LPS-induced apoptotic cell death and increased ROS has been demonstrated in HepG2 cells (Raza et al., 2016).

Our third hypothesis was that dietary PlsEtn may suppress colon inflammatory mediators and histological damage due to the abundance of vinyl ether linkages at the *sn-1* position. Here we investigated the effect of diets containing 0.1% purified EtnGpl from ascidian muscle with high PlsEtn (87.3 mol% PlsEtn in EtnGpl) and from porcine liver with low PlsEtn (7.2 mol% PlsEtn in EtnGpl) levels and consisting of relatively similar n-3/n-6 ratio by supplementing with 1% fish oil on the impairment of colon lining using dextran sulfate sodium (DSS)-induced colitis in mice.

1.5.2.4. Dextran sulfate sodium (DSS)-induced colitis in vivo

Inflammatory bowel disease (IBD) is categorized as either Crohn's disease (CD) or ulcerative colitis (UC). IBD is directly associated with an increased risk of colorectal cancer (Perše and Cerar, 2012). Induction of colonic mucosa damage from chronic inflammation as a form of IBD by use of dextran sodium sulfate is the most common mouse experimental model due to the ability to conduct the experiment in a rapid, simple, reproducible, and controlled manner. The desired level of intestinal inflammation (acute, chronic or relapsing) can be achieved by adjusting the concentration level of DSS (Eichele and Kharbanda, 2017). Acute colitis is induced by continuous administration of 2 - 5% for about 4-9 days, while chronic colitis may be induced by continuous administration of low concentration or cyclic administration (Perše and Cerar, 2012). DSS is water soluble, negatively charged sulfated polysaccharide and the most severe murine colitis with similarities to human UC results from administration of 40-50 kDa DSS in drinking water (Chassing et al., 2015). DSS induces inflammation in the colon by acting directly as a chemical toxin to epithelial cells, leading to the destruction of the epithelial cells. The mechanism underlying DSS-induced intestinal inflammation is unclear but it is suggested that DSS damages the epithelial monolayer lining, which leads to the movement of the luminal bacteria into the

cells of colon mucosa layers. This in turn allows the distribution of pro-inflammatory intestinal content into the colon mucosa (Eichele and Kharbanda, 2017).

※ DSS mode of action is by direct injury to the colon epithelial cells resulting in intestinal inflammation, which is distinct from DHM administration that is first metabolized in the liver, and then transported via the bile duct to the intestinal cells where it induces colon carcinogenesis.

2. CHAPTER 2: DIETARY ETHANOLAMINE PLASMALOGEN AMELIORATES COLON MUCOSA INFLAMMATORY STRESS AND PRE-CANCEROUS ACF IN 1,2-DMH-INDUCED COLON CARCINOGENESIS MICE MODEL: PROTECTIVE ROLE OF VINYL ETHER LINKAGE

2.1. ABSTRACT

Ethanolamine plasmalogen (PlsEtn), a sub-class of ethanolamine glycerophospholipids (EtnGpl), is a universal phospholipid in mammalian membranes. Several researchers are interested in the relationship between colon carcinogenesis and colon PlsEtn levels. Here, we evaluated the functional role of dietary purified EtnGpl from the ascidian muscle (87.3 mol% PlsEtn in EtnGpl) and porcine liver (7.2 mol% PlsEtn in EtnGpl) in 1,2-dimethylhydrazine (DMH)-induced aberrant crypt foci (ACF) *in vivo*, and elucidated the possible underlying mechanisms behind it. Dietary EtnGpl suppressed DMH-induced aberrant crypt with one foci (AC1) and total ACF formation ($P < 0.05$). ACF suppression by dietary ascidian muscle EtnGpl was higher compared with dietary porcine liver EtnGpl. Additionally, dietary EtnGpl decreased DMH-induced oxidative damage, overproduction of TNF- α , and expression of apoptosis-related proteins in the colon mucosa. The effect of dietary ascidian muscle EtnGpl showed superiority compared with dietary porcine liver EtnGpl. Our results demonstrate the mechanisms by which dietary PlsEtn suppresses ACF formation and apoptosis. Dietary PlsEtn attained this suppression by reducing colon inflammation and oxidative stress hence a reduction in DMH-induced intestinal impairment. These findings provide new insights about the functional role of dietary PlsEtn during colon carcinogenesis.

2.2. INTRODUCTION

Ethanolamine glycerophospholipid (EtnGpl) is a major phospholipid after choline glycerophospholipids (ChoGpl) in all biological membranes. EtnGpl exists in three forms, according to the nature of linkage at sn-1 and sn-2 positions: 1,2-diacyl-sn-glycero-3-phosphoethanolamine (PtdEtn), 1-0-alkyl-2-acyl-sn-glycero-3-phosphoethanolamine, and 1-0-alkenyl-2-acyl-sn-glycero-3-phosphoethanolamine (PlsEtn). The latter form, containing the vinyl ether (alkenyl) linkage, is referred to as plasmalogen (Pls). The vinyl ether moiety in the sn-1 position consists of fatty alcohols mainly 16:0, 18:0, or 18:1 (Braverman and Moser, 2012). At the sn-2 position, PlsEtn are enriched in polyunsaturated fatty acids (PUFA). PlsEtn, especially those from seafood sources are abundant in 20:5n-3 (EPA) and 22:6n-3 (DHA), preferentially providing precursors for the synthesis of anti-inflammatory eicosanoids and docosanoids (Yamashita et al., 2016a).

Ethanolamine plasmalogen content in mammalian species varies greatly depending on the tissue source. For instance, in human tissues, PlsEtn levels in EtnGpl differ significantly; the brain and nervous system contain 60-90%, the plasma and red blood cells, 50-60%, the kidney, 20-45%, the skeletal muscle, 10-25%, while the liver contains the lowest levels, at about 2-5% (Braverman and Moser, 2012). In the colon, PlsEtn accounts for approximately 35% of EtnGpl (Dueck et al., 1996). The vinyl ether linkage in PlsEtn is highly susceptible to oxidative stress and has the propensity to acquire an inverted HII hexagonal shape, which is linked with its role in scavenging reactive oxygen species (ROS) and in membrane fusion, respectively (Leßig and Fuchs, 2009). PlsEtn is also involved in signal transduction, membrane trafficking, and generation of lipid second messengers (Braverman and Moser, 2012).

PlsEtn is a foreseeable functional food, and in the recent past, has attracted considerable interest as a functional lipid (Braverman and Moser, 2012; Messias et al., 2018). Indeed, a deficiency in the biosynthesis of plasmalogen has been associated with various disorders like Alzheimer's disease (AD), Down syndrome, Zellweger syndrome and rhizomelic chondrodysplasia punctata (RCDP) (Braverman and Moser, 2012; Yamashita et al., 2016b). We have shown that the extrinsic supply of PlsEtn bearing n-3 PUFA suppresses neuronal apoptosis through the mitochondrial pathway and improves impaired memory in a rat model of AD (Yamashita et al., 2015; 2016a). In addition, EPA-enriched PlsEtn rather than EPA-enriched PtdEtn alleviated amyloid β -induced neurotoxicity by inhibiting oxidative stress, neural injury, apoptosis, and neuro-inflammation, which depended on the vinyl ether linkage in the sn-1 position (Che et al., 2018a). However, the functional role of dietary PlsEtn in the health of intestines remains unknown.

Currently, colon cancer is increasingly becoming a devastating disease of both sexes worldwide, despite advances in diagnosis and treatment. Colon cancer ranks third and second among all cancer-related diseases in incidence and mortality, respectively (Bray et al., 2018). Concomitantly, chronic colon inflammation has been associated with the risk of developing colon malignancy (Bartsch and Nair, 2006). Chronic inflammatory processes induce oxidative stress and lipid peroxidation due to excessive pro-inflammatory cytokines and reactive oxygen/nitrogen species (ROS/RNS) production. These lead to DNA damage, apoptosis, cell homeostasis dysregulation, and dedifferentiation, which accentuates a chronic inflammation-related disease pathogenesis like cancer (Bartsch and Nair, 2006). Recently, PlsEtn metabolism has been reported to be profoundly dysregulated in dedifferentiated colon mucosa (Lopez et al., 2018). This indicates that PlsEtn may play a key role in protecting normal colon mucosa from a transition to hyper-proliferative and adenomatous polyps. However, the biological function of dietary PlsEtn and its underlying molecular mechanisms especially during colon mucosa pathophysiology, remain elusive.

Fish oil is the most common rich source of n-3 PUFA, specifically EPA and DHA (Gil, 2002). Dietary supplementation of n-3 PUFA increases their proportion in cell membrane phospholipids in a dose-dependent manner, partly at the expense of arachidonic acid (ARA, 20:4n-6), an n-6 PUFA. The n-3 and n-6 PUFA provide precursors for the synthesis of different types of eicosanoids, which mediate anti- and pro-inflammatory effects, respectively (Wall et al., 2010). Indeed, an increased dietary intake of n-6 PUFA correlates with an increased incidence of inflammatory bowel disease (IBD) in humans while an increased dietary consumption of n-3 to n-6 PUFA from marine products results in an attenuation of chronic colon inflammation (Djuric et al., 2017). Therefore, the alteration of dietary n-3/n-6 PUFA ratio is considered an important determining factor in colon cancer progression.

In light of the demonstrated superiority of PlsEtn over PtdEtn in neuroprotective functions (Che et al., 2018a) and the relationship of PlsEtn levels and a dysfunction in the colon mucosa (Lopez et al., 2018) as aforementioned, we hypothesized that dietary intake of PlsEtn may suppress colon inflammatory stress and subsequent formation of colon precancerous lesions (aberrant crypt foci – ACF) possibly due to a high presence of alkenyl (vinyl ether) linkages. In the present study, we elucidated the effect of diets supplemented with purified EtnGpl consisting of high and low PlsEtn ratios on the formation of ACF using a 1,2-dimethylhydrazine (DMH)-induced colon carcinogenesis mice model. Basal diet supplemented with fish oil only, therefore consisting of almost similar n-3/n-6 PUFA ratio to the EtnGpl diets, was used as reference for negative and positive controls because dietary n-3 PUFA is reported to alleviate colon inflammation as described above. Administered EtnGpl were prepared from ascidian (*Halocynthia roretzi*) muscle which contains a high PlsEtn ratio (Yamashita et al., 2014a) and porcine liver, which contains low PlsEtn (Braverman and Moser, 2012), while fish oil was sourced from skipjack tuna (*Katsuwonus pelamis*). In addition, the effect of diets with differing PlsEtn ratios compared to the basal diet on apoptosis and inflammation in the colon and the alteration of tissues lipid composition were investigated.

2.3. MATERIAL AND METHODS

2.3.1. Materials and Reagents

Freeze-dried ascidian muscle was provided by Yaizu Suisankagaku Industry Co., Ltd. (Shizuoka, Japan) while the porcine liver was purchased from local meatpackers in Hokkaido, Japan. Fish oil from skipjack tuna (*K. pelamis*) was provided by Nippon Suisan Kaisha Ltd. (Tokyo, Japan). Standard phospholipid species were purchased from Avanti Polar Lipids, Inc. (Alabaster, AL, USA) and PlsEtn-18:0/20:5 was purified according to the method reported previously (Yamashita et al., 2014b).

2.3.2. Preparation of EtnGpl and Experimental Diets

2.3.2.1. Preparation and Purification of Ascidian Muscle EtnGpl

Extraction of EtnGpl from ascidian muscle was done as described by Yamashita et al., (2014) with some modifications as shown in Figure 2.1 using organic solvents. The ascidian muscle powder was thawed for about 30 min and neutral lipids removed by washing the powder with 2.0 L cold acetone (-20°C) for 30 min. The residue, 600 g of ascidian muscle was extracted twice with 2.0 L of hexane-ethanol-water (6:11:1, v/v). The filtrate was evaporated to dryness using a vacuum rotary evaporator (Yamato rotary evaporator RE300, Tokyo, Japan) and 1 L of hexane-ethanol-water (2:1:1, v/v) was added. The mixture was transferred into a separating funnel and allowed to stand for 1 h. The upper phase (crude lipid) was evaporated to dryness and dissolved in small amount of chloroform-methanol (2:1, v/v), then 1 L of cold acetone was added, followed by addition of 25 mL 10% MgCl₂ in methanol. The resulting crude complex lipid was dissolved in chloroform and subjected to silica gel column chromatography (300 g of silica) with the following solvent system: chloroform, chloroform-acetone (4:1, v/v), acetone, chloroform-methanol (4:1, v/v) and chloroform-methanol (3:2, v/v). EtnGpl was confirmed using TLC and the fraction was evaporated to dryness. The dried EtnGpl fraction was further purified by dissolving in chloroform-methanol-ammonium hydrate (70:24:2, v/v) and subjected to silica gel column chromatography (200 g of silica) with the following solvent system: chloroform-methanol-ammonium hydrate 70:24:2, 65:25:3, 65:35:3, 60:40:3 and 50:50:3. EtnGpl was confirmed using TLC and the purified ascidian muscle EtnGpl fraction evaporated to dryness and dissolved in 40 mL of C:M (2:1).

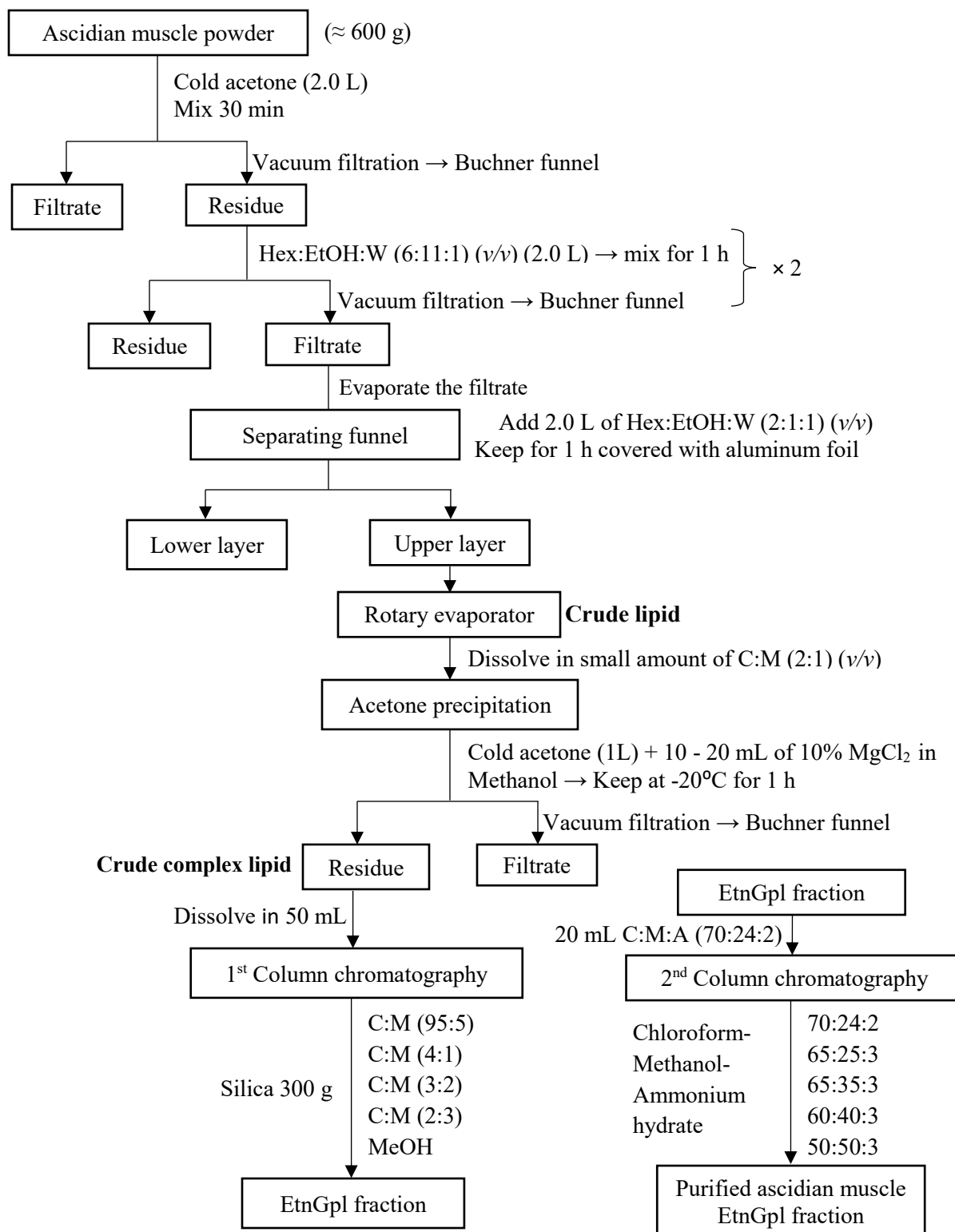


Figure 2.1 Preparation and purification of ascidian muscle EtnGpl

2.3.2.2. Preparation and purification of Porcine Liver EtnGpl

Frozen porcine liver was thawed and dipped in physiological saline solution (0.9% NaCl with 1% EDTA-2Na) for about 10 min and then cut in to pieces and homogenized in a mixer (Nissei Ace homogenizer, Tokyo, Japan) at 6,000 rpm for 30 sec. The homogenate was weighed into freeze drying bottles, frozen at -80°C overnight and freeze-dried (Yamato Scientific Co. Ltd, Tokyo, Japan) for 72 h. The freeze-dried sample was weighed, crushed, and kept at -20°C until use.

Extraction of EtnGpl from porcine liver was done according to our previous report (Yamashita et al., 2014b) with some modifications as shown in Figure 2.2. Neutral lipids were removed by washing twice with 1.2 L of cold acetone containing 0.2% BHT. The residue, 430 g of porcine liver was extracted twice with 1.2 L of chloroform-methanol (2:1, v/v) containing 0.2% BHT. The supernatant was treated as described by Folch et al., (1957). The resulting crude lipid was dissolved in chloroform-methanol (2:1, v/v) and 1 L of cold acetone was added, followed by addition of 25 mL 10% MgCl₂ in methanol. The resulting crude complex lipid was dissolved in chloroform and subjected to silica gel column chromatography twice as described above. EtnGpl was confirmed using TLC and the purified porcine liver EtnGpl fraction evaporated to dryness and dissolved in 40 mL of C:M (2:1).

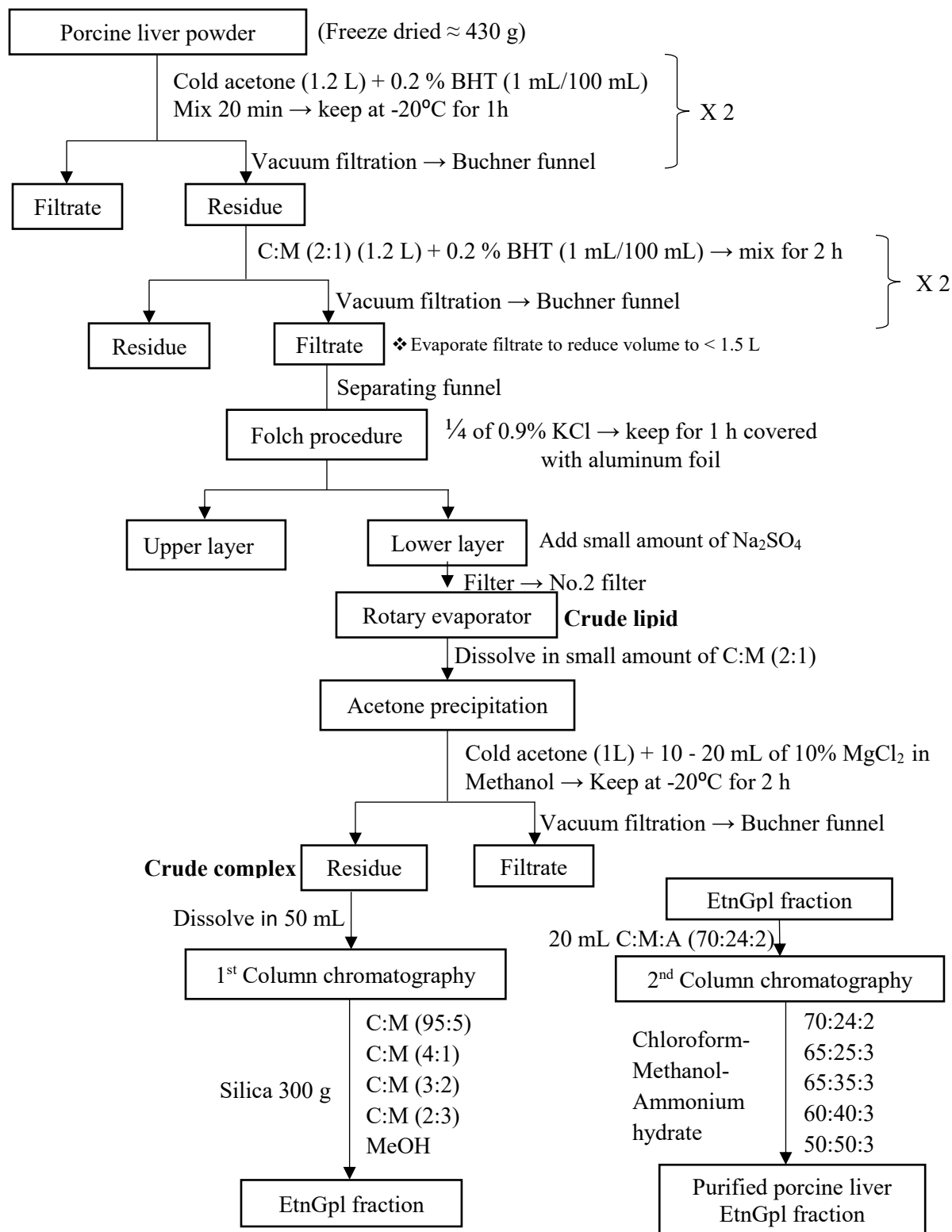


Figure 2.2 Preparation and purification of porcine liver EtnGpl

2.3.2.3. Experimental Diets

Three experimental diets were prepared; basal diet for blank and control mice groups, and porcine liver EtnGpl and ascidian muscle EtnGpl diets based on AIN-93G diet. The AIN-93G diet was slightly modified by reducing soy oil content to 6% and supplementing with 1% fish oil (10 g/kg) to form the basal diet. Precisely, 1 kg of porcine liver and ascidian muscle EtnGpl diets were prepared by adding 0.1% purified porcine liver and ascidian muscle EtnGpl (1 g/kg diet), respectively, to the basal diet. Briefly, 0.1% porcine liver and ascidian muscle EtnGpl (dissolved in Chloroform-methanol 2:1, v/v) was dried to a constant weight. The dried EtnGpl fractions were each dissolved in 4 mL of hexane-ethanol (2:1, v/v) and 10 g of soy added. The mixture was dried in a vacuum rotary evaporator to a constant weight and placed in a vacuum desiccator covered with aluminum foil overnight. The basal diet was prepared in a similar manner but with no addition of EtnGpl.

The ingredients for each diet were mixed following the order shown in Table 2.1. The solid ingredients were mixed using a plastic mixing paddle by hand after adding each of the ingredient in the mixing bowl and the mixing bowl was then mounted on the mixer. Oil from the desiccator was mixed with fish oil and added to the mixed ingredients, then the flask was rinsed by the remaining 50 g of soy oil. Endotoxin free water was added (430 mL) and mixing done until the mixture formed a consistent thick elastic dough. The dough was molded into 10 g round pieces. To prevent oxidation of lipids in the diet, diets were kept in air-sealed bags, in the dark, at -20°C until use.

- ❖ Porcine liver and ascidian muscle EtnGpl for incorporation into the diet were calculated based on phospholipid concentration (mol). Concentration of sample analyzed by GC = $\left(\frac{Alkenyl + Acyl}{2}\right) \mu M$. Then the concentration of GC analyzed sample was multiplied by the amount of chloroform-methanol (2:1, v/v) used to dissolve the purified EtnGpl and molecular weight of phospholipid (775) to get the mass concentration of EtnGpl (g EtnGpl/chloroform-methanol mL).
- ❖ Porcine liver EtnGpl contained low PlsEtn level (7.2 mol% PlsEtn in EtnGpl) while ascidian muscle EtnGpl contained high PlsEtn (83.7 mol% PlsEtn in EtnGpl).
- ❖ 1% fish oil was added to the three experimental diets to attain relatively similar n-3/n-6 PUFA ratio. In addition, the current recommended ratio of n-3/n-6 PUFA is 2:1 to 5:1, while the World Health Organization (WHO) recommended level is at 5:1 to 10:1 (World Health Organization Fat and Oils in human Nutrition, 1994; Zhang et al., 2019).

Table 2.1 Modified AIN-93G diet to form the basal diet, porcine liver and ascidian muscle EtnGpl diets prepared by adding 0.1% of the respective EtnGpl to the basal diet.

| AIN-93G basal diet | | | | AIN-93G basal diet + EtnGpl | | | |
|-------------------------------|-----------------------|-------------|-------------|--|-----------------------|---------|--------|
| Blank and control diet (1 kg) | | | | Porcine liver and ascidian muscle EtnGpl diet (1 kg) | | | |
| Ingredients | | % | g | Ingredients | | % | g |
| 1 | BHT | 0.0014% | 0.014 | 1 | BHT | 0.0014% | 0.014 |
| 2 | Choline | 0.3% | 2.5 | 2 | Choline | 0.3% | 2.5 |
| 3 | L-Cystine | 0.3% | 3.0 | 3 | L-Cystine | 0.3% | 3.0 |
| 4 | Cellulose | 5.0% | 50.0 | 4 | Cellulose | 5.0% | 50.0 |
| 5 | Sucrose | 10.0% | 100.0 | 5 | Sucrose | 10.0% | 100.0 |
| 6 | α -Corn starch | 13.2% | 132.0 | 6 | α -Corn starch | 13.2% | 132.0 |
| 7 | Casein lactic | 20.0% | 200.0 | 7 | Casein lactic | 20.0% | 200.0 |
| 8 | Cornstarch | 39.75% | 397.49 | 8 | Cornstarch | 39.75% | 397.49 |
| 9 | Vitamin | 1.0% | 10.0 | 9 | Vitamin | 1.0% | 10.0 |
| 10 | Minerals | 3.5% | 35.0 | 10 | Minerals | 3.5% | 35.0 |
| 11 | Fish oil | 1.0% | 10.0 | 11 | Fish oil | 1.0% | 10.0 |
| 12 | Soy oil | 6.0% | 60.0 | 12 | Soy oil | 6.0% | 60.0 |
| | | 100% | 1000 | 13 | EtnGpl | 0.1% | 1.0 |
| 13 | Water | 430 mL | | 14 | Water | 430 mL | |

EtnGpl, ethanolamine glycerophospholipids; *BHT*, Butylated hydroxytoluene

2.3.3. Animals and Experimental design

Female BALB/c mice were obtained from Japan SLC, Inc (Shizuoka, Japan) at 4 weeks of age and housed in pathogen-free conditions in micro-isolator cages at $22 \pm 1^\circ\text{C}$ under a 12 h light/dark cycle. The mice were randomized into four groups (n=8) after acclimation for 1 week with CE-2 diets (CLEA Japan, Inc, Tokyo, Japan). Blank group was orally fed with basal diet and administered intraperitoneally (i.p.) saline. The control group was orally fed with basal diet and administered i.p. DMH. The porcine liver group was orally fed with porcine liver EtnGpl diet and administered i.p. DMH. The ascidian muscle group was orally fed with ascidian muscle EtnGpl diet and administered i.p. DMH (Figure 2.3). Furthermore, the four groups were divided into two categories; the first category was used to confirm colon ACF formation (n=4) and the second category to analyze the levels of apoptosis-related proteins, TNF- α , and lipid composition in colon mucosa (n=4). After one week of adaptive feeding with the respective experimental diet *ad libitum*, the mice were administered with 15 mg/kg i.p.

1,2-DMH-HCl in saline once a week for 4 weeks followed by 25 mg/kg i.p. 1,2-DMH once a week for 5 weeks and provided daily with the experimental diet (about 5 g/day/mouse). At the end of the experimental diet (10 weeks), the mice were fasted for 12 h and euthanized with sodium pentobarbital (50 mg/kg BW, i.p.). All animal experiments protocols were approved by the Animal Care and Use Committee and were performed according to Obihiro University Guidelines (Permit Number: 18-149).

❖ **Routine activities**

The diets were changed daily while the cages, beddings, and drinking water were replaced weekly during *i.p.* administration.

❖ ***i.p.* 1,2-DMH preparation**

DMH for *i.p.* administration was prepared based on average weight of mouse, which was 20g and injection volume of 100 µl per mouse. Precisely, 15 mg/kg and 25 mg/kg *i.p.* 1,2-DMH were prepared by dissolving 30 and 50 mg of DMH, respectively in autoclaved saline (0.9% NaCl with 1mM EDTA-2Na) using 15 mL sterile conical centrifuge tubes. The pH of the mixture was adjusted to 7.0 using 0.5 N NaOH. Blank group *i.p.* saline was prepared by adjusting the pH of 10 mL autoclaved saline with 0.25 N NaOH to 7.0. The solutions were filtered into sterile conical centrifuge tubes using cellulose acetate membrane filters, pore size 0.45 µm (ADVANTEC®, Toyo Roshi Kaisha Ltd, Tokyo, Japan).

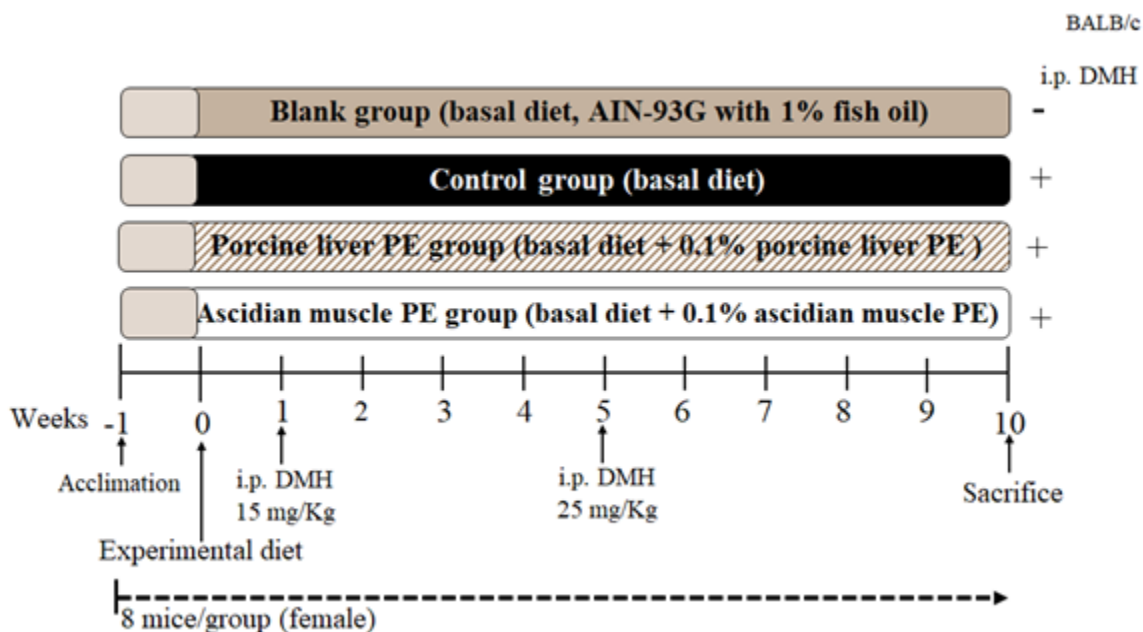


Figure 2.3 Experimental design of *i.p.* DMH-induced colon carcinogenesis in mice for 10 weeks.

After 1 week of acclimation with chow diet *ad lib*, the experimental diets were introduced and changed everyday (about 5 g/mice/day). After 1 week of experimental diet adaptive feeding, the mice were intraperitoneally

administered with 1,2-DMH-HCl (4 weeks at 15 mg/kg and 5 weeks at 25 mg/kg i.p. DMH). Diet intake was recorded everyday and body weight recorded once a week prior to DMH administration. At sacrifice, the mice were further grouped into two; for colon ACF scoring (n = 4/group) and for colon mucosa apoptosis and lipid analysis (n = 4/group). Body weight, colon length, spleen and liver weight were recorded for all mice.

2.3.4. Blood, Tissues, and Colon Mucosa Preparation

Plasma (n=8) was prepared from freshly collected blood from the heart of euthesized mice. The blood was placed in Eppendorf tubes with 10 mg/mL EDTA-2Na dissolved in saline to a final concentration of 0.1% (v/v) and centrifuged first and second time at 1,200 and 1,800 rpm, respectively for 15 min at 4 °C to separate red blood cells (RBC) from the plasma. The plasma was kept at -80 °C until use. The liver and spleen (n=8) were separated, washed with cold saline, dried (with Kim paper towel), and weighed. The liver was then homogenized with cold phosphate buffer solution (PBS) containing 1mM EDTA to make a 30% homogenate using a digital homogenizer (As one corporation, Osaka, Japan) at 940 rpm under an ice bath condition. The homogenate was aliquoted in Eppendorf tubes and kept at -80°C until use. The colon was resected from the part with cecum to the proximal anus. To obtain colon mucosa, excised colon (n=4) was rinsed with cold saline followed by cold protease inhibitor in PBS. Colon mucosa was scraped using a glass slide, homogenized with 1 mL PBS containing Protease inhibitor cocktail set III (Fujifilm Wako Pure Chemical Corp., Gunma, Japan) and then Triton X-100 was added to a final concentration of 1%. The colon mucosa homogenate was aliquoted and kept at -80 °C until use.

2.3.5. Identification of Aberrant Crypt Foci (ACF)

ACFs in the colon (n=4) were identified and quantified as described previously with some modifications (Yamashita et al., 2017). The resected colon was rinsed with cold saline and filled with 10% neutral buffered formalin solution for 24 h. Each colon was opened longitudinally from the caecum to the anus and stained with 0.1% methylene blue solution in saline for 1 min at room temperature (25 °C). ACFs were counted depending on crypt multiplicity; the number of aberrant crypts (AC 1, 2 and 3 or more) was identified under a light microscope (Bird, 1995; Arai et al., 2013).

2.3.6. TNF- α and Apoptosis Array Assays

TNF- α levels were measured using a Mouse TNF- α ELISA kit (FUJIFILM Wako Shibayagi Corp., Gunma, Japan). Levels of apoptosis-related proteins were examined using Mouse Apoptosis Array Kit (R&D Systems, Minneapolis, MN, USA). After freezing and thawing the colon mucosa homogenate, according to the manufacture's protocol, the proteins were detected. The detected apoptosis-related proteins were: B-cell

lymphoma 2 (Bcl-2); Bcl/leukemia x (Bcl-x); catalase; claspin; (MCL-1); p27 cyclin-dependent kinase 4 inhibitor 1B (p27/Kip1); X-linked inhibitor of apoptosis (XIAP); Bcl-xL/Bcl-2 associated death promoter (Bad); cytochrome c; second mitochondria-derived activator of caspase/direct inhibitor of apoptosis-binding protein with low pI (SMAC/Diablo); fibroblast-associated (Fas); TNF receptor 1 (TNF R1); TNF-related apoptosis-inducing ligand receptor 2 (TRAIL R2); cleaved caspase-3; p53; hypoxia-inducible transcription factor (HIF)-1 α ; heme oxygenase (HO)-1; HO-2; heat shock protein (HSP)27; HSP60; HSP70.

2.3.7. Lipid Extraction and Assay

2.3.7.1. Total lipids and phospholipid fraction from liver homogenate

Extraction of total lipids from the 30% mice liver homogenate samples was done as described by Folch et al., (1957). Briefly, 0.5 mL of the homogenate samples was added to 2.5 mL of C:M (2:1) containing 0.002% BHT. The mixture was vortexed thoroughly and centrifuged at 3,000 rpm for 10 min. Total lipids were extracted for the second time by adding 1.8 mL of C:M (10:1) to the upper layer, the mixture was vortexed and centrifuged at 3,000 rpm for 10 min. The lower layers from the two extractions were combined and 2.4 mL of chloroform: methanol: water (3:48:47) added, vortexed and centrifuged at 3,000 rpm for 10 min. The lower layer was dried under N₂ flux, dissolved in 1 mL of C:M (2:1) and kept at -30°C until use. To obtain phospholipid fraction, 1 mL of the extracted total lipids was dried by N₂ flux and dissolved in 200 μ l of chloroform-isopropanol (2:1), and then loaded onto a silica Sep-Pak cartridge (Waters, Tokyo, Japan) activated with 1.5 mL of methanol and equilibrated with 1.5 mL of chloroform-isopropanol (2:1). The sample was loaded and eluted with 1.5 mL of chloroform-isopropanol (2:1) to remove non-polar compounds. The cartridge was then loaded with 1.5 mL of methanol and the eluted methanol solution collected as phospholipid fraction. FAME and DMA prepared from the lipid extracts were analyzed by gas chromatography (Yamashita et al., 2019). Phospholipid species were analyzed by LC-MS/MS operated in the multiple reaction monitoring (MRM) mode.

2.3.7.2. Phospholipid fraction from plasma and colon mucosa

Phospholipid fraction in plasma and colon mucosa was extracted as previously described in our report (Otoki et al., 2017). Briefly, crude phospholipid fraction was extracted by adding 80 μ l of the thawed plasma and colon mucosa in Eppendorf tubes, thoroughly mixed with 20 μ l of 25 μ M EDTA in water and 500 μ l of 0.002% BHT in methanol. The mixture was centrifuged at 7,000 rpm for 15 min and the supernatant collected (600 μ l). The precipitate was re-extracted with 500 μ l of methanol and centrifuged at 7,000 rpm for 15 min. The two supernatants were combined to yield a total volume of 1100 μ l of plasma crude phospholipid. To remove polar compounds, the extracted crude phospholipid was pretreated with Sep-Pack Plus silica cartridges (Waters, Milford, MA, USA). The cartridges were conditioned (activated) with 1.5 mL of methanol (500 μ l \times 3), then

500 µl of plasma crude phospholipid loaded onto the cartridge followed by an additional 1.5 mL (500 µl × 3) to elute the residual phospholipids. The purified phospholipid fraction (2 mL) was analyzed for fatty acid and aldehyde composition using GC-FID, while PlsEt_n molecular species were analyzed by LC-M/MS operated in the multiple reaction monitoring (MRM) mode.

2.3.7.3. Fatty acid and aldehyde analysis

Fatty acids and aldehydes were analyzed from the lipid extracts as follows. Fatty acid methyl esters (FAME) and dimethyl acetals (DMA) were prepared by incubating 0.1 mL of dried lipid extract with 1.8 mL of methanol, 0.2 mL of acetyl chloride and 0.1 mL of internal standard (17:0, 2 mg/mL) at 100°C for 2 h (Rodr et al., 1998). The methylated mixture was cooled and 3 mL of hexane and 0.5 mL of distilled water added, vortexed, and centrifuged (3,000 rpm for 10 min), followed by addition of 0.5 mL of 2% KHCO₃ to the hexane phase (upper layer). The mixture was vortexed, centrifuged (3,000 rpm for 10 min) and the hexane phase (upper layer) dried under N₂ flux to recover FAME and DMA. FAME and DMA were concentrated by adding 0.5 mL of hexane and stored at -20°C until analysis by gas chromatography with flame ionization detector (GC-FID) (GC-2010, Shimadzu, Japan). The GC column was CP-SIL 88 (50 m × 0.25 mm i.d., 0.2 µm, Varian USA) with oven cycle program of 80°C to 160°C at 10°C/min for 8 min, followed by 160°C to 220°C at 2°C/min for 30 min and a final column temperature of 220°C for 10 min. Injection and detection temperatures were 230°C and 240°C, respectively and the column flow rate was 0.7 mL/min. Sample injection was 2 µl manually. Identification of individual FAME and DMA peaks was done by comparison of retention time with bovine heart lipid extract as standard and quantification against internal standard (C17:0).

2.3.7.4. Phospholipid analysis

Phospholipid content was determined according to the method described by Rouser et al., (1970). Briefly, 1 mL of chlorine peroxide (perchloric acid) was added to dried sample in long tubes (15 mm × 180 mm) and covered with a marble then heated at 200°C for 90 min. After cooling, 5 mL distilled water, 1 mL 2.5% ammonium molybdate solution, 1 mL 10% ascorbate solution and 2 mL distilled water were added in that order and contents vortexed after each addition. The standard solutions (0, 2, 5, 10, 15 and 20 µg P) were prepared with the same procedure and at the same time with the samples but NOT heated at 200°C for 90 min. The tubes were incubated at 100°C for 10 min, cooled and absorbance determined at 820 nm. A multiplier of 25 was used based on the general phosphorus content in phosphatidylcholine.

- ❖ Phosphate stock solution was prepared by dissolving 0.2193 g KH₂PO₄ in 50 mL of distilled water (1 mg phosphorus/mL). Phosphate standard solution was then prepared by diluting the stock solution 100 times with distilled water to form 10 µg P/mL. Standard solutions were prepared as

- follows: 0, 0.2, 0.5, 1.0, 1.5, 2.0 mL (0, 2, 5, 10, 15, and 20 µg P, respectively) were each added in to tubes (15 mm × 180 mm).
- ❖ The sample was diluted 100 times with chloroform-methanol (2:1, v/v).
 - ❖ Phospholipid amount = P amount × 25 and phospholipid mol = P amount/31 (Average M.W of phospholipid and P is 775 and 31, respectively).

2.3.8. Other Assays

2.3.8.1. 2-Thiobarbituric Acid Reactive Substances (TBARS)

Lipid peroxidation in the tissues is a consequence of initiation of oxidative stress upon attack of cell membrane lipids by free radicals. Malonaldehyde (MDA) is the most abundant product arising from lipid peroxidation and has been widely used as an index of oxidative stress.

TBARS to determine lipid peroxidation in diets, colon mucosa (n=4), and liver homogenates (n=8) were determined according to the method by Ohkawa et al., (1979) with some modifications. Briefly, 100 µl of 30% liver homogenate and the standard solutions were each added into 10 mL screw cap test tubes and 1.5 mL acetic buffer solution (pH 3.5 adjusted with KOH), 1.5 mL 0.8% thiobarbituric acid (TBA reagent, dissolved in warm water), 0.2 mL 8.1% SDS solution, 1.0 mL distilled water, and 50 µl 0.8% BHT in acetic acid were added. The mixture was vortexed and allowed to stand at 5°C (ice cubes in water) for 60 min. Then heated in boiling water for 60 min, cooled and 1.0 mL distilled water and 5.0 mL n-butanol/pyridine (15:1 v/v) were added, vortexed and centrifuged at 3,000 rpm for 10 min. The upper phase was collected with Pasteur pipette and absorbance read at 532 nm.

- ❖ The concentration of the sample was determined from malonaldehyde (MDA) standard curve and then multiplied by the sample volume, which gives the concentration of supernatant in the cuvette only, so moles of TBARS per sample weight were calculated by taking into account the volume of the supernatant (5 mL).
- ❖ To prepare the MDA standard curve, 1,1,3,3-tetramethoxypropane (TEP) stock solution (precursor for MDA) was prepared by adding 50 µl of TEP in 100 mL of methanol (5 mM/L). The standard solution was prepared by diluting the stock solution 1,000 times with methanol (5 µM/L). Then standards 0, 0.05, 0.1, 0.2, 0.5 and 1.0 µM/L were prepared by adding 0, 10, 20, 40, 100 and 200 µL of standard solution, respectively into screw cap test tubes.

2.3.8.2. Total Cholesterol

Total cholesterol in liver homogenates (n=8) was determined using total cholesterol kit (T-Cho Enzymatic method) (FUJIFILM Wako Shibayagi Corp., Gunma, Japan). Briefly, 200 µl of total lipid extract was dried

under nitrogen flux, then dissolved in 200 μ l of 2-propanol, followed by addition of 3.0 mL of color reagent solution. The mixture was then incubated at 37 °C for 5 min, and the absorbance read at 600 and 700 nm. The color reagent and standard curve from cholesterol standard solution were prepared according to the manufacturer's instructions.

2.3.8.3. Total Protein Content

Total protein amounts of samples were measured by the DC Protein Assay kit (Bio-rad, Hercules, CA, USA). Briefly, 100 μ l of standard and 1000 μ l of sample were pipetted into dry test tubes and 500 μ l of reagent A added followed by 4.0 mL of reagent B. The mixture was vortexed immediately. After 15 minutes, the absorbance was read at 750 nm (Absorbance stable for at least 1 h).

- ❖ Protein stock solution (20 mg/mL) was prepared by dissolving 100 mg of Albumin from Bovine Serum in 5 mL of D.W using 15 mL sterile conical centrifuge tube. Protein standard solution was then prepared by serial dilution of the stock solution with D.W into 1.25, 2.5, 5, and 10 mg/mL protein. Standard curve was prepared each time the assay was performed.

2.3.9. Statistical Analysis

The results are represented as means \pm SEM. All data were subjected to analysis of variance using SPSS software (version 17.0; SPSS Inc., Chicago, IL, USA). Differences between the means were tested using one-way ANOVA followed by Tukey's post-hoc test. Values of $P < 0.05$ were considered statistically significant.

2.4. RESULTS

2.4.1. EtnGpl Fractions from Ascidian Muscle and Porcine Liver

The main carbon chains in purified ascidian muscle EtnGpl were 18:0, EPA, and DHA, while PlsEtn-18:0/20:5, PlsEtn-18:0/22:6 and PtdEtn-18:0/22:6 were the main diradylphospholipid species (Table 1). The PlsEtn level in purified ascidian muscle EtnGpl was 87.3 mol% in EtnGpl. The main carbon chains in purified porcine liver EtnGpl were 18:0, 18:2n-6, and ARA, and the main diradylphospholipid species was PtdEtn-18:0/20:4. PlsEtn levels in porcine liver EtnGpl were lower (7.2 mol% in EtnGpl) than that of ascidian muscle EtnGpl. Ascidian muscle EtnGpl had higher ratios of n-3/n-6 and (EPA+DHA)/ARA than porcine liver EtnGpl.

Table 2.2 Composition of acyl and alkenyl chains (A), and phospholipid species (B) of prepared EtnGpl (mol%)

| A | Porcine | Ascidian | B | Porcine | Ascidian |
|----------------|--------------|---------------|---------------------------------|--------------|---------------|
| | liver EtnGpl | muscle EtnGpl | | liver EtnGpl | muscle EtnGpl |
| Acyl (mol%) | | | Species <i>sn-1/sn-2</i> (mol%) | | |
| 16:0 | 8.0 | 1.0 | PlsEtn-18:0/18:1 | 0.4 | 2.2 |
| 18:0 | 36.6 | 3.4 | PlsEtn-18:0/20:4 | 2.1 | 3.5 |
| 18:1n-9 | 6.1 | 2.4 | PlsEtn-18:0/20:5 | Traces | 53.1 |
| 18:2n-6 | 9.3 | nd | PlsEtn-18:0/22:6 | 0.2 | 12.4 |
| 18:3n-6 | 0.2 | 0.8 | PlsCho-18:0/18:1 | nd | Traces |
| 20:3n-6 | 1.4 | nd | PlsCho-18:0/20:4 | nd | nd |
| 20:4n-6 | 27.5 | 1.9 | PlsCho-18:0/22:6 | nd | nd |
| 20:5n-3 | 0.6 | 35.6 | PtdEtn-18:0/18:1 | 5.6 | 0.8 |
| 22:5n-3 | 2.3 | 0.4 | PtdEtn-18:0/20:4 | 69.2 | 0.5 |
| 22:6n-3 | 2.3 | 8.7 | PtdEtn-18:0/22:6 | 5.5 | 7.4 |
| n-3/n-6 | 1.0 | 11.0 | PtdCho-18:0/18:1 | Traces | Traces |
| (EPA+DHA)/ARA | 0.1 | 23.8 | PtdCho-18:0/20:4 | Traces | Traces |
| Alkenyl (mol%) | | | PtdCho-18:0/22:6 | Traces | Traces |
| 16:0ol | 1.2 | 5.5 | LysoPlsEtn-16:0 | Traces | Traces |
| 18:0ol | 2.1 | 34.8 | LysoPlsEtn-18:0 | Traces | 0.5 |
| 18:1ol | 0.3 | 3.4 | LysoPlsCho-16:0 | nd | nd |
| Total | 3.6 | 43.7 | LysoPlsCho-18:0 | nd | nd |
| | | | LysoPtdEtn-16:0 | 0.1 | Traces |
| | | | LysoPtdEtn-18:0 | 0.3 | 0.1 |

EtnGpl ethanolamine glycerophospholipids, *DHA* docosahexaenoic acid (22:6n-3), *ARA* arachidonic acid (20:4n-6), *PlsEtn/Cho* ethanolamine/choline plasmalogen, *PtdEtn/Cho* phosphatidylethanolamine/choline, *Lyso-PtdEtn/Cho* Lysophosphatidylethanolamine/choline, *Lyso-PlsEtn/Cho* Lysoethanolamine/choline plasmalogen, *nd* not detected.

2.4.2. Fish and Soy Oil Acyl and Alkenyl Chains

The acyl and alkenyl chains of fish and soy oil are as shown in Table 2.3. The fish oil contained 31.2 mol% DHA (22:6n-3) and 6.7 mol% EPA (20:5n-3). The major saturated (SFA) and monounsaturated fatty acid were palmitic acid (16:0, 21.4 mol%) and oleic acid (18:1n-9, 13.0 mol%). The major n-3 PUFA, DHA and EPA had the highest proportion (37.9 mol%) while n-6 ARA was 2.2 mol%. This led to the high ratio of n-3/n-6 and (EPA+DHA)/ARA. Soy oil mainly contained palmitic acid, oleic acid and linoleic acid as the main acyl chains,

while the ratio of n-3/n-6, and (EPA+DHA)/ARA were low due to low levels of n-3. Alkenyl chains were not detected in both fish and soy oil.

Table 2.3 Composition of acyl and alkenyl chains (mol%) in fish and soy oil

| | Fish oil | Soy oil |
|-----------------|----------|---------|
| Acyl (mol%) | | |
| 16:0 | 21.4 | 11.5 |
| 18:0 | 4.6 | 4.2 |
| 18:1n-9 | 13.0 | 23.5 |
| 18:2n-6 | 1.5 | 54.2 |
| 18:3n-3 | 0.6 | 6.6 |
| 20:3n-6 | nd | nd |
| 20:4n-6 | 2.2 | nd |
| 20:5n-3 | 6.7 | nd |
| 22:5n-3 | 1.0 | nd |
| 22:6n-3 | 31.2 | nd |
| n-3/n-6 | 9.0 | 0.1 |
| (EPA + DHA)/ARA | 17.5 | 0.0 |
| Alkenyl (mol%) | | |
| 16:0ol | nd | nd |
| 18:0ol | nd | nd |
| 18:1ol | nd | nd |
| Total | nd | nd |

Fish oil from skipjack tuna (*K. palemis*); *nd* not detected.

2.4.3. Diet Lipid Composition

The main acyl chains in the diets were palmitic acid, oleic acid, linoleic acid, and DHA while ARA was prominent in porcine liver EtnGpl diet (Table 2.4). The ratio of (EPA+DHA)/ARA in the porcine liver EtnGpl diet was lower than that of basal and ascidian muscle EtnGpl diets due to the high levels of ARA in porcine liver EtnGpl. All the other acyl chains levels were relatively the same among the diets resulting in a similar n-3/n-6 ratio. Importantly, ascidian muscle EtnGpl diet had a higher abundance of alkenyl chains i.e. plasmalogens than porcine liver EtnGpl and basal diets.

Table 2.4 Composition of acyl and alkenyl chains ($\mu\text{mol}/100\text{g}$) in the experimental diet

| | Basal diet | Porcine liver EtnGpl diet | Ascidian muscle EtnGpl diet |
|---|------------|---------------------------|-----------------------------|
| Acyl ($\mu\text{mol}/100\text{ g}$) | | | |
| 16:0 | 2896.6 | 2916.0 | 2899.1 |
| 18:0 | 935.1 | 1021.2 | 943.4 |
| 18:1n-9 | 4748.7 | 4764.9 | 4754.6 |
| 18:2n-6 | 9920.2 | 9945.0 | 9920.2 |
| 18:3n-3 | 1217.7 | 1219.1 | 1219.6 |
| 20:3n-6 | 4.0 | 4.8 | 4.0 |
| 20:4n-6 | 83.0 | 145.3 | 87.7 |
| 20:5n-3 | 243.3 | 244.5 | 330.4 |
| 22:5n-3 | 36.7 | 41.4 | 37.6 |
| 22:6n-3 | 1142.4 | 1146.8 | 1163.1 |
| n-3/n-6 | 0.3 | 0.3 | 0.3 |
| (EPA + DHA)/ARA | 16.7 | 9.6 | 17.0 |
| Alkenyl ($\mu\text{mol}/100\text{g}$) | | | |
| 16:0ol | nd | 3.2 | 13.5 |
| 18:0ol | 3.7 | 9.0 | 88.7 |
| 18:1ol | nd | 0.7 | 8.2 |
| Total | 3.7 | 13.0 | 110.4 |

The experimental diet was a modified AIN-93G diet by reducing soy oil content to 6% and supplemented with 1 % fish oil (10 g/kg diet) to form the basal diet. Ascidian muscle and porcine liver EtnGpl diets were 0.1% ascidian muscle and porcine liver EtnGpl (1 g/kg diet), respectively added to the basal diet. *nd* not detected.

2.4.4. Animal and Tissues Data

Experimental diet intake at week 1 and 10, and TBARS levels in the diet, an indicator of peroxidation, remained relatively the same among the groups (Table 2.5). Mice at week 0 had the same weight among the groups and their weight increased during the experimental period. At week 10, DMH-treated mice had higher TBARS levels in the colon mucosa and liver compared to the blank group. Dietary ascidian muscle EtnGpl suppressed the DMH-induced TBARS levels in colon mucosa and lowered the total cholesterol in liver tissue compared to the control group. DMH treatment in the control group had no effect on phospholipid content in colon mucosa, liver, and plasma compared with the blank group. DMH treatment in the control group also had no effect on total lipid content in the colon mucosa and liver among the groups, while those of the plasma was

not analyzed since they were used up. Dietary EtnGpl did not affect all other parameters, including TBARS levels, in the liver when compared to the control group.

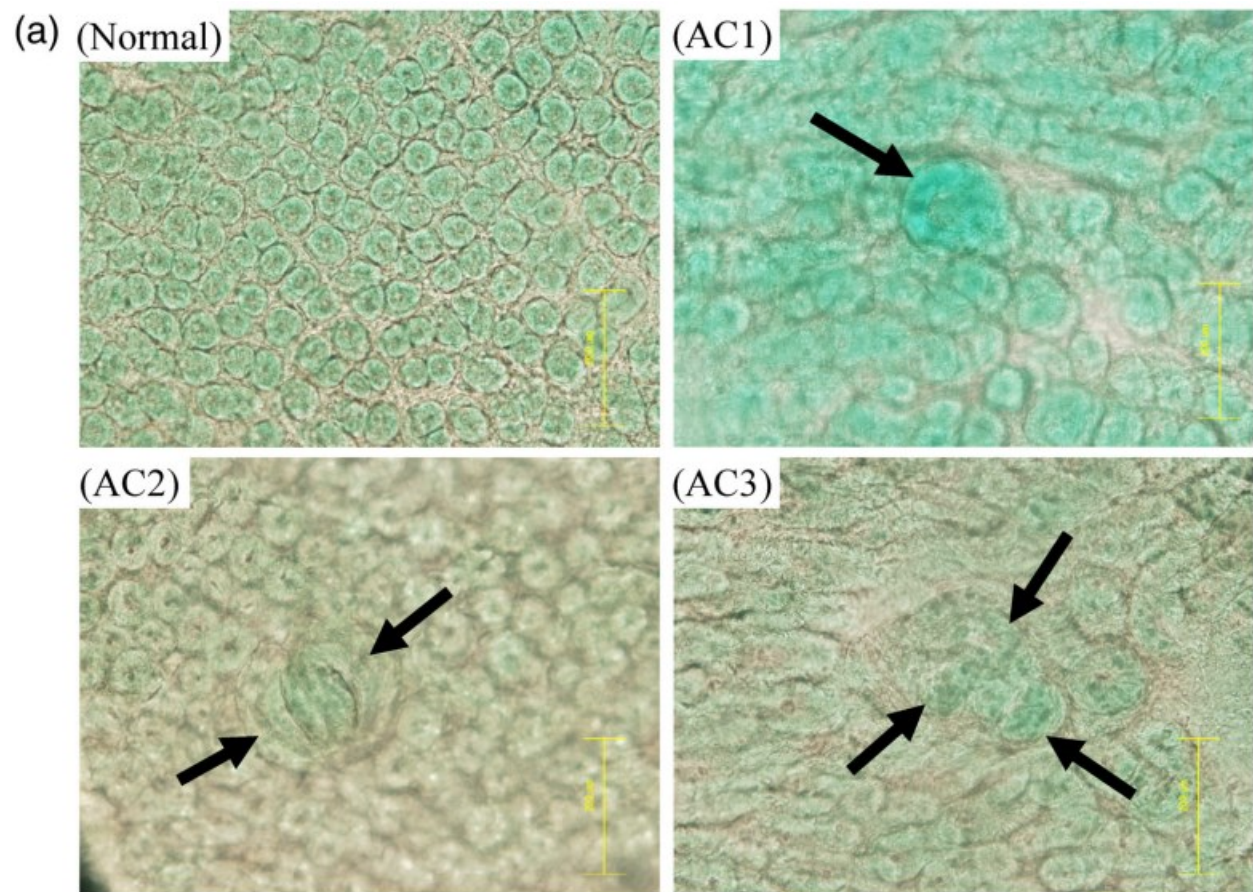
Table 2.5 Daily diet intake, body, liver and spleen weights, colon length and TBARS after 10 weeks of the animal experiment

| | Group i,p DMH | Blank - | Control + | Porcine liver + | Ascidian muscle + |
|-----------------------------------|------------------|---------------------------|---------------------------|---------------------------|---------------------------|
| Diet | | | | | |
| Intake (g/day, week 1) | | 4.0 ± 0.1 ^a | 4.1 ± 0.1 ^a | 4.0 ± 0.1 ^a | 3.9 ± 0.1 ^a |
| Intake (g/day, week 10) | | 3.6 ± 0.1 ^a | 3.6 ± 0.1 ^a | 4.0 ± 0.1 ^a | 4.0 ± 0.1 ^a |
| TBARS (µmol/100 g of diet) | | 10.4 ± 1.2 ^a | 10.4 ± 1.2 ^a | 9.1 ± 2.4 ^a | 8.5 ± 2.1 ^a |
| Body | | | | | |
| Weight (g, week 0) | | 14.1 ± 0.3 ^a | 14.1 ± 0.4 ^a | 13.6 ± 0.2 ^a | 14.4 ± 0.4 ^a |
| Weight (g, week 10) | | 22.2 ± 0.3 ^a | 21.0 ± 0.5 ^{ab} | 20.2 ± 0.3 ^b | 21.1 ± 0.4 ^{ab} |
| Spleen | | | | | |
| Weight (g) | | 0.10 ± 0.0 ^b | 0.13 ± 0.0 ^{ab} | 0.14 ± 0.0 ^a | 0.13 ± 0.0 ^{ab} |
| Colon | | | | | |
| Length (cm) | | 10.9 ± 0.2 ^a | 11.4 ± 0.2 ^a | 11.6 ± 0.2 ^a | 11.4 ± 0.2 ^a |
| Colon mucosa | | | | | |
| TBARS (nmol/mg protein) | | 0.2 ± 0.0 ^b | 0.9 ± 0.2 ^a | 0.4 ± 0.0 ^{ab} | 0.3 ± 0.1 ^b |
| Total lipid (µg/mg protein) | | 215.4 ± 27.7 ^a | 291.2 ± 36.6 ^a | 161.3 ± 52.5 ^a | 107.9 ± 26.6 ^a |
| Phospholipid (nmol/mg protein) | | 64.3 ± 7.9 ^a | 51.3 ± 12.7 ^a | 55.6 ± 7.2 ^a | 63.5 ± 6.1 ^a |
| Liver | | | | | |
| Weight (g) | | 0.8 ± 0.0 ^a | 0.8 ± 0.0 ^{ab} | 0.7 ± 0.0 ^b | 0.8 ± 0.0 ^{ab} |
| TBARS (nmol/mg protein) | | 1.4 ± 0.3 ^b | 3.8 ± 0.3 ^a | 4.5 ± 0.3 ^a | 4.2 ± 0.3 ^a |
| Total lipid (µg/mg protein) | | 490.5 ± 46.5 ^a | 539.3 ± 15.8 ^a | 393.2 ± 52.1 ^a | 460.1 ± 29.4 ^a |
| Phospholipid (nmol/mg protein) | | 294.1 ± 17.1 ^a | 283.1 ± 12.9 ^a | 289.9 ± 12.7 ^a | 272.1 ± 7.4 ^a |
| Total cholesterol (µg/mg protein) | | 10.7 ± 0.9 ^{ab} | 12.0 ± 0.8 ^a | 10.2 ± 0.7 ^{ab} | 8.6 ± 0.7 ^b |
| Plasma | | | | | |
| Phospholipid (nmol/mL) | | 389.4 ± 51.8 ^a | 567.1 ± 56.1 ^a | 509.5 ± 82.0 ^a | 544.3 ± 47.1 ^a |

Mean ± SEM, $n = 8$. Different letters indicate significant difference at $P < 0.05$ determined by ANOVA (Tukey's test).

2.4.5. Dietary PE Inhibits AC Development and Suppresses ACF Formation

To demonstrate the effect of dietary EtnGpl on ACF, we scored AC that formed in the colon depending on crypt multiplicity. Normal colon epithelial cells shown represent the blank group (Figure 2.4a). DMH treatment in the control group significantly increased the number of ACs at all stages compared to that of the blank group (Figure 2.4b, $P < 0.05$). We observed a significant inhibition of AC 1 in porcine liver and ascidian muscle groups compared with the control group ($P < 0.05$), while AC 2 and 3 in ascidian muscle group showed reduced AC formation compared with the control group. Moreover, total ACF formation was significantly suppressed in the dietary EtnGpl groups compared to that of the control group ($P < 0.05$).



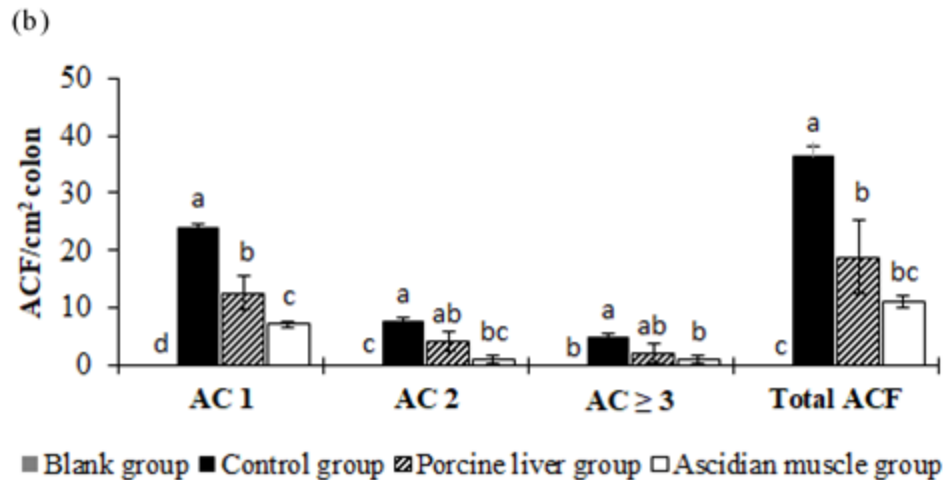


Figure 2.4 Effect of dietary EtnGpl on ACF formation in 1,2-DMH-treated mice.

(a) Histology of aberrant crypt foci (ACF) showing different number of crypts; normal colon, 1 crypt (AC1), 2 crypts (AC2), and 3 crypts (AC3). Methylene blue staining ($\times 100$). Scale bar indicates 50 μm for normal colon and 200 μm for AC1, AC2, and AC3. (b) Dietary EtnGpl inhibits AC development and suppresses ACF formation in 1,2-DMH-treated mice. Means \pm SEM, $n = 4$. Different letters indicate significant difference at $P < 0.05$ determined by ANOVA (Tukey's test).

2.4.6. Dietary EtnGpl Reduces the Levels of Apoptosis Related Proteins and TNF- α

After 10 weeks of treatment, we evaluated the levels of apoptosis-related proteins (i.e., death receptors, catalase antioxidant enzyme, and TNF- α ligand) in the colon mucosa (Figure 2.5). Regarding the levels of apoptosis-related proteins, DMH treatment in the control group significantly increased relative levels of Bcl-x and caspase-3 and significantly lowered the relative levels of Bcl-2 and XIAP compared with the blank group ($P < 0.05$). Furthermore, the level of cleaved caspase-3 and catalase were significantly higher in the control group than the blank group. Dietary EtnGpl showed a decrease in the relative levels of apoptosis-related proteins when compared to those of the control group. Furthermore, dietary ascidian muscle EtnGpl significantly suppressed the relative expression of all the proteins examined ($P < 0.05$). Importantly, the ratio of pro- and anti-apoptosis Bcl-2 family proteins (Bad vs. Bcl-2, Bcl-x and MCL-1) in the blank, control, porcine liver, and ascidian muscle groups were relatively the same: at 0.6, 0.5, 0.5, and 0.6, respectively. Moreover, DMH treatment increased the relative levels of TNF- α in the control group compared with those of the blank group. The DMH-induced TNF- α relative expression in the colon mucosa was significantly suppressed by dietary ascidian muscle EtnGpl ($P < 0.05$).

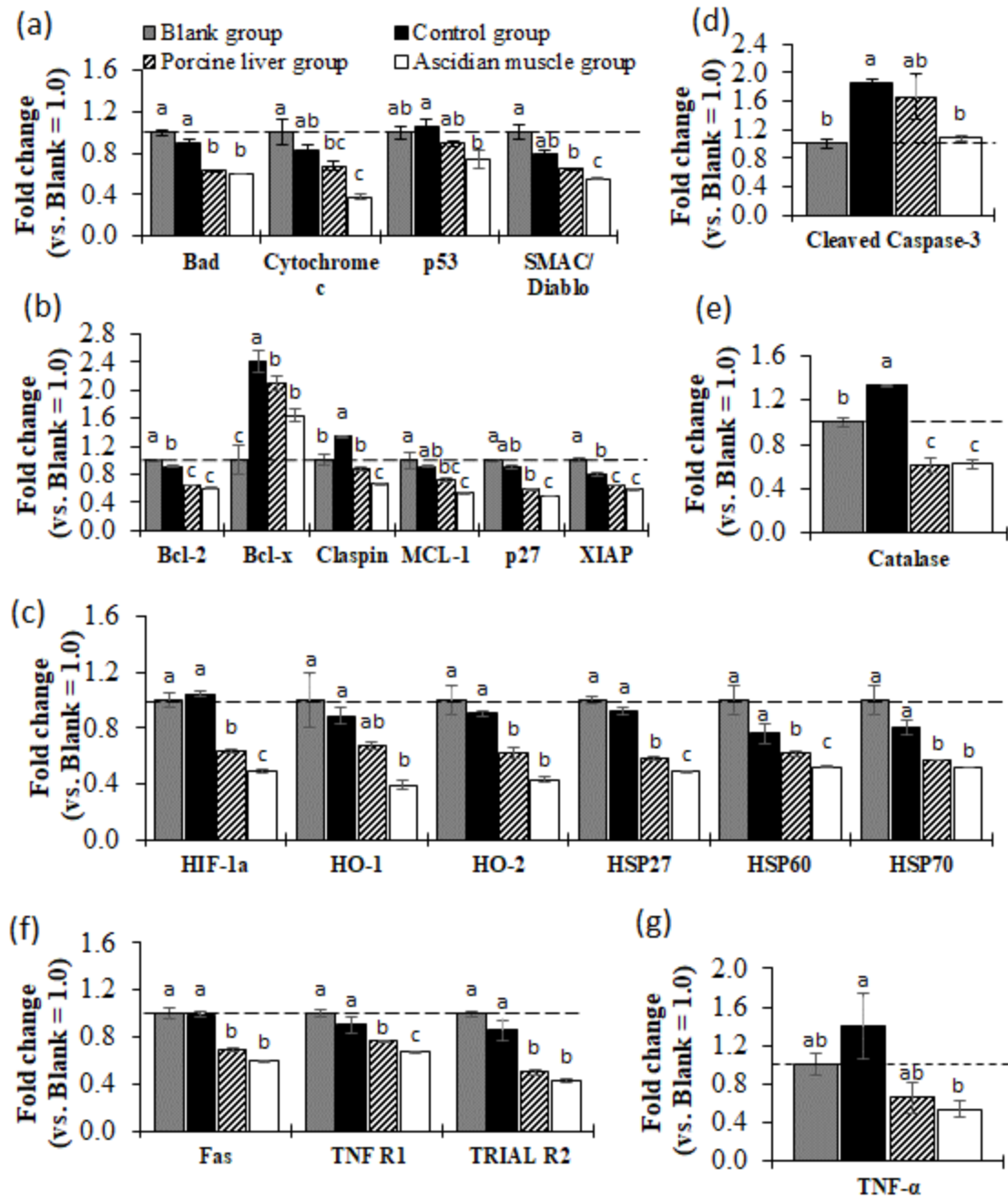


Figure 2.5 Dietary EtnGpl suppresses the induction of apoptosis and related downstream death signaling cascade in colon epithelial cells of 1,2-DMH-treated mice (fold change vs. blank).

(a) Pro-apoptosis proteins. (b) Anti-apoptosis proteins. (c) Other apoptosis related proteins. (d) Cysteine protease. (e) Anti-oxidant enzyme. (f) Death receptors. (g) TNF- α death ligand. The dashed line indicates the Blank group = 1.0. Different letters indicated significant differences at $P < 0.05$ determined by ANOVA (Tukey's test)

2.4.7. Alteration of Phospholipid Species in the Plasma, Liver, and Colon Mucosa

After 10 weeks of treatment, DMH administration in the control group led to a reduction in PlsEtn-18:0/18:1, PlsEtn-18:0/22:6, PlsCho-18:0/20:4 and PlsCho-18:0/22:6 levels in the plasma compared with the blank group (Table 2.6). Notably, dietary EtnGpl, particularly ascidian muscle EtnGpl, significantly increased all phospholipid species that were decreased by DMH administration.

Table 2.6 Phospholipid species level (nmol/mL) in plasma after 10 weeks of treatments

| Group | Blank | Control | Porcine liver | Ascidian muscle |
|------------------------------|-------------------------|-------------------------|-------------------------|-------------------------|
| i.p. DMH | - | + | + | + |
| Species (<i>sn-1/sn-2</i>) | | | | |
| PlsEtn (nmol/mL plasma) | | | | |
| 18:0/18:1 | 0.1 ± 0.0 ^{ab} | 0.1 ± 0.0 ^b | 0.1 ± 0.0 ^{ab} | 0.1 ± 0.0 ^a |
| 18:0/20:4 | 0.9 ± 0.1 ^a | 0.7 ± 0.1 ^a | 0.9 ± 0.1 ^a | 1.2 ± 0.2 ^a |
| 18:0/20:5 | Traces ^b | 0.1 ± 0.0 ^b | 0.1 ± 0.0 ^b | 0.2 ± 0.0 ^a |
| 18:0/22:6 | 1.8 ± 0.2 ^{ab} | 1.2 ± 0.1 ^b | 1.2 ± 0.1 ^{ab} | 1.8 ± 0.2 ^a |
| PlsCho (nmol/mL plasma) | | | | |
| 18:0/18:1 | Traces ^a | Traces ^a | Traces ^a | Traces ^a |
| 18:0/20:4 | 0.4 ± 0.0 ^a | 0.2 ± 0.0 ^b | 0.2 ± 0.0 ^b | 0.4 ± 0.0 ^a |
| 18:0/22:6 | 1.3 ± 0.1 ^a | 0.5 ± 0.1 ^c | 0.4 ± 0.1 ^c | 0.9 ± 0.1 ^b |
| PtdEtn (nmol/mL plasma) | | | | |
| 18:0/18:1 | 0.1 ± 0.0 ^a | 0.2 ± 0.0 ^a | 0.2 ± 0.0 ^a | 0.1 ± 0.0 ^a |
| 18:0/20:4 | 5.2 ± 0.8 ^a | 6.7 ± 0.8 ^a | 5.8 ± 0.5 ^a | 6.1 ± 0.8 ^a |
| 18:0/22:6 | 2.9 ± 0.5 ^a | 3.9 ± 0.5 ^a | 2.7 ± 0.3 ^a | 3.4 ± 0.4 ^a |
| PtdCho (nmol/mL plasma) | | | | |
| 18:0/18:1 | 14.0 ± 1.2 ^a | 17.9 ± 1.1 ^a | 16.0 ± 1.0 ^a | 16.8 ± 1.6 ^a |
| 18:0/20:4 | 81.6 ± 6.1 ^a | 65.1 ± 5.1 ^a | 63.2 ± 8.5 ^a | 59.5 ± 3.8 ^a |
| 18:0/22:6 | 38.5 ± 3.3 ^a | 33.3 ± 1.8 ^a | 30.6 ± 4.3 ^a | 33.6 ± 2.3 ^a |
| LysoPlsEtn (nmol/mL plasma) | | | | |
| 16:0 | 0.1 ± 0.0 ^a |
| 18:0 | 0.1 ± 0.0 ^a |
| LysoPlsCho (nmol/mL plasma) | | | | |
| 16:0 | 0.1 ± 0.0 ^a |

| | | | | |
|-----------------------------|-------------------------|-------------------------|-------------------------|-------------------------|
| 18:0 | Traces ^a | Traces ^b | Traces ^{ab} | Traces ^{ab} |
| LysoPtdEtn (nmol/mL plasma) | | | | |
| 16:0 | 1.9 ± 0.3 ^a | 1.7 ± 0.1 ^a | 1.7 ± 0.1 ^a | 1.7 ± 0.2 ^a |
| 18:0 | 1.2 ± 0.2 ^a | 1.2 ± 0.1 ^a | 1.3 ± 0.1 ^a | 1.3 ± 0.1 ^a |
| LysoPtdCho (nmol/mL plasma) | | | | |
| 16:0 | 58.5 ± 6.2 ^a | 52.9 ± 5.1 ^a | 51.7 ± 4.3 ^a | 50.4 ± 5.6 ^a |
| 17:0 | 2.5 ± 0.3 ^a | 2.4 ± 0.3 ^a | 2.1 ± 0.2 ^a | 2.1 ± 0.3 ^a |
| 18:0 | 25.5 ± 3.3 ^a | 24.1 ± 2.8 ^a | 23.6 ± 2.3 ^a | 23.8 ± 2.9 ^a |

Mean ± SEM, $n = 8$. Different letters indicate significant difference at $P < 0.05$ determined by ANOVA (Tukey's test).

In the liver tissue, DMH treatment in the control group lowered PlsCho-18:0/20:4, PlsCho-18:0/22:6 and PtdCho-18:0/20:4, while PtdEtn-18:0/18:1 and PtdEtn-18:0/18:1 were increased in comparison with the blank group (Table 2.7). The DMH-induced increases in liver phospholipid species were lowered by dietary ascidian muscle EtnGpl.

Table 2.7 Phospholipid species level (pmol/mg protein) in liver after 10 weeks of treatments

| Group | Blank | Control | Porcine liver | Ascidian muscle |
|------------------------------|---------------------------|---------------------------|---------------------------|---------------------------|
| i.p. DMH | - | + | + | + |
| Species (<i>sn-1/sn-2</i>) | | | | |
| PlsEtn (pmol/mg protein) | | | | |
| 18:0/18:1 | 5.4 ± 0.4 ^a | 6.2 ± 0.6 ^a | 6.2 ± 0.6 ^a | 5.8 ± 0.6 ^a |
| 18:0/20:4 | 270.9 ± 23.9 ^a | 212.8 ± 25.6 ^a | 263.5 ± 24.0 ^a | 192.4 ± 19.4 ^a |
| 18:0/20:5 | 7.0 ± 0.7 ^a | 9.0 ± 2.0 ^a | 7.4 ± 1.1 ^a | 9.9 ± 0.8 ^a |
| 18:0/22:6 | 301.9 ± 24.3 ^a | 235.5 ± 24.5 ^a | 239.2 ± 18.3 ^a | 221.1 ± 17.9 ^a |
| PlsCho (pmol/mg protein) | | | | |
| 18:0/18:1 | 0.2 ± 0.0 ^a | 0.2 ± 0.0 ^a | 0.1 ± 0.0 ^a | 0.2 ± 0.0 ^a |
| 18:0/20:4 | 8.4 ± 0.7 ^a | 3.2 ± 0.2 ^b | 3.5 ± 0.3 ^b | 4.6 ± 0.6 ^b |
| 18:0/22:6 | 20.4 ± 1.8 ^a | 7.8 ± 1.0 ^b | 7.5 ± 0.6 ^b | 12.3 ± 1.4 ^b |
| PtdEtn (pmol/mg protein) | | | | |
| 18:0/18:1 | 161.5 ± 12.1 ^b | 232.0 ± 18.7 ^a | 254.3 ± 18.7 ^a | 159.7 ± 19.1 ^b |

| | | | | |
|------------------------------|-----------------------------|-----------------------------|-----------------------------|-----------------------------|
| 18:0/20:4 | 4828.3 ± 224.4 ^a | 4142.6 ± 388.9 ^a | 4220.5 ± 272.0 ^a | 4648.2 ± 402.8 ^a |
| 18:0/22:6 | 5102.9 ± 308.7 ^a | 5393.6 ± 414.9 ^a | 5261.2 ± 292.5 ^a | 4511.9 ± 365.3 ^a |
| PtdCho (pmol/mg protein) | | | | |
| 18:0/18:1 | 720.7 ± 63.9 ^{ab} | 887.6 ± 64.1 ^a | 856.8 ± 60.3 ^a | 611.4 ± 64.6 ^b |
| 18:0/20:4 | 3561.9 ± 222.2 ^a | 2472.6 ± 202.8 ^b | 2575.7 ± 180.0 ^b | 2692.6 ± 269.7 ^b |
| 18:0/22:6 | 1569.1 ± 83.2 ^a | 1382.6 ± 91.9 ^a | 1291.5 ± 89.1 ^a | 1552.4 ± 135.7 ^a |
| LysoPlsEtn (pmol/mg protein) | | | | |
| 16:0 | 7.8 ± 1.4 ^a | 6.7 ± 0.5 ^a | 6.7 ± 0.5 ^a | 10.2 ± 3.7 ^a |
| 18:0 | 15.3 ± 3.9 ^a | 10.4 ± 2.5 ^a | 10.4 ± 2.5 ^a | 48.5 ± 39.4 ^a |
| LysoPlsCho (pmol/mg protein) | | | | |
| 16:0 | 0.2 ± 0.0 ^a | 0.2 ± 0.0 ^a | 0.2 ± 0.0 ^a | 0.2 ± 0.1 ^a |
| 18:0 | nd | nd | nd | nd |
| LysoPtdEtn (pmol/mg protein) | | | | |
| 16:0 | 409.0 ± 66.4 ^a | 331.3 ± 34.6 ^a | 332.6 ± 33.1 ^a | 459.7 ± 107.2 ^a |
| 18:0 | 557.1 ± 107.1 ^a | 525.0 ± 56.4 ^a | 531.4 ± 56.8 ^a | 489.2 ± 114.5 ^a |
| LysoPtdCho (pmol/mg protein) | | | | |
| 16:0 | 7.8 ± 1.7 ^a | 5.6 ± 0.7 ^a | 7.6 ± 0.9 ^a | 7.3 ± 1.9 ^a |
| 17:0 | 185.9 ± 43.8 ^a | 134.0 ± 16.5 ^a | 185.2 ± 20.3 ^a | 180.6 ± 42.3 ^a |
| 18:0 | 121.0 ± 28.1 ^a | 96.1 ± 10.8 ^a | 128.0 ± 14.9 ^a | 102.2 ± 21.7 ^a |

Mean ± SEM, $n = 8$. Different letters indicate significant difference at $P < 0.05$ determined by ANOVA (Tukey's test).

In the colon mucosa, induction of colon carcinogenesis in the control group resulted in lower levels of PlsEtn-18:0/18:1, PlsEtn-18:0/20:4, PlsCho-18:0/18:1, PlsCho-18:0/20:4), PtdEtn-18:0/18:1, PtdCho-18:0/18:1, and PtdCho-18:0/20:4 compared with those of the blank group (Table 2.8). On the other hand, dietary EtnGpl increased all phospholipid species that were decreased by DHM administration as well as PlsEtn-18:0/20:5 and lysoPtdEtn-16:0. Importantly, ascidian muscle EtnGpl led to an increase in the aforementioned phospholipid species in comparison with porcine liver EtnGpl.

Table 2.8 Phospholipid species level (pmol/mg protein) in colon mucosa after 10 weeks of treatments

| | Group | Blank | Control | Porcine liver | Ascidian muscle |
|------------------------------|----------|-------|---------|---------------|-----------------|
| | i.p. DMH | - | + | + | + |
| Species (<i>sn-1/sn-2</i>) | | | | | |

| | | | | |
|----------------------------------|----------------------------|---------------------------|----------------------------|----------------------------|
| PlsEtn (pmol/mg protein) | | | | |
| 18:0/18:1 | 53.6 ± 6.4 ^{ab} | 39.6 ± 8.3 ^b | 62.0 ± 4.3 ^{ab} | 91.6 ± 16.9 ^a |
| 18:0/20:4 | 158.8 ± 12.0 ^a | 96.5 ± 16.6 ^b | 142.5 ± 23.7 ^a | 221.3 ± 45.4 ^a |
| 18:0/20:5 | 20.7 ± 2.8 ^b | 21.0 ± 4.8 ^b | 36.2 ± 5.6 ^{ab} | 39.6 ± 3.4 ^a |
| 18:0/22:6 | 76.8 ± 5.0 ^a | 63.1 ± 10.0 ^a | 85.4 ± 10.5 ^a | 125.6 ± 27.6 ^a |
| PlsCho (pmol/mg protein) | | | | |
| 18:0/18:1 | 3.7 ± 0.1 ^{ab} | 2.1 ± 0.4 ^b | 3.5 ± 0.2 ^{ab} | 4.7 ± 1.0 ^a |
| 18:0/20:4 | 7.8 ± 0.9 ^{ab} | 4.8 ± 1.0 ^b | 6.7 ± 0.4 ^{ab} | 9.9 ± 1.9 ^a |
| 18:0/22:6 | 4.2 ± 0.3 ^a | 3.4 ± 0.6 ^a | 4.4 ± 0.5 ^a | 5.9 ± 0.9 ^a |
| PtdEtn species (pmol/mg protein) | | | | |
| 18:0/18:1 | 289.2 ± 22.3 ^{ab} | 170.9 ± 35.6 ^b | 263.9 ± 31.7 ^{ab} | 375.8 ± 74.8 ^a |
| 18:0/20:4 | 472.4 ± 76.3 ^a | 276.0 ± 53.8 ^a | 343.4 ± 53.8 ^a | 598.3 ± 134.6 ^a |
| 18:0/22:6 | 122.1 ± 10.8 ^a | 98.5 ± 14.9 ^a | 111.6 ± 17.2 ^a | 186.2 ± 41.0 ^a |
| PtdCho (pmol/mg protein) | | | | |
| 18:0/18:1 | 173.8 ± 12.2 ^{ab} | 131.2 ± 18.8 ^b | 186.7 ± 12.4 ^{ab} | 264.6 ± 47.3 ^a |
| 18:0/20:4 | 264.5 ± 24.2 ^{ab} | 181.5 ± 34.2 ^b | 210.0 ± 18.5 ^{ab} | 348.3 ± 62.1 ^a |
| 18:0/22:6 | 34.2 ± 3.7 ^a | 30.5 ± 4.6 ^a | 35.4 ± 3.0 ^a | 52.1 ± 10.3 ^a |
| LysoPlsEtn (pmol/mg protein) | | | | |
| 16:0 | 39.1 ± 4.1 ^a | 40.4 ± 9.7 ^a | 94.0 ± 15.8 ^a | 115.5 ± 32.3 ^a |
| 18:0 | 26.0 ± 2.6 ^a | 27.7 ± 6.0 ^a | 73.1 ± 14.4 ^a | 76.7 ± 19.9 ^a |
| LysoPlsCho (pmol/mg protein) | | | | |
| 16:0 | 7.9 ± 1.7 ^a | 7.6 ± 2.4 ^a | 15.1 ± 2.7 ^a | 21.0 ± 6.5 ^a |
| 18:0 | 0.7 ± 0.2 ^a | 0.9 ± 0.3 ^a | 1.8 ± 0.4 ^a | 2.3 ± 0.7 ^a |
| LysoPtdEtn (pmol/mg protein) | | | | |
| 16:0 | 26.2 ± 1.5 ^b | 37.7 ± 12.6 ^b | 49.2 ± 2.1 ^{ab} | 86.9 ± 29.2 ^a |
| 18:0 | 78.9 ± 7.0 ^a | 81.7 ± 14.0 ^a | 175.6 ± 22.9 ^a | 222.2 ± 53.5 ^a |
| LysoPtdCho (pmol/mg protein) | | | | |
| 16:0 | 143.7 ± 4.9 ^a | 163.3 ± 55.0 ^a | 249.6 ± 14.6 ^a | 367.2 ± 105.6 ^a |
| 17:0 | 9.0 ± 0.6 ^a | 7.9 ± 2.5 ^a | 13.5 ± 0.8 ^a | 18.8 ± 5.1 ^a |
| 18:0 | 78.2 ± 3.6 ^a | 81.9 ± 19.9 ^a | 147.4 ± 11.3 ^a | 192.8 ± 52.8 ^a |

Mean \pm SEM, $n = 4$. Different letters indicate significant difference at $P < 0.05$ determined by ANOVA (Tukey's test).

2.4.8. Alteration of Acyl and Alkenyl Chains Composition in the Plasma, Liver, and Colon Mucosa

After 10 weeks of dietary EtnGpl administration, acyl and alkenyl chains in the phospholipid fractions of mice liver, plasma, and colon mucosa were analyzed. In the plasma, administration of DMH in the control group did not alter the composition of acyl and alkenyl chains except for an 18:2n-6 increase, compared to the blank group (Table 2.9). Similarly, supplementation with dietary EtnGpl in DHM-treated groups did not alter acyl and alkenyl chains compared to the control group.

Table 2.9 Composition of acyl and alkenyl chains (mol%) in plasma phospholipid fraction after 10 weeks of treatments

| Group | Blank | Control | Porcine liver | Ascidian muscle |
|----------------|-----------------------------|-----------------------------|-----------------------------|-----------------------------|
| i.p. DMH | - | + | + | + |
| Acyl (mol%) | | | | |
| 16:0 | 31.0 \pm 1.8 ^a | 28.1 \pm 0.9 ^a | 31.5 \pm 1.5 ^a | 27.8 \pm 0.9 ^a |
| 18:0 | 15.6 \pm 1.5 ^a | 14.0 \pm 0.7 ^a | 18.7 \pm 2.5 ^a | 13.1 \pm 0.4 ^a |
| 18:1n-9 | 12.8 \pm 1.2 ^a | 15.4 \pm 1.0 ^a | 13.7 \pm 1.0 ^a | 14.7 \pm 0.4 ^a |
| 18:2n-6 | 16.4 \pm 1.6 ^b | 21.4 \pm 0.7 ^a | 17.5 \pm 1.3 ^a | 21.0 \pm 0.8 ^a |
| 18:3n-3 | 0.8 \pm 0.1 ^a | 0.7 \pm 0.1 ^a | 1.0 \pm 0.2 ^a | 0.7 \pm 0.1 ^a |
| 20:4n-6 | 9.9 \pm 1.3 ^a | 8.0 \pm 0.5 ^a | 7.4 \pm 0.6 ^a | 7.8 \pm 0.3 ^a |
| 20:5n-3 | 1.3 \pm 0.6 ^a | 0.9 \pm 0.3 ^a | 0.7 \pm 0.6 ^a | 2.2 \pm 0.9 ^a |
| 22:5n-3 | 0.6 \pm 0.1 ^a | 0.4 \pm 0.1 ^a | 0.5 \pm 0.2 ^a | 0.4 \pm 0.0 ^a |
| 22:6n-3 | 5.5 \pm 0.7 ^a | 5.0 \pm 0.4 ^a | 4.3 \pm 0.5 ^a | 5.4 \pm 0.4 ^a |
| n-3/n-6 | 0.3 \pm 0.0 ^a |
| (EPA+DHA)/ARA | 0.7 \pm 0.1 ^a | 0.7 \pm 0.1 ^a | 0.7 \pm 0.1 ^a | 1.0 \pm 0.1 ^a |
| Alkenyl (mol%) | | | | |
| 16:0ol | 0.1 \pm 0.0 ^a | 0.1 \pm 0.1 ^a | 0.1 \pm 0.0 ^a | 0.1 \pm 0.0 ^a |
| 18:0ol | 0.7 \pm 0.7 ^a | 0.4 \pm 0.1 ^a | 0.4 \pm 0.1 ^a | 0.6 \pm 0.1 ^a |
| 18:1ol | Traces | nd | nd | nd |
| Total | 0.8 \pm 0.4 ^a | 0.5 \pm 0.1 ^a | 0.6 \pm 0.2 ^a | 0.7 \pm 0.2 ^a |

Mean \pm SEM, $n=8$

In the liver, DMH treatment in the control, porcine liver and ascidian muscle groups altered acyl chain compositions (Table 2.10). Notably, DMH treatment in the control group significantly lowered the 18:0ol alkenyl chain ratio and total plasmalogens (alkenyls) compared with the blank group. The observed decrease in 18:0ol and total alkenyls was improved by dietary EtnGpl, with ascidian muscle group, showing a significant increase compared to porcine liver group ($P < 0.05$)

Table 2.10 Composition of acyl and alkenyl chains (mol%) in liver phospholipid fraction after 10 weeks of treatments

| Group | Blank | Control | Porcine liver | Ascidian muscle |
|----------------|-------------------------|--------------------------|--------------------------|-------------------------|
| i.p. DMH | - | + | + | + |
| Acyl (mol%) | | | | |
| 16:0 | 29.5 ± 1.1 ^a | 27.5 ± 0.3 ^b | 26.9 ± 0.3 ^b | 27.0 ± 0.4 ^b |
| 18:0 | 16.1 ± 1.1 ^b | 17.1 ± 0.1 ^a | 17.3 ± 0.2 ^a | 17.3 ± 0.1 ^a |
| 18:1n-9 | 8.2 ± 2.2 ^a | 9.1 ± 0.2 ^b | 8.8 ± 0.1 ^{ab} | 8.8 ± 0.1 ^{ab} |
| 18:2n-6 | 14.0 ± 0.4 ^c | 15.5 ± 0.2 ^{ab} | 14.7 ± 0.1 ^{bc} | 15.6 ± 0.2 ^a |
| 18:3n-3 | 0.3 ± 0.0 ^a | 0.3 ± 0.0 ^{ab} | 0.2 ± 0.0 ^c | 0.2 ± 0.0 ^{bc} |
| 20:4n-6 | 12.5 ± 1.6 ^a | 10.3 ± 0.3 ^b | 11.5 ± 0.1 ^a | 10.5 ± 0.3 ^b |
| 20:5n-3 | 0.3 ± 0.0 ^b | 0.5 ± 0.1 ^a | 0.5 ± 0.0 ^a | 0.6 ± 0.0 ^a |
| 22:5n-3 | 0.3 ± 0.0 ^c | 0.4 ± 0.0 ^b | 0.5 ± 0.0 ^{ab} | 0.5 ± 0.0 ^a |
| 22:6n-3 | 15.9 ± 1.8 ^a | 15.7 ± 0.3 ^a | 16.1 ± 0.2 ^a | 15.6 ± 0.2 ^a |
| n-3/n-6 | 0.6 ± 0.1 ^a | 0.6 ± 0.0 ^a | 0.6 ± 0.0 ^a | 0.6 ± 0.0 ^a |
| (EPA+DHA)/ARA | 1.3 ± 1.3 ^b | 1.6 ± 0.1 ^a | 1.4 ± 0.0 ^{ab} | 1.5 ± 0.0 ^{ab} |
| Alkenyl (mol%) | | | | |
| 16:0ol | Traces ^a | Traces ^a | Traces ^a | Traces ^a |
| 18:0ol | 0.3 ± 0.0 ^a | 0.2 ± 0.0 ^b | 0.3 ± 0.0 ^{ab} | 0.3 ± 0.0 ^a |
| 18:1ol | nd | nd | nd | nd |
| Total | 0.3 ± 0.0 ^b | 0.2 ± 0.0 ^c | 0.3 ± 0.0 ^{bc} | 0.4 ± 0.0 ^a |

Mean ± SEM, n=8

In the colon mucosa, administration of DMH in the control group did not alter the composition of acyl and alkenyl chains except for an 18:2n-6 increase, compared to the blank group (Table 2.11). Similarly, supplementation with dietary EtnGpl in DHM-treated groups did not alter acyl and alkenyl chains compared to the control group.

Table 2.11 Composition of acyl and alkenyl chains (mol%) in colon mucosa phospholipid fraction after 10 weeks of treatments

| Group | Blank | Control | Porcine liver | Ascidian muscle |
|-----------------|-------------------------|-------------------------|-------------------------|-------------------------|
| i.p. DMH | - | + | + | + |
| Acyl (mol%) | | | | |
| 16:0 | 28.9 ± 1.9 ^a | 29.1 ± 0.8 ^a | 33.2 ± 2.3 ^a | 40.7 ± 5.3 ^a |
| 18:0 | 10.3 ± 1.8 ^a | 9.1 ± 1.2 ^a | 14.7 ± 1.8 ^a | 16.1 ± 3.8 ^a |
| 18:1n-9 | 27.9 ± 2.1 ^a | 30.3 ± 1.5 ^a | 23.8 ± 2.7 ^a | 18.7 ± 5.1 ^a |
| 18:2n-6 | 18.2 ± 1.9 ^a | 17.1 ± 0.9 ^a | 12.5 ± 1.5 ^a | 10.5 ± 3.8 ^a |
| 18:3n-3 | 0.8 ± 0.2 ^a | 0.9 ± 0.1 ^a | 0.5 ± 0.2 ^a | 0.5 ± 0.2 ^a |
| 20:4n-6 | 1.3 ± 0.5 ^a | 0.9 ± 0.2 ^a | 2.8 ± 1.0 ^a | 1.9 ± 0.5 ^a |
| 20:5n-3 | 1.4 ± 1.1 ^a | 0.2 ± 0.1 ^a | 0.3 ± 0.1 ^a | 0.5 ± 0.2 ^a |
| 22:5n-3 | 0.4 ± 0.1 ^a | 0.4 ± 0.1 ^a | 0.7 ± 0.1 ^a | 1.1 ± 0.4 ^a |
| 22:6n-3 | 0.9 ± 0.0 ^a | 1.0 ± 0.2 ^a | 1.2 ± 0.1 ^a | 1.4 ± 0.3 ^a |
| n-3/n-6 | 0.2 ± 0.1 ^a | 0.2 ± 0.0 ^a | 0.2 ± 0.0 ^a | 0.7 ± 0.4 ^a |
| (EPA + DHA)/ARA | 4.2 ± 3.3 ^a | 1.4 ± 0.4 ^a | 0.7 ± 0.2 ^a | 1.6 ± 0.8 ^a |
| Alkenyl (mol%) | | | | |
| 16:0ol | 0.3 ± 0.2 ^a | nd | nd | Traces ^a |
| 18:0ol | 0.6 ± 0.2 ^a | 0.5 ± 0.2 ^a | 1.0 ± 0.0 ^a | 1.1 ± 0.4 ^a |
| 18:1ol | nd | nd | nd | 0.1 ± 0.1 ^a |
| Total | 0.8 ± 0.4 ^a | 0.5 ± 0.2 ^a | 1.0 ± 0.2 ^a | 1.3 ± 0.5 ^a |

Mean ± SEM, n=4

2.5. DISCUSSION

Levels of PlsEtn and its related species are lower in inflamed colon mucosa and dysregulated in adenomatous polyps (Fan et al., 2015; Lopez et al., 2018). Furthermore, dietary fat can alter colon mucosal lipids, and many studies have provided evidence of a strong correlation between colon cancer and dietary factors, especially dietary fat (Yusof et al., 2012; Sakita et al., 2017; Castelló et al., 2019). The onset and progression of colon cancer associates chronic colon inflammation and oxidative stress (Coussens and Werb, 2002). Therefore, dietary PlsEtn may be used as a therapy for intestinal disorders. Here, we show that EtnGpl derived from dietary sources with high and low PlsEtn ratios suppress the formation of ACF, which are regarded as pre-cancerous lesions in the colon. To advance our understanding on the possible underlying mechanisms of this, we

determined the effects of dietary EtnGpl diets with differing PlsEtn ratios and same n-3/n-6 ratios on DMH-induced oxidative damage, apoptosis-related proteins, and TNF- α in the colon mucosa. We further determined the alterations of acyl and alkenyl chains and phospholipid species in mouse tissues. We demonstrated, for the first time, that dietary PlsEtn and its molecular species, especially from marine invertebrates, have the potential to improve impaired intestinal mucosa *in vivo* by inhibiting inflammatory and oxidative stress leading to suppression of ACF and apoptosis.

In the present study, DMH treatment in the control group increased not only colon ACF formation but also levels of TBARS, an index of lipid peroxidation, in the liver and colon mucosa ([Figure 2.4](#) and [Table 2.5](#)). In addition, DMH treatment increased the levels of TNF- α , several anti-apoptosis proteins, cleaved caspase 3, and catalase in the colon mucosa ([Figure 2.5](#)). DMH is metabolically activated into the highly reactive methyl diazonium ion in the liver and is either transported into the colon through excretion into the bile or directly from blood circulation (Fiala and Stathopoulos, 1984). Intraperitoneal administration of DMH has been shown to induce inflammatory and oxidative stress as well as ACF formation (Moulaoui et al., 2018; Yamashita et al., 2019). Colon cancer can be induced by dedifferentiation-associated epigenetic regulations by chronic inflammation (Bartsch and Nair, 2006). Moreover, carcinogenic metabolites of DMH in a mouse model have been implicated in the methylation of DNA bases in proliferative compartments of crypts in colon epithelial cells, which lead to elevated apoptotic levels, preventing restoration of homeostasis (Perše and Cerar, 2011).

Ingestion of dietary EtnGpl inhibited AC development and suppressed total DMH-induced ACF formation compared to the control group ([Figure 2.4](#)). Ascidian muscle EtnGpl diet with a high concentration of PlsEtn and a porcine liver EtnGpl diet with a low concentration of PlsEtn suppressed total ACF by 69% and 48%, respectively, compared to the control diet that had the same ratio of n-3/n-6 to the EtnGpl diets. Since the addition of fish oil resulted in attaining similar n-3/n-6 ratio among the three experimental diets ([Table 2.4](#)), our results reveal that the suppression of ACF formation in the colon might be dependent on the levels of PlsEtn in the diet. PlsEtn bearing EPA has been shown to significantly reduce neuro-inflammation compared with PtdEtn bearing EPA, which was attributed to the vinyl ether linkage in the *sn*-1 position (Che et al., 2018a). This could further indicate the specific effect of PlsEtn during the development of colon pathophysiology. To our knowledge, this study provides the first evidence on the beneficial effect of dietary PlsEtn in colon health and disease. Our study further provides evidence indicating that the food functionality of PlsEtn in the suppression of ACF may depend highly on the abundance of alkenyl linkages (vinyl ether linkages).

In this study, DMH administration in the control group increased the levels of TNF- α , apoptosis-related proteins, and TBARS in colon mucosa, which were subsequently suppressed by dietary EtnGpl, especially

ascidian muscle EtnGpl ([Figure 2.5](#) and [Table 2.5](#)). The balance of anti- and pro-apoptotic Bcl-2 family proteins determines the fate of cells (survival or death), and in our study, the ratio remained the same in all treatments. The role of TNF- α as a major mediator of inflammation and apoptosis is well documented. The majority of TNF- α biological activity is mediated by the death receptor TNFR1 while TNF- α levels during chronic colon inflammation are elevated (Hofmanová et al., 2014). This explains the inhibition of the TNFR1 and cleaved caspase-3 (ascidian muscle group > porcine liver group) in our study, which suggests suppression of the extrinsic apoptosis signaling cascade by dietary EtnGpl depended on the vinyl ether linkages in the *sn*-1 position. Furthermore, the inhibition of catalase activity by dietary EtnGpl indicates a decrease in colon inflammation, which suggests the suppression of oxidative stress. Indeed, patients suffering from oxidative stress i.e. cardiovascular disease, diabetes, tumor, inflammation, and anemia have increased catalase activity, which was suppressed by intake of Vitamin E supplement (Al-Abrash et al., 2000). Contrary results show that patients with inflammatory bowel disease (IBD) have decreased catalase activity compared to controls, however their superoxide dismutase and glutathione peroxidase anti-oxidant enzymes activity were increased and normalized during remission phase (Iborra et al., 2011). Overall, our results indicate that dietary PlsEtn has the potential to inhibit colon inflammation and oxidative stress depending on the abundance of vinyl ether linkages. Consequently, this leads to the inhibition of death receptor apoptosis pathways via suppression of TNF- α in the colon mucosa.

Induction of colon carcinogenesis by DMH reduced PlsEtn molecular species levels in colon mucosa compared with the blank group ([Table 2.8](#)). These results suggest that chemically induced colon carcinogenesis inhibits *de novo* synthesis of PlsEtn and/or that chronic inflammation consumes PlsEtn as a way of protecting cells. Dietary PlsEtn is hydrolyzed in the intestines by pancreatic phospholipase A2 (PLA2) into lysoPlsEtn and fatty acid (FA) from the *sn*-2 position. The lysoPlsEtn and FA micelles are absorbed into the enterocytes and through the Land's cycle, some are re-esterified into PlsEtn. The products then form chylomicrons, which are secreted into the lymphatic system and enter circulation (Zhang et al., 2019). Remarkably, dietary EtnGpl, especially ascidian muscle EtnGpl, increased the levels of PlsEtn, PlsCho, PtdCho, and lysoPtdEtn species in the colon mucosa. Contrary to our results, levels of PlsEtn and PlsCho in human malignant colonic tissues were found to be elevated compared with normal tissues, probably due to rapid cellular growth, which requires a higher amount of membrane phospholipids (Dueck et al., 1996). Rats fed with PlsEtn for one week had a significant increase in caecum PlsEtn levels and a slight increase in colon PlsEtn levels, which was similar to our results (Nishimukai et al., 2003). PtdEtn has a remarkable anti-oxidative effect at pH 7.0, which is a similar pH condition in the colon (Hara et al., 2000). The anti-oxidant effect of PlsEtn has been shown to degrade the vinyl ether linkages rapidly with a considerable delay in oxidation of PUFA double bonds in the *sn*-2 position,

which makes Pls a scavenger of peroxy radicals in biological membranes (Reiss et al., 1997; Hahnel et al., 1999). Therefore, the increase in the levels of colon mucosa PlsEtn species (ascidian muscle group > porcine liver group) in our study contributed to the resistance against oxidative stress and lipid peroxidation from DMH-induced carcinogenesis, hence a reduction in the intestinal impairment observed in the ascidian muscle and porcine liver groups compared to the control group (Figure 1B). Moreover, in the intestine, administrated PlsEtn is degraded into lysoPlsEtn and PUFA, and some of the lysoPlsEtn is preferentially re-esterified into PlsEtn-18:0/20:4, which was in agreement with our results (Nishimukai et al., 2011). In this study, the vinyl-ether linkages in undigested PlsEtn and the degraded lysoPlsEtn, which are known to have high anti-oxidative properties, and PUFA lipolysis from PlsEtn, that are thought to be metabolized into eicosanoids and docosanoids, offered protection to the colon mucosa during carcinogenesis (Yamashita et al., 2016a). Despite the alteration in tissue phospholipid species, the phospholipid content in DMH-treated groups was similar to that of the blank group. This indicates that the alteration of lipid profiles is a tissue compensatory response to maintain cellular phospholipid levels during a deficiency and/or surplus status. During RCDP disease, PtdEtn has been shown to compensate PlsEtn deficiency in order to maintain an optimal phospholipid composition (Dorninger et al., 2015).

Treatment with DMH in the control group increased liver's total cholesterol, while dietary ascidian muscle EtnGpl led to a concomitant decrease in total cholesterol, and with no effect on PlsEtn species compared to the control group (Table 2.5 and 2.8). However, dietary ascidian muscle EtnGpl restored the pool of Pls in the liver after DMH treatment. (Table 2.10). PlsEtn has also been reported to control cholesterol biosynthesis (Honscho et al., 2015), and that cholesterol is the source for bile acids in the liver. In this ACF model, bile acids carry carcinogens from the liver to the colon, and bile acids metabolized by intestinal bacteria lead to an accumulation of secondary bile acids, such as deoxycholic acid, which are carcinogens and are involved in the progression of colon cancer (Nagengast et al., 1995; Jia et al., 2018). Therefore, dietary PlsEtn may normalize liver lipid metabolism and protect the colon from ACF formation. Further *in vivo* and *in vitro* studies are required to understand the tissue-specific function of PlsEtn in detail and to clarify the relevant mechanisms surrounding it. Our study indicates the functional role of dietary PlsEtn during colon cancer initiation stage, therefore *in vitro* studies using human colon cancer cells may possibly help to elucidate the functional role of PlsEtn in colon cancerous tumors.

2.6. CONCLUSION

Ingestion of dietary EtnGpl, especially with high levels of PlsEtn suppressed ACF formation and colon mucosa apoptosis by inhibiting the apoptosis signaling pathway, and suppressing inflammation and oxidative stress by downregulating the activity of TNF- α in the colon mucosa. These results suggest that PlsEtn abundance

is potentially beneficial as a dietary therapy for pathological colon conditions such as chronic inflammation and cancer.

3. CHAPTER 3: ETHANOLAMINE PLASMALOGEN SUPPRESSES APOPTOSIS IN HUMAN INTESTINAL TRACT CELLS *IN VITRO* BY ATTENUATING INDUCED INFLAMMATORY STRESS

3.1. ABSTRACT

Ethanolamine plasmalogen (PlsEtn) is a subtype of ethanolamine glycerophospholipids (EtnGpl). Recently, PlsEtn has attracted increasing research interest due to its beneficial effects in health and disease; however, its functional role in colonic health has not been well established. This study was conducted to determine mechanism underlying the antiapoptotic effect of PlsEtn in human intestinal tract cells under induced inflammatory stress. Lipopolysaccharide (LPS) induced apoptosis of differentiated Caco-2 cells, which was suppressed by EtnGpl in a dose-dependent manner. Cells treated with ascidian muscle EtnGpl containing high levels of PlsEtn demonstrated a lower degree of apoptosis, and downregulated TNF- α and apoptosis-related proteins compared to those treated with porcine liver EtnGpl containing low PlsEtn. This indicates PlsEtn exerted the observed effects, which provided protection against induced inflammatory stress. Overall, our results suggest PlsEtn with abundant vinyl ether linkages is potentially beneficial in preventing the initiation of inflammatory bowel disease (IBD) and colon cancer.

3.2. INTRODUCTION

Ethanolamine plasmalogen (PlsEtn), a sub-class of ethanolamine glycerophospholipids (EtnGpl) is a universal phospholipid in mammalian membranes. PlsEtn contains a vinyl-ether (alkenyl) linkage at the *sn*-1 position, whereas at the *sn*-2 position, it is enriched with polyunsaturated fatty acids (PUFA) (Brites et al., 2004; Braverman and Moser, 2012). Marine sources such as sea squirt and mussel muscles are enriched with n-3 PUFA, notably docosahexaenoic acid (DHA, 22:6n-3) and eicosapentaenoic acid (EPA, 20:5n-3), while land sources such as pig and cattle muscles are enriched with n-6 PUFA arachidonic acid (ARA, 20:4n-6) at the *sn*-2 position (Yamashita et al., 2014b, 2016a). The vinyl ether linkage in PlsEtn has high oxidative potential, which enables the scavenging of free radicals and singlet oxygen, in addition to altering membrane properties (Brites et al., 2004; Braverman and Moser, 2012). Increased cellular levels of PlsEtn bearing n-3 PUFA have shown potential for the prevention of neurodegenerative disorders like Alzheimer's disease (Yamashita et al., 2017a). It has also been reported that PlsEtn is involved in the development of other diseases such as Parkinson's disease and atherosclerosis (Ding et al., 2020; Mawatari et al., 2020). Consequently, several researchers are currently interested in the association between colon carcinogenesis and PlsEtn levels.

Currently, colon cancer is a major health problem in both developed and developing nations. Worldwide, colon cancer ranks third in incidence and fourth in mortality rates among cancers (Bray et al., 2018). Chronic colon inflammation has been associated with an increased risk of colon cancer initiation and promotion (Bartsch and Nair, 2006). Chronic inflammation is associated with excessive colon cell death (apoptosis), and on the other hand, disturbed regulation of colon cell death, leading to uncontrolled growth of cells (resistance to apoptosis), contributes to colon cancer promotion (Yang et al., 2009; Hofmanová et al., 2014). Patients with chronic colon inflammation exhibit increased levels of pro-inflammatory cytokines such as interleukin (IL)-6, IL-1 β , IL-8, and TNF- α (Krzystek-korpacka et al., 2013). This inflammatory microenvironment facilitates crosstalk with infiltrating immune cells to create a pro-carcinogenic environment (Hofmanová et al., 2014).

It is well established that several endogenous regulatory molecules play a key role in regulating intestinal homeostasis, but their presence is significantly influenced by dietary compounds (Hofmanová et al., 2014). Dietary compounds come into direct contact with the colonic epithelium cells and may affect growth, differentiation, and cell death within the tissue (Hossain et al., 2009). In the recent past, research interest on benefits of PlsEtn in health and disease has increased (Braverman and Moser, 2012; Messias et al., 2018); however, its functional role in colonic health is not well established. [In Chapter 2 study](#), we have shown that diet with high PlsEtn level and same ratio of n-3/n-6 as diet with low PlsEtn level has higher suppression of aberrant crypt foci (ACF) formation and apoptosis compared to the diet with low PlsEtn level. The observed suppression was a consequence of higher down-regulation of pro-inflammatory mediator TNF- α and oxidative stress in 1,2-dimethylhydrazine (DMH)-treated mice (Nguma et al., 2020). This suggests that the abundance of dietary PlsEtn changed the colon epithelial microenvironment, and conferred a low susceptibility to carcinogenesis.

Based on our previous study, the aim of this study was to clarify the functional role of PlsEtn and the molecular mechanisms underlying its effects on colonic health. In this study, we investigated the effects of extrinsic PlsEtn from ascidian muscle and porcine liver EtnGpl on inflammatory-stressed differentiated Caco-2 cells as a human intestinal tract *in vitro* model, and the possible underlying mechanisms. Extrinsic EtnGpl from ascidian (*Holacynthis roretzi*) muscle contained a high PlsEtn ratio and high EPA and DHA while porcine liver EtnGpl contained low PlsEtn ratio and high ARA ([Chapter 2, Table 2.2](#)).

3.3. MATERIALS AND METHODS

3.3.1. Materials

Materials used in the cell culture experiment were purchased as follows: human colon carcinoma cell line Caco-2 from Riken Gene Bank (Tsukuba, Japan); Dulbecco's modified Eagle's medium (DMEM), trypsin-

EDTA ($\times 10$), and protease inhibitor cocktail for use with mammalian cell and tissue extracts from Sigma-Aldrich, Inc. (Missouri, MO, USA); lysis buffer 17 from R&D Systems (Minneapolis, MN, USA); phosphate-buffered saline (PBS) from Nissui (Tokyo, Japan); fetal bovine serum (FBS) from Biowest (Nuaille, France); penicillin-streptomycin-amphoteric B ($\times 100$), MEM non-essential amino acids ($\times 100$), lipopolysaccharide (LPS), and bovine serum albumin (BSA) fatty acid free from Fujifilm Wako Pure Chemical Corp. (Gunma, Osaka, Japan) and phospholipid species from Avanti Polar Lipids (Alabaster, AL, USA). PlsEtn-18:0/20:5 was purified according to our previously reported method (Yamashita et al., 2014b).

3.3.2. Ascidian muscle and porcine liver EtnGpl preparation

Purified ascidian muscle and porcine liver EtnGpl were prepared as previously described in our study (Yamashita et al., 2014b). Purified EtnGpl were dissolved in ethanol to a stock solution of 10 mM and diluted to 0.5% ethanol by adding to DMEM containing 0.1% BSA at time of use.

3.3.3. Cell culture

The human colon carcinoma cell line Caco-2 was cultured in DMEM supplemented with 10% heat-inactivated FBS (v/v), 1% penicillin-streptomycin-amphoteric B (v/v), and 1% non-essential amino acids (v/v) in an incubator at 37 °C and 5% CO₂ under humid conditions. Cells were continuously passaged at 1.5×10^6 cells/mL in 100-mm dishes every 3-4 days. Differentiated Caco-2 cells were obtained by seeding Caco-2 cells, and when they reached > 90 % confluence, they were designated as day 0 and incubated for 21 days to differentiate. In this study, differentiated Caco-2 cell medium was changed to DMEM with 0.1% BSA containing 50 µg/mL LPS (control), LPS, and ascidian muscle or porcine liver EtnGpl (1 to 50 µM), and a blank treatment. The dose levels of EtnGpl used in this study were based on our previous study in which 5 to 50 µM of EtnGpl increased the viability of serum-starved Neuro-2A cells (Yamashita et al., 2015).

3.3.4. Cell viability

Caco-2 cells at a concentration of 2.0×10^5 were seeded into 24-well plates (Nunc, Rochester, NY) containing 1 mL of culture medium. The cells were incubated for the indicated times and conditions. Differentiated Caco-2 cells were then treated with LPS (50 µg/mL) and EtnGpl in a dose-dependent manner (1, 10, 20, and 50 µM) for 48 h, followed by rinsing with pre-warmed PBS, trypsinized, and counted using a counting chamber (EM-Techcolor; Hirschmann, Eberstadt, Germany).

3.3.5. Apoptosis detection

Caco-2 cells at a concentration of 1.0×10^5 were seeded in eight-well Lab-Tek™ chamber slides (Thermo Scientific, Waltham, MA) containing 0.5 mL of culture medium. Differentiated Caco-2 cells were then treated

with 50 μ M EtnGpl and LPS for 24 h. Apoptotic cells were visualized and determined by double staining method using the TACS 2 TdT-Flour in situ apoptosis detection kit (Trevigen) as per manufacturer's instruction followed by 4',6-diamidino-2-phenylindole (DAPI) staining under a fluorescence microscope (BX-51; Olympus, Tokyo, Japan). The percentage of apoptotic cells was determined morphologically after DAPI staining by counting cells with characteristic convoluted budding and blebbing of the membrane and fragmented nuclei under a fluorescence microscope (BX-51; Olympus, Tokyo, Japan) (Harada-Shiba et al., 1998; Narayanan et al., 2004; Yamashita et al., 2017b).

To confirm the results of morphological analysis, the relative levels of apoptosis-related proteins were examined using the Human Apoptosis Array Kit (R&D Systems, Minneapolis, MN). Briefly, Caco-2 cells were seeded in 100-mm dishes (1.5×10^6 cells) and incubated as indicated. Differentiated Caco-2 cells were treated with 50 μ M EtnGpl and LPS (50 μ g/mL) for 24 h and then rinsed with cold PBS, followed by lysis with cold lysis buffer 17 containing 10 μ L/mL protease inhibitor cocktail. Membranes coated with 35 different anti-apoptosis-related antibodies were exposed to the cell lysate, and apoptosis-related proteins were detected according to the manufacturer's protocol. Data of captured antibody pixel densities from an image of the developed X-ray film were acquired using ImageJ software. The detected apoptosis-related proteins were denoted as follows: Bcl-xL/Bcl-2 associated death promoter (Bad), Bcl-2-associated X protein (Bax), B-cell lymphoma 2 (Bcl-2), Bcl/leukemia x (Bcl-x), pro-caspase 3, cleaved caspase 3, catalase, cytosolic inhibitors of apoptosis-1 (cIAP-1), cytosolic inhibitors of apoptosis-2 (cIAP-2), claspin, clusterin, cytochrome c, TNF receptor 1 (TNF R1), TNF-related apoptosis-inducing ligand receptor 1 (TRAIL R1), TRAIL R2, Fas associated protein with death domain (FADD), fibroblast-associated (Fas), hypoxia-inducible transcription factor (HIF)-1 α , heme oxygenase (HO)-1, HO-2, heat shock protein (HSP)27, HSP60, HSP70, high temperature requirement protein A2 (HTRA2/Omi), livin, paraoxonase 2 (PON2), cyclin-dependent kinase 4 inhibitor 1 (p21), cyclin-dependent kinase 4 inhibitor 1 (p27), phosphorylated p53 at serine 15 [phospho-p53 (S15)], phospho-p53 (S46), phospho-p53 (S392), phospho-Rad17 (S635), second mitochondria-derived activator of caspase/direct inhibitor of apoptosis-binding protein with low pI (SMAC/Diablo), surviving, and X-linked inhibitor of apoptosis (XIAP).

3.3.6. Cytokine array

Relative cytokine levels were determined using a Human Cytokine Array Kit (R&D Systems, Minneapolis, MN). The cells were cultured, incubated, and treated as indicated in the analysis of apoptosis-related proteins. Membranes coated with 36 different anti-cytokine antibodies were exposed to the cell lysate, and cytokines were detected according to the manufacturer's protocol. Then, data were acquired as described above. The detected cytokines were denoted as follows: Chemokine (C-C motif) ligand 1 (CCL1/I-309), Chemokine (C-C motif)

ligand 2 (CCL2)/Monocyte chemoattractant protein 1 (MCP-1), Macrophage inflammatory protein-1 alpha (MIP-1 α :CCL3)/Macrophage inflammatory protein-1 beta (MIP-1 β :CCL4), Regulated on activation, normal T cell expressed and secreted (RANTES), CD-40 Ligand, Complement Component 5a (C5/C5a), Growth related oncogene-alpha (GRO- α), Interferon- γ -induced protein 10 (IP-10), Interferon-inducible T cell alpha chemoattractant (I-TAC), Stromal cell-derived factor 1 (SDF-1), Granulocyte colony stimulating factor (G-CSF), Granulocyte macrophage colony-stimulating factor (GM-CSF), Intercellular adhesion molecule 1 (ICAM-1), Interferon-gamma (IFN- γ), Interleukins (IL-1 α , IL-1 β , IL-1ra, IL-2, IL-4, IL-5, IL-6, IL-8, IL-10, IL-12p70, IL-13, IL-16, IL-17A, IL-17E, IL-18, IL-21, IL-27, IL-32a), Macrophage migration inhibitory factor (MIF), Plasminogen activator inhibitor-1 (PAI-1:Serpine E1), Tumor necrosis factor-alpha (TNF- α), and Triggering receptor expressed on myeloid cells 1 (TREM-1).

3.3.7. TNF- α assay

TNF- α levels were quantified using a Human TNF- α ELISA kit (FUJIFILM Wako Shibayagi Corp., Gunma, Japan). Briefly, the cells were cultured and incubated, as indicated. The differentiated cells were treated for 24 h, and the cell lysates were collected as described. Additionally, differentiated Caco-2 cells were treated with 50 μ M EtnGpl for 16 h followed by LPS (50 μ g/mL) treatment for 24 h to confirm whether LPS inhibited the functionality and/or uptake of EtnGpl by differentiated Caco-2 cells. The cell lysates (20 μ L) were added to 96-well microplates with the standards, and the assay was performed according to the manufacturer's protocol. Absorbance at 450 nm and 620 nm was read using a 96-well microplate read (ThermoScientific Multiskan FC version 2.5, Finland). Protein contents of samples were measured using a DC Protein Assay kit (Bio-rad, CA, USA).

3.3.8. Lipid extraction and assay

To determine the uptake of extrinsic EtnGpl by differentiated Caco-2 cells, fatty acid methyl esters (FAME), dimethyl acetals (DMA), and phospholipid species in cell lysates were analyzed over a period of 24 h. Briefly, differentiated Caco-2 cells were treated with 50 μ M EtnGpl for 0, 2, 4, 8, 16, and 24 h with 0.1% BSA instead of 10% FBS. At each time interval, the cell surface binding lipids were removed by washing the cells twice with 20 mmol/L Tris-HCl, 2 mol/L NaCl, pH 4.0 (Kinoshita and Shimokado, 1999). The cells were scraped off the plate, ultrasonicated for 10 s on ice, and stored at -80 $^{\circ}$ C until use. Total lipids were extracted according to the Folch method (Folch et al., 1957). To obtain the phospholipid fraction, 1 mL of the extracted total lipids was dried by N₂ flux and dissolved in 200 μ L of chloroform-isopropanol (2:1), and then loaded onto a silica Sep-Pak cartridge (Waters, Tokyo, Japan) in which very fine particles had been removed by passing 1.5 mL of methanol and equilibrated with 1.5 mL of chloroform-isopropanol (2:1). The loaded sample was eluted with 1.5 mL of

chloroform-isopropanol (2:1) to remove non-polar compounds, followed by elution with 1.5 mL of methanol, and the eluted methanol solution was collected as the phospholipid fraction. FAME and DMA prepared from the lipid extracts were analyzed by gas chromatography (Yamashita et al., 2019). Phospholipid species were analyzed by LC-MS/MS in multiple reaction monitoring (MRM) mode (Otoki et al., 2017).

3.3.9. Statistical analysis

The results are represented as mean \pm SEM. All data were subjected to analysis of variance using SPSS software (version 17.0; SPSS Inc., Chicago, IL, USA). Differences between the means were tested using one-way ANOVA followed by Tukey's post hoc test. $P < 0.05$ was considered statistically significant.

3.4. RESULTS

3.4.1. EtnGpl Fraction from Ascidian Muscle and Porcine Liver

The PlsEtn level in ascidian muscle was 87.3 mol% of EtnGpl. The prominent acyl carbon chains in ascidian muscle EtnGpl were 18:0, EPA, and DHA while PlsEtn-18:0/20:5, PlsEtn-18:0/22:6, and phosphatidylethanolamine (PtdEtn)-18:0/22:6 were the main phospholipid species ([Chapter 2, Table 2.2](#)). Porcine liver contained lower PlsEtn, 7.2 mol% of EtnGpl compared to ascidian muscle. The prominent acyl carbon chains in porcine liver EtnGpl were 18:0, 18:2n-6, and ARA, while PtdEtn-18:0/20:4 was the main phospholipid species. Ascidian muscle EtnGpl had higher ratios of n-3/n-6 and (EPA+DHA)/ARA compared to porcine liver EtnGpl.

3.4.2. Extrinsic EtnGpl Enhances Cell Viability of Differentiated Caco-2 cells under Inflammatory Stress

Figure 3.1 shows that differentiated Caco-2 cells stimulated with LPS (control) had significantly reduced cell viability compared to the blank (untreated cells) ($P < 0.05$). Treatment of differentiated Caco-2 cells with increasing concentrations of EtnGpl under LPS-induced inflammatory stress increased the cell viability in a dose-dependent manner (Figure 3.1). Cells treated with ascidian muscle and porcine liver EtnGpl at 20 and 50 μ M showed significantly higher cell viability than those treated with LPS ($P < 0.05$). Moreover, ascidian muscle EtnGpl led to significantly higher cell viability compared to porcine liver EtnGpl at 20 and 50 μ M ($P < 0.05$).

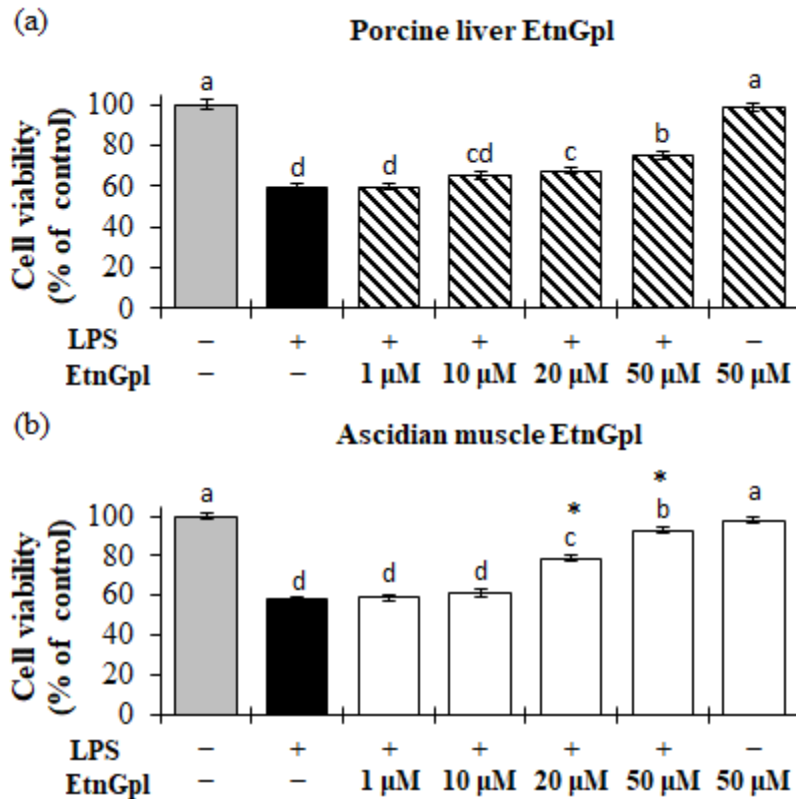


Figure 3.1 Cell viability during LPS induced inflammatory stress in differentiated Caco-2 cells.

Differentiated Caco-2 cells were cultured for 48 h with 1-50 μ M of (a) porcine liver EtnGpl and (b) ascidian muscle EtnGpl containing LPS (50 μ g/mL). Cell viability was estimated by counting viable cells under a light microscope in two independent experiments. Values represent means \pm SEM, $n = 8$. Different letters indicate significant differences at $P < 0.05$ determined by ANOVA (Tukey's test). *Asterisks* indicate significantly higher cell viability in ascidian muscle than porcine liver EtnGpl treatment (t-test, $*P < 0.05$).

3.4.3. Extrinsic EtnGpl Inhibits Apoptosis by Modulating Apoptosis Related Proteins in Inflammatory Stressed Differentiated Caco-2 Cells

Induction of apoptosis by LPS and the subsequent inhibition by extrinsic EtnGpl was measured by identifying apoptotic cells in TUNEL assay and cells that showed characteristic morphological changes determined by DAPI staining (Figure 3.2a-d). DAPI staining of differentiated Caco-2 cells treated with LPS showed blebbing of membrane, and aggregated and fragmented nuclei (Figure 3.2b). Differentiated Caco-2 cells exposed to LPS showed significantly greater number of apoptotic-like cells when compared to the blank ($P < 0.05$) (Figure 3.2e). When differentiated Caco-2 cells were exposed to LPS and EtnGpl, the degree of apoptotic cell death was significantly reduced compared with the LPS treatment, with ascidian muscle EtnGpl showing greater suppression of apoptosis compared to porcine liver EtnGpl ($P < 0.05$).

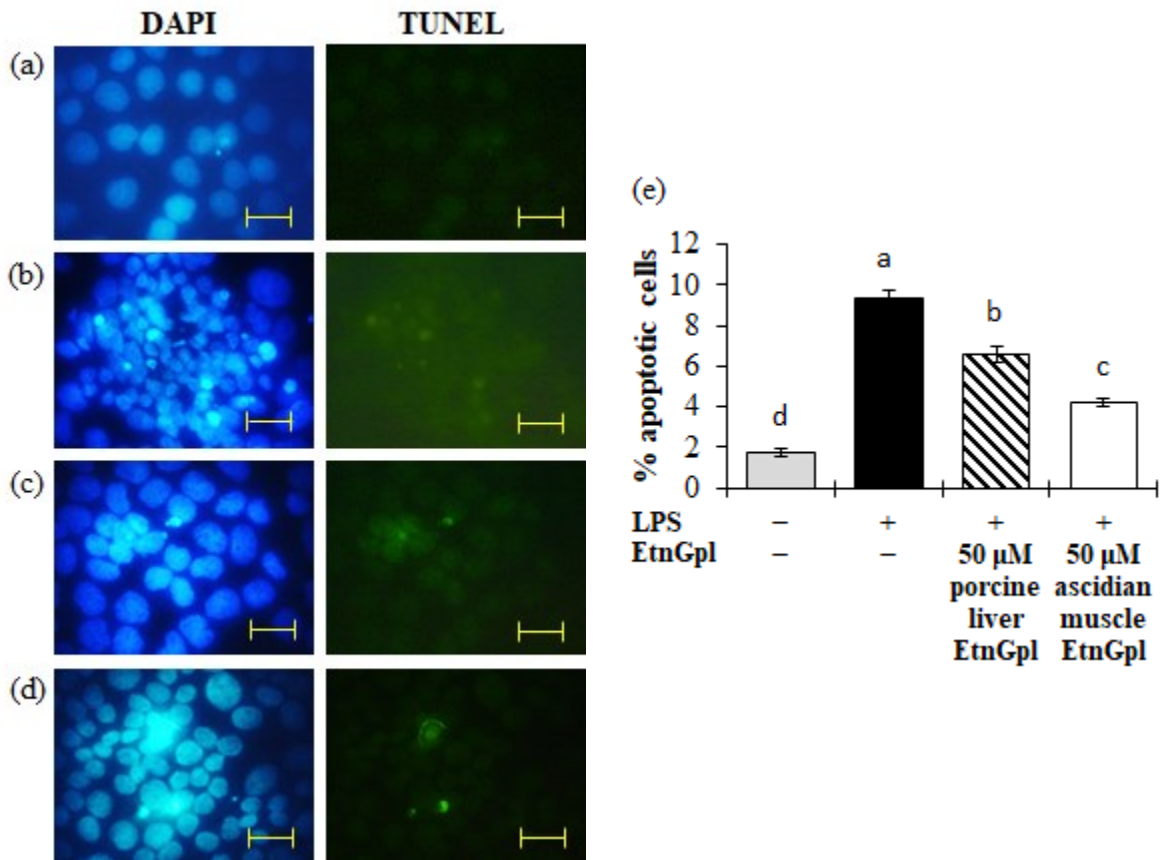


Figure 3.2 Apoptotic cells during LPS induced inflammatory stress in differentiated Caco-2 cells.

Apoptotic cells during LPS induced inflammatory stress in differentiated Caco-2 cells. Differentiated Caco-2 cells were cultured for 48 h with 50 μM porcine liver or ascidian muscle EtnGpl containing LPS (50 μg/mL) and then stained with TdT-mediated dUTP nick end labeling (TUNEL) immunofluorescence followed by staining with 4',6-diamidino-2-phenylindole (DAPI). Representative images (objective, 100×). (a) Blank. (b) LPS (control). (c) LPS + 50 μM porcine liver EtnGpl. (d) LPS + 50 μM ascidian muscle EtnGpl. Scale bar indicates 20 μm. (e) Induction of apoptosis in differentiated Caco-2 cells by LPS. Values represent means ± SEM, n = 3. Different letters indicate significant differences at $P < 0.05$, determined by ANOVA (Tukey's test).

To gain further insight on inhibition of apoptosis by EtnGpl during LPS-induced inflammatory stress, we evaluated the relative levels of apoptosis-related proteins (Figure 3.3). LPS-treated differentiated Caco-2 cells showed significantly higher levels of proapoptotic Bad and cytochrome c compared to blank cells ($P < 0.05$). Furthermore, LPS treatment significantly upregulated apoptosis executioner pro-caspase 3, TNF R1 death receptor and P-p53 (S392) antibody protein ($P < 0.05$), and showed a tendency to up-regulate SMAC/Diablo and cleaved caspase 3 compared to the blank cells. Notably, co-treatment with LPS and ascidian muscle EtnGpl

significantly downregulated the relative levels of Bad, cytochrome c, and SMAC/Diablo proapoptotic proteins, caspase 3 and cleaved caspase 3 apoptosis executioner proteins compared to the LPS-treated cells ($P < 0.05$). On the other hand, although LPS and porcine liver EtnGpl co-treatment downregulated the aforementioned apoptosis-related proteins, the effect was less remarkable compared to that observed with LPS and ascidian muscle EtnGpl co-treatment.

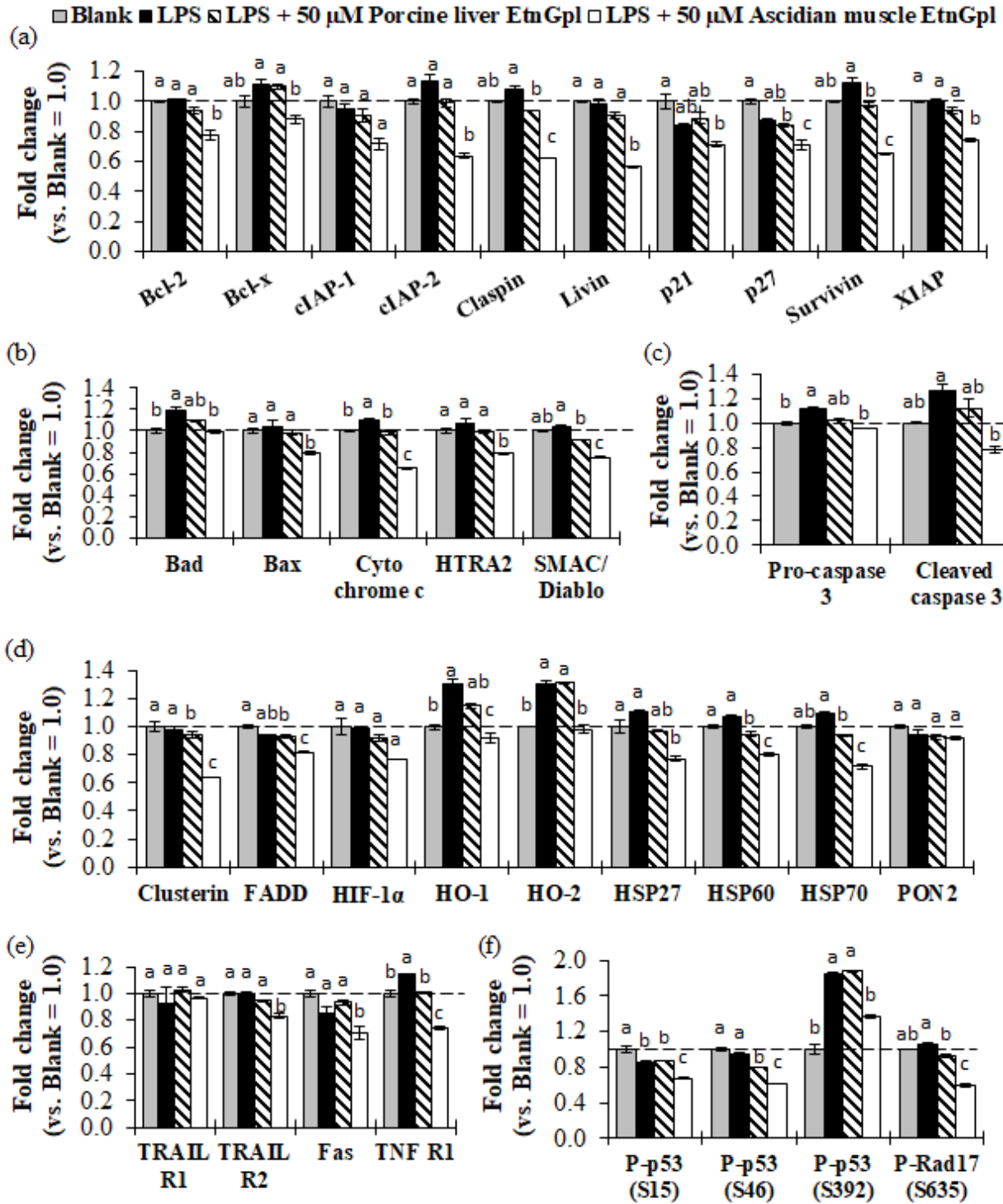


Figure 3.3 Relative levels of apoptosis-related proteins (fold change vs. blank) during LPS induced inflammatory stress in differentiated Caco-2 cells.

(a) Antiapoptotic proteins. (b) Proapoptotic proteins. (c) Cysteine proteases. (d) Other apoptosis-related proteins. (e) Death receptors. (f) Antibody proteins. The dashed line indicates the blank group = 1.0. Different letters indicated significant difference at $P < 0.05$ determined by ANOVA (Tukey's test).

3.4.4. Extrinsic EtnGpl Ameliorates Inflammation in Differentiated Caco-2 Cells by Lowering Cytokine Levels

A cytokine array assay was conducted to determine the effect of extrinsic EtnGpl on human intestinal tract cells under inflammatory stress (Figure 3.4). Treatment of differentiated Caco-2 cells with LPS led to higher relative levels of eight pro-inflammatory cytokines, anti-inflammatory cytokines, MCP-1, MIP-1 β , and SDF-1 chemokines and CD-40 ligand and G-CSF cytokines, while C5/C5a, GRO α , IP-10 and IL-8 chemokines were decreased compared to the blank cells (Figure 3.4a-d). Co-treatment with LPS and ascidian muscle EtnGpl downregulated eleven pro-inflammatory cytokines, four anti-inflammatory cytokines, four chemokines, and SDF-1 chemokine, while co-treatment with LPS and porcine liver EtnGpl downregulated five pro-inflammatory cytokines, two anti-inflammatory cytokines and SDF-1 chemokine (Figure 3.4a-d). However, four chemokines were upregulated in porcine liver EtnGpl-treated cells compared to LPS-treated cells.

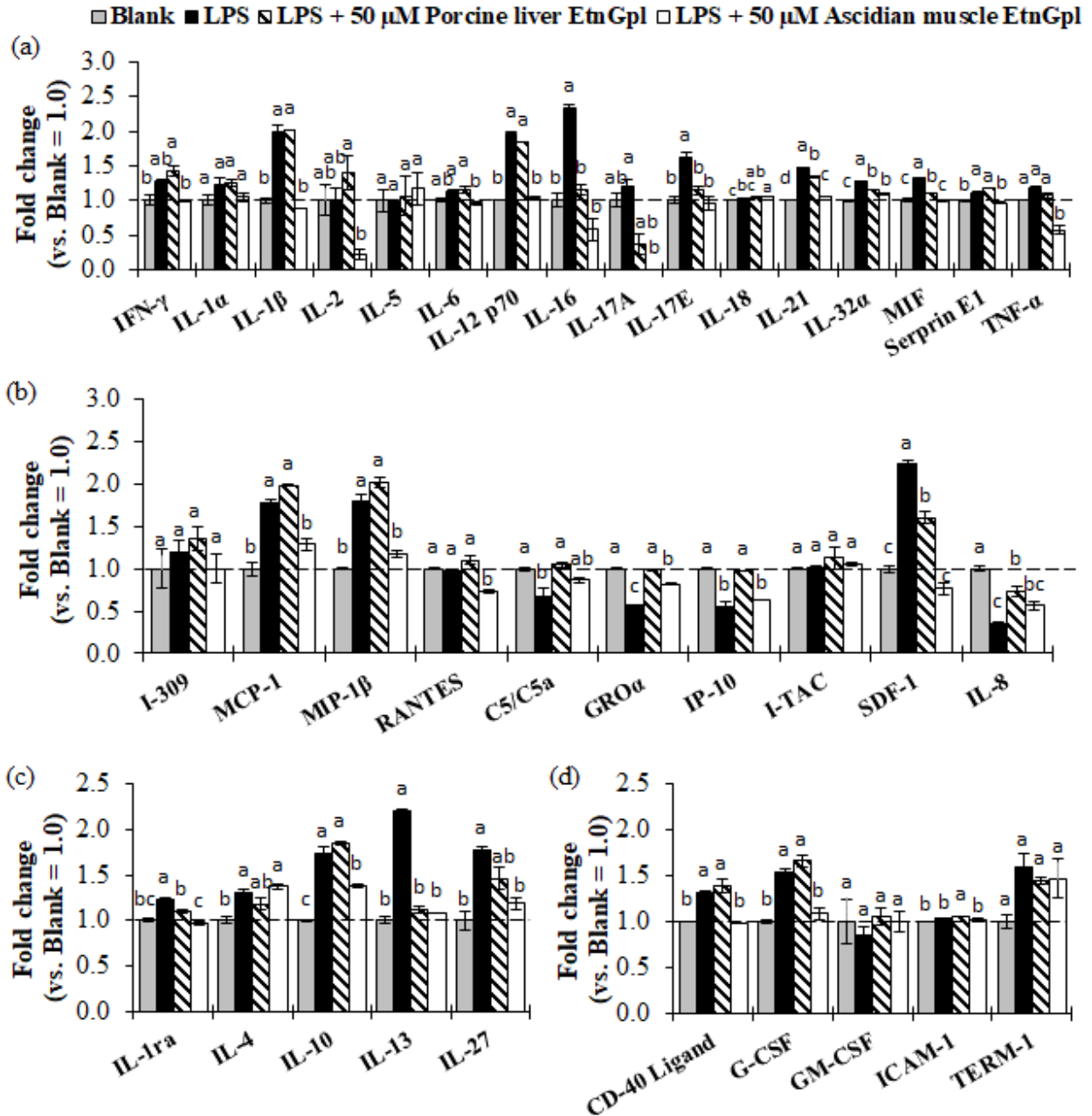


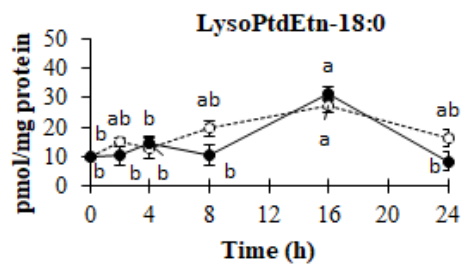
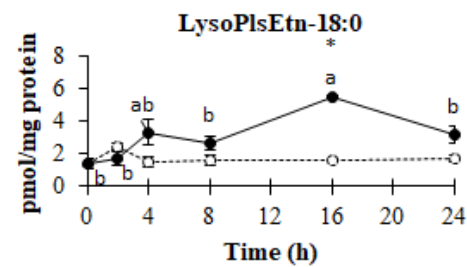
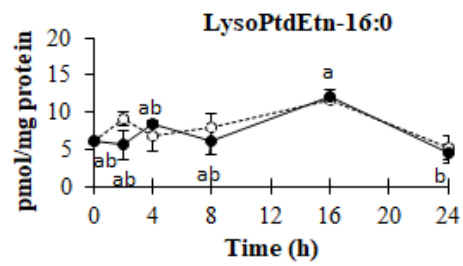
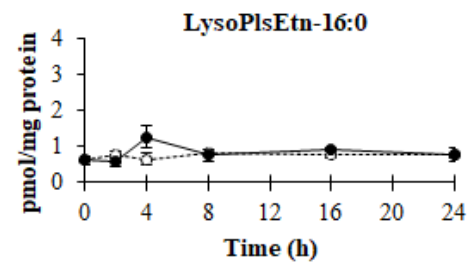
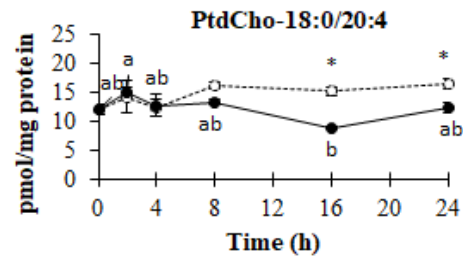
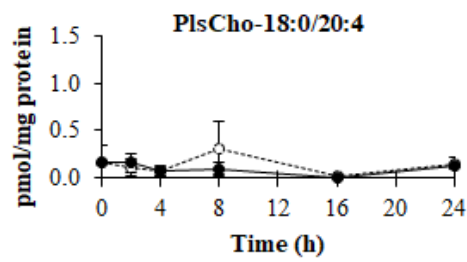
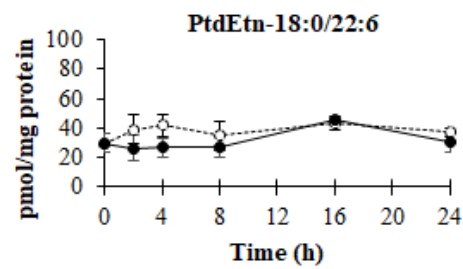
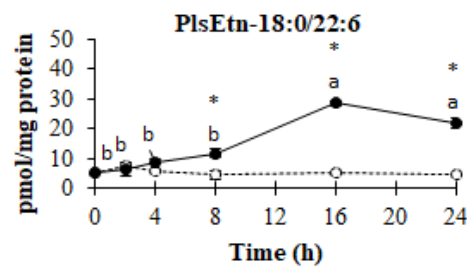
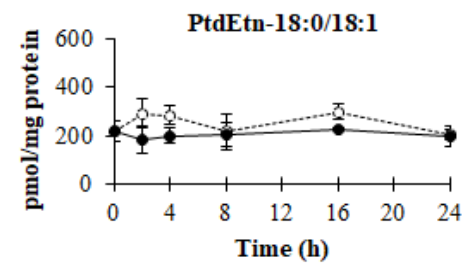
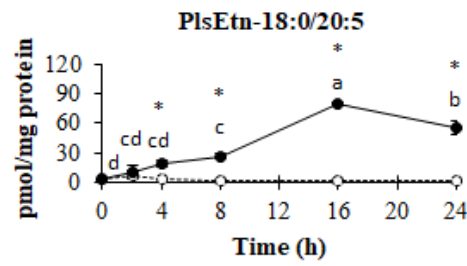
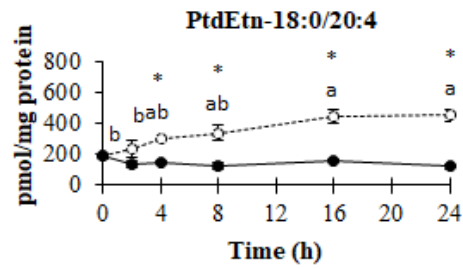
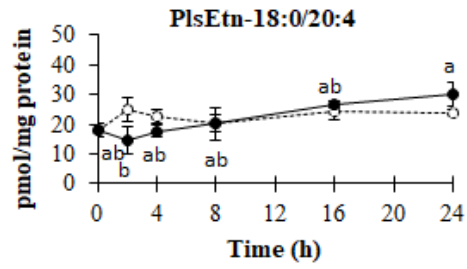
Figure 3.4 Relative levels of cytokine (fold change vs. blank group = 1.0) during LPS induced inflammatory stress in differentiated Caco-2 cells.

(a) Pro-inflammatory cytokines. (b) Chemokines. (c) Anti-inflammatory cytokines. (d) Other cytokines. The dashed line indicates the blank group = 1.0. Different letters indicated significant difference at $P < 0.05$ determined by ANOVA (Tukey's test).

3.4.5. Uptake of Extrinsic EtnGpl by Differentiated Caco-2 Cells

The lipid composition of the cell lysate was determined to characterize the phospholipid species, acyl and alkenyl carbon chains of EtnGpl taken up by differentiated Caco-2 cells over time (Figure 3.5 and 3.6). Acyl and alkenyl carbon chains of EtnGpl taken up by differentiated Caco-2 cells under LPS treatment were analyzed over time (Figure 3.7). As shown in Figure 3.5, we observed that the levels of PlsEtn-18:0/20:4, PlsEtn-18:0/20:5, and PlsEtn-18:0/22:6 from ascidian muscle EtnGpl moved up from 0 to 24 h, with a peak at 16 h except for PlsEtn-18:0/20:4. The levels of PtdEtn-18:0/20:4 from porcine liver EtnGpl showed a steady increase from 0 to 24 h. The levels of choline plasmalogen (PlsCho) and the other PtdEtn and phosphatidylcholine (PtdCho) species from ascidian muscle and porcine liver EtnGpl remained unchanged during the exposure time except for PtdCho-18:0/20:4 from ascidian muscle EtnGpl, which showed a decrease. Meanwhile, EtnGpl hydrolysis products, lysoPlsEtn-18:0 levels from ascidian muscle EtnGpl showed an increase during the 24 h uptake time with a peak at 16 h, while lysoPtdEtn-16:0 and 18:0 from ascidian muscle and porcine liver EtnGpl increased in a similar manner with a peak at 16 h.

In addition, we determined the change in acyl and alkenyl carbon chains over time. As shown in Figure 3.6, we observed that 18:0ol and EPA levels from ascidian muscle EtnGpl moved up from 0 to 24 h and reached a peak at 16 h. DHA from ascidian muscle EtnGpl moved down in the first 4 h followed by an increase up to 24 h, with a peak at 16 h. Alkenyl and acyl carbon chains remained unchanged during porcine liver EtnGpl uptake. On the other hand, the changes in acyl and alkenyl carbon chains under LPS treatment over time are shown in Figure 3.7. We observed a sharp increase in the first 2 h followed by steady increase up to 24 h of 18:0ol, EPA and DHA from ascidian muscle EtnGpl. For porcine liver EtnGpl uptake, we observed a steady increase in ARA over time while the other acyl and alkenyl carbon chains remained unchanged.



--○-- 50 μM Porince liver EtnGpl —●— 50 μM Ascidian muscle EtnGpl

Figure 3.5 Time-dependent changes of various phospholipids in differentiated Caco-2 cells.

Values represent means ± SEM, $n = 3$. Different letters indicate significant differences at $P < 0.05$ among same EtnGpl treatment determined by ANOVA (Tukey's test). *Asterisks* indicate significant difference between cells treated with different EtnGpl. (t-test, $*P < 0.05$).

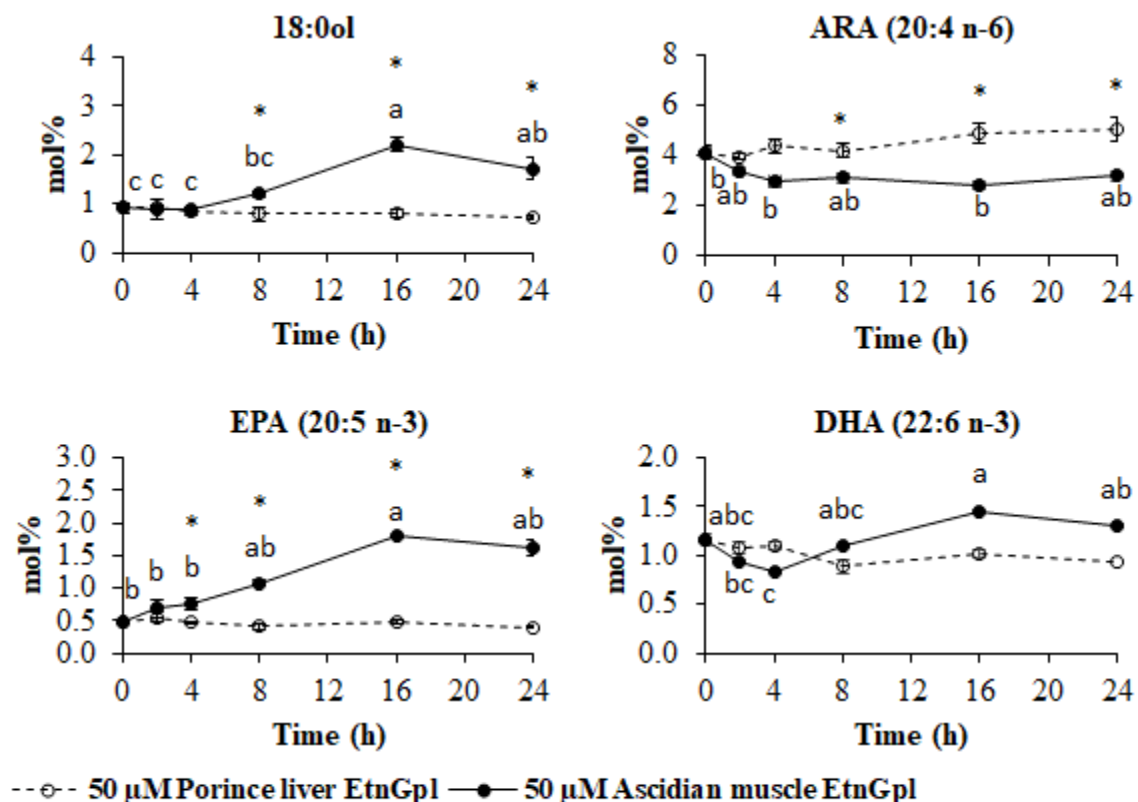


Figure 3.6 Time-dependent changes of phospholipid carbon chain composition in differentiated Caco-2 cells after treatment with 50 μM porcine liver and ascidian muscle EtnGpl.

Values represent means ± SEM, $n = 3$. Different letters indicate significant differences at $P < 0.05$ among same EtnGpl treatment determined by ANOVA (Tukey's test). *Asterisks* indicate significantly higher level at a given time-point ($P < 0.05$, t-test).

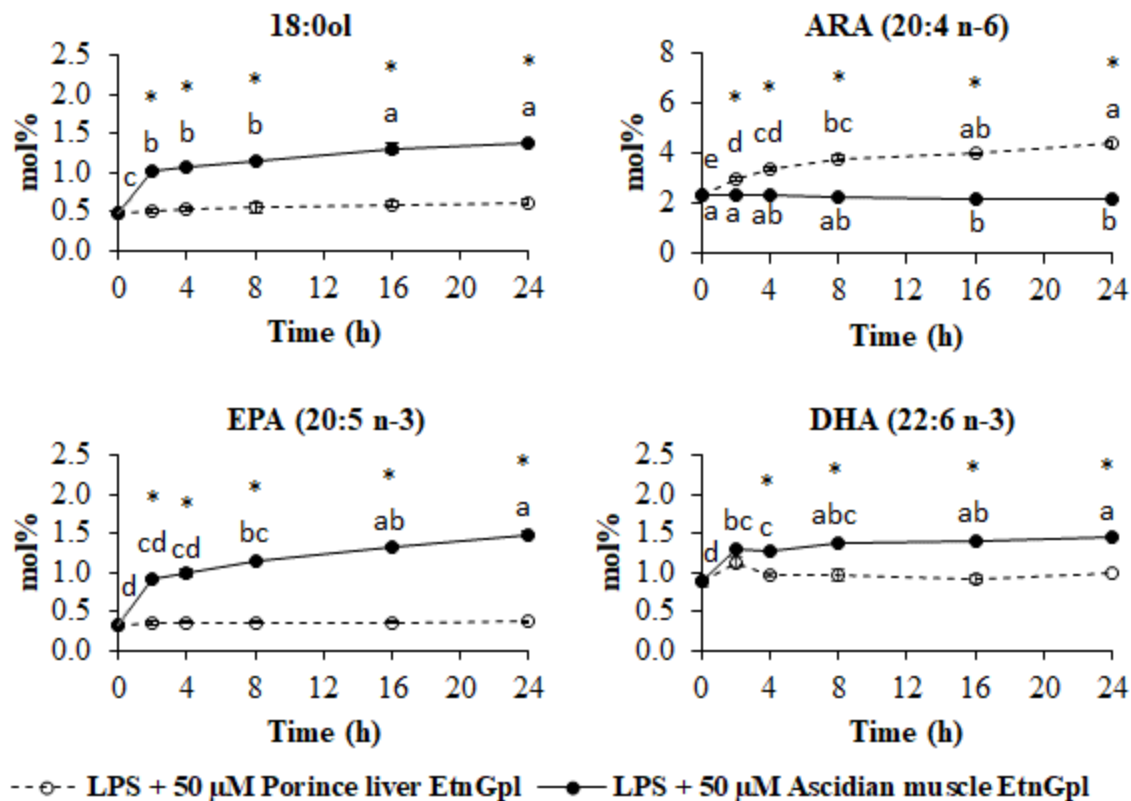


Figure 3.7 Time-dependent changes of phospholipid carbon chain composition in differentiated Caco-2 cells after treatment with LPS + 50 μM porcine liver and ascidian muscle EtnGpl.

Values represent means ± SEM, $n = 3$. Different letters indicate significant differences at $P < 0.05$ among same EtnGpl treatment determined by ANOVA (Tukey's test). Asterisks indicate significantly higher level at a given time-point ($P < 0.05$, t-test).

3.4.6. Extrinsic EtnGpl Suppresses TNF- α in Differentiated Caco-2 Cells under Inflammatory Stress

TNF- α is a major mediator of inflammation and apoptosis in cells. To examine if EtnGpl suppressed inflammation and apoptosis, TNF- α was quantified in differentiated Caco-2 cells with LPS and EtnGpl-treatment using an ELISA kit (Figure 3.8). Differentiated Caco-2 cells treated with LPS for 24 h demonstrated upregulation of TNF- α compared to the blank cells. Cells cultured for 24 h in the presence of LPS and EtnGpl exhibited lower levels of TNF- α compared with LPS- treated cells. Moreover, cells treated with LPS and ascidian muscle EtnGpl showed significantly reduced TNF- α levels (almost similar to those in blank cells) compared to LPS-treated cells ($P < 0.05$). In addition, TNF- α levels were lower in LPS and ascidian muscle EtnGpl-treated cells than in LPS and porcine liver EtnGpl-treated cells. On the other hand, there were no significant differences ($P < 0.05$) in TNF- α levels between differentiated Caco-2 cells co-treated with EtnGpl and LPS in the same medium and those

treated with EtnGpl first followed by LPS. The treatment of the cells with EtnGpl for 16 h was based on our uptake experiment, which showed that uptake of EtnGpl by differentiated Caco-2 cells reached a peak at 16 h. This suggests that the uptake of EtnGpl by the cells led to the observed functionality during LPS-induced inflammatory stress.

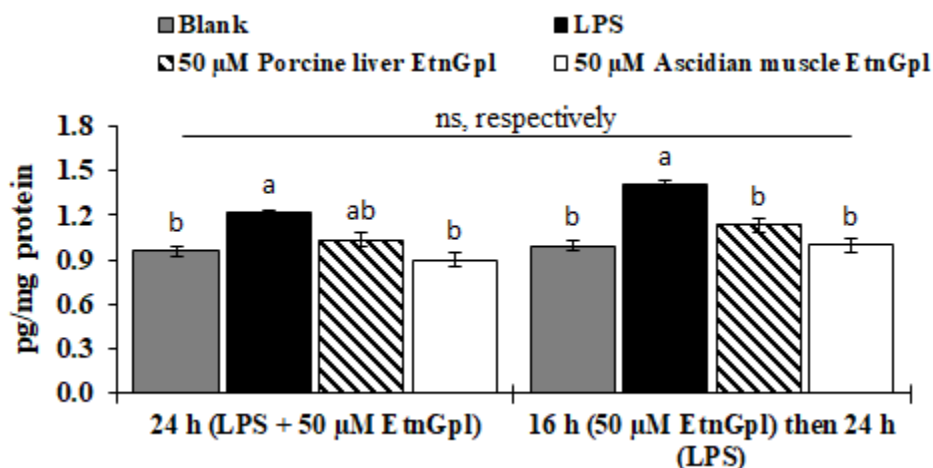


Figure 3.8 TNF- α levels during LPS induced inflammatory stress in differentiated Caco-2 cells

(a) Differentiated Caco-2 cells were cultured for 24 h with LPS + 50 μ M EtnGpl and in another experiment differentiated -2 cells Caco were treated with 50 μ M EtnGpl for 16 h (pre-treatment) and then treated with 50 μ g/mL of LPS for 24 h (post-treatment after EtnGpl was taken up). Values represent means \pm SEM, $n = 3$. Different letters indicate significant differences at $P < 0.05$ determined by ANOVA (Tukey's test). *ns*, not significant (t-test, $*P < 0.05$).

3.5. DISCUSSION

In the present study, we demonstrate that an increase in intracellular PlsEtn levels is associated with anti-inflammatory and antiapoptotic effects in human intestinal tract cells. We employed LPS for the induction of inflammatory stress *in vitro*, which has been extensively used in studies on pro-inflammatory and proapoptotic responses in differentiated Caco-2 cells (Yamashita et al., 2017b; Jutanom et al., 2020). Moreover, *in vitro* epithelial cell studies have been shown to play a critical role in understanding specific aspects related to IBD (McKay et al., 1997). Here, using an *in vitro* model, we observed that in comparison to extrinsic EtnGpl with low PlsEtn content, the one having high PlsEtn content and distinct PUFA at the *sn-2* position showed superior inhibition of inflammation and apoptosis in human intestinal tract cells under LPS-induced inflammatory stress via downregulation of inflammatory cytokines and modulation of apoptosis-related proteins. Extrinsic EtnGpl from the ascidian muscle was found to maintain higher intracellular levels of PlsEtn species compared to that

from the porcine liver. These results suggest that the uptake of PlsEtn by colon epithelial cells provides protection against induced inflammatory stress by suppressing apoptosis. This evidence shows a clear relationship between increased PlsEtn levels in colon epithelial cells and attenuation of tissue injury during induced stress.

Chronic colon inflammation has been closely associated with the development of inflammatory bowel disease (IBD) and colon cancer (Coussens and Werb, 2002; Bartsch and Nair, 2006). Chronic inflammation induced by stress stimuli has been linked to the deregulation of apoptosis, which disrupts normal cellular homeostasis (Fulda et al., 2010). In neuronal cells under serum starvation, EtnGpl containing high PlsEtn levels suppresses the activities of caspases 3, 8, and 9, which are involved in the mitochondrial and death receptor pathways (Yamashita et al., 2016a). In our study, LPS treatment upregulated proapoptotic Bad and cytochrome c, while co-treatment with LPS and EtnGpl downregulated their relative levels (ascidian muscle > porcine liver EtnGpl) ([Figure 3.3b](#)). Moreover, the uptake of ascidian muscle EtnGpl resulted in higher levels of PlsEtn species, EPA, and DHA compared to porcine liver EtnGpl. Based on these findings, we suggest that the uptake of PlsEtn might have limited the release of proapoptotic cytochrome c into the cytosol. The release of cytochrome c activates initiator caspase 9, which, in turn, activates the apoptosis executioner caspase 3 (Yang et al., 2009). Our results further confirmed the possibility of a limited release of cytochrome c due to the downregulation of apoptosis executioner pro-caspase 3 and cleaved caspase-3 by LPS and EtnGpl co-treatment (ascidian muscle > porcine liver EtnGpl) compared to LPS treatment ([Figure 3.3c](#)). Moreover phosphorylation of p53 protein is known to trigger the induction of apoptosis via activation of proapoptotic related protein leading to the release of cytochrome c (Yogosawa and Yoshida, 2018). We observed that LPS treatment upregulated P-p53 (S392) and not P-p53 (S15 and S46), however, all were downregulated by ascidian muscle EtnGpl and LPS co-treatment. Upon DNA damage, phosphorylation of p53 at S394 is within its COOH-terminal region that enhances p53 DNA binding activity while that of p53 at S15 and S46 is within its NH₂-terminal region that promotes dissociation of MDM2, which might possibly explain the observed differences (Ozaki and Nakagawara, 2011). Taken together, this explains the observed effect on cell viability and suppression of apoptotic cells by PlsEtn (ascidian muscle EtnGpl > porcine liver EtnGpl > LPS).

TNF- α is known to control inflammatory cell populations and mediate many other aspects of the inflammatory process, contributing to the disruption of the intestinal epithelial barrier (Coussens and Werb, 2002). It has been shown that i.p. administration of plasmalogens (Pls) reduces the expression of TNF- α in the hippocampus of LPS-treated mice (Ifuku et al., 2012). In our *in vitro* study, we found that extrinsic EtnGpl suppressed the LPS-induced high levels of TNF- α . Furthermore, TNF- α is implicated in the induction of apoptosis involving the death receptor TNF-R1 via the extrinsic apoptosis pathway (Yang et al., 2009). In the present study, we observed that extrinsic EtnGpl lowered the relative levels of TNF-R1 induced by LPS (ascidian

muscle > porcine liver EtnGpl) ([Figure 3.3c](#)). It is possible that EtnGpl might have suppressed caspase-dependent apoptosis via the extrinsic pathway. Cytokines are important in the pathogenesis of colon inflammation, and their manipulation can reduce disease severity and maintain remission. Cellular secretion of pro-inflammatory cytokines mediates many responses, including apoptosis during chronic colon inflammation (Sanchez-muñoz et al., 2008). We showed here that an increase in pro-inflammatory cytokines by LPS treatment was downregulated by extrinsic EtnGpl (ascidian muscle > porcine liver EtnGpl), which possibly generated a favorable microenvironment for the survival of the cells.

PlsEtn has been shown to form more condensed and thicker membranes, possibly due to the vinyl ether linkage at the *sn*-1 position (Rubio et al., 2018). Furthermore, EPA-PlsEtn exerts a better effect in lowering amyloid- β levels in CHO-APP/PS1 cells *in vitro*, which is partly attributed to the vinyl ether linkage (Che et al., 2018b). In the present study, the observed increase in PlsEtn levels in differentiated Caco-2 cells (ascidian muscle > porcine liver EtnGpl) might have influenced the intracellular microenvironment differently. Moreover, chemically induced inflammatory stress is associated with reactive oxygen species (ROS), and ROS play a central role in the regulation of main pathways in apoptosis (Redza-dutordoir and Averill-bates, 2016). However, the vinyl ether linkage at the *sn*-1 position makes Pls more susceptible to oxidative stress (Wallner and Schmitz, 2011). Indeed, it has been demonstrated that one vinyl ether double bond in Pls can scavenge two peroxy radicals (Hahnel et al., 1999; Leßig and Fuchs, 2009). This might partly explain the superior antiapoptotic effect of the ascidian muscle EtnGpl over porcine liver EtnGpl observed in our study ([Figure 3.1](#) and [3.2](#)). Therefore, PlsEtn might have acted as an antioxidant and protected cells from LPS-induced inflammatory stress.

Ascidian muscle EtnGpl containing EPA and DHA had a superior antiapoptotic effect compared to porcine liver EtnGpl containing ARA. Extrinsic ascidian muscle EtnGpl yielded higher levels of intracellular PlsEtn containing DHA and EPA compared to porcine liver EtnGpl ([Figure 3.5](#), [3.6](#) and [3.7](#)). PlsEtn-selective phospholipase A₂ is activated by inflammation, and quarried EPA and DHA give rise to eicosanoids and docosanoids, which serve as inflammation-resolving mediators (Farooqui, 2010; Calder, 2015). This changes the pattern of cellular inflammatory mediators and decreases chemically induced colonic damage and inflammation (Empey et al., 1991). In this study, ascidian muscle EtnGpl, which led to increased PlsEtn containing EPA and DHA, showed higher suppression of apoptotic responses in the cells. Furthermore, since ARA is metabolized to form eicosanoids that serve as inflammatory mediators, the observed increase in PtdEtn-containing ARA with porcine liver EtnGpl could possibly explain the relatively similar levels of a few pro-inflammatory cytokines between porcine liver EtnGpl-treated cells and LPS-treated cells.

During intestinal absorption of phospholipids, fatty acids are released as a result of hydrolysis at the *sn*-2, which yields lysophospholipids (Cohn et al., 2010). Lysophospholipids have been identified as biologically

active lipid mediators (McMullen et al., 2020). For instance, lysoPtdCho bearing DHA have been shown to exhibit anti-inflammatory effects *in vivo* and *in vitro* in mouse and macrophage models, respectively (Hung et al., 2011). In the present study, we observed an increase in lysoPlsEtn-18:0 from ascidian muscle EtnGpl and an increase in lysoPtdEtn-18:0 from both EtnGpl treatments (Figure 3.5). This possibly suggests their involvement in suppressing colon inflammation and apoptosis during LPS-induced stress. We have recently demonstrated that lysoEtnGpl improves the absorption kinetics of PlsEtn *in vivo* in the plasma of mice through re-esterification (Yamashita et al., 2020b). Therefore, it would be interesting to elucidate the protective role of lysoPlsEtn vis-à-vis PlsEtn during colon inflammation and carcinogenesis *in vivo* and *in vitro*. Thus, further detailed studies to clarify the food functionality of lysoPlsEtn in the colon should be conducted.

3.6. CONCLUSION

In conclusion, our findings provide evidence that the elevation of PlsEtn in colon epithelial cells might contribute to the alleviation of stress-induced inflammation and apoptosis responses. The resulting intracellular antiapoptotic effect was achieved via suppression of pro-inflammatory cytokines and inhibition of proapoptotic proteins. Our present research findings suggest that the intake of PlsEtn with abundant vinyl ether linkages and n-3 PUFA efficiently inhibits the downstream inflammatory and apoptotic signaling cascade in the colon (Figure 3.9). Therefore, PlsEtn derived from food sources with high vinyl ether linkages and n-3 PUFA is potentially beneficial in averting the initiation of IBD and colon cancer, which are strongly associated with chronic colon inflammation.

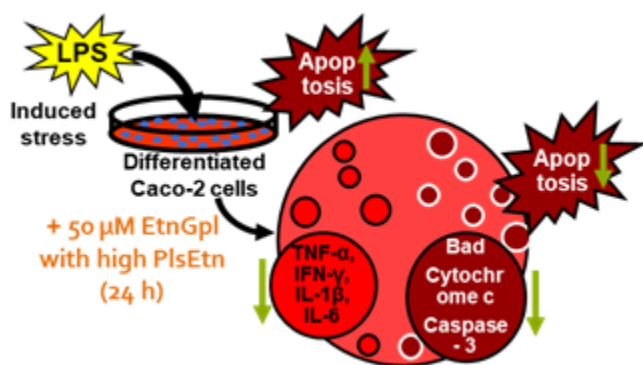


Figure 3.9 Schematic illustration of antiapoptotic effect of PlsEtn in differentiated Caco-2 cells under LPS-treatment

Differentiated Caco-2 cells were treated with 50 μM EtnGpl with LPS for 24 h. EtnGpl with high PlsEtn level suppressed pro-inflammatory cytokines and apoptosis-related proteins, hence a decrease in the degree of apoptotic cells

4. CHAPTER 4: DIETARY ETHANOLAMINE PLASMALOGEN AMELIORATES DEXTRAN SULFATE SODIUM-INDUCED COLITIS IN MICE

4.1. ABSTRACT

Ethanolamine plasmalogen (PlsEtn), abundant in marine creatures, is a unique subclass of glycerophospholipid (EtnGpl) due to the vinyl ether linkage at the sn-1 position of the glycerol moiety. Dietary PlsEtn has been reported to have several health benefits; however, its functional role during colon pathophysiology remains elusive. The aim of the present study was to investigate the anti-colitis effect of dietary EtnGpl with high (86.2 mol%) and low (7.7 mol%) PlsEtn levels in dextran sulfate sodium (DSS)-induced colitis mice model. Colitis was induced in vivo by administering 1.5% DSS. Two groups of mice received AIN-93G diet with 1% fish oil (blank and control group) and another two groups of mice receive AIN-93G diet with 1% fish oil and either high PlsEtn level (ascidian muscle group) or low PlsEtn level (porcine liver group). After 38 days, DSS treatment shortened the colon length, decreased the body weight, and increased spleen weight, compared to the blank group, which were improved by dietary EtnGpl, with ascidian muscle group showing superior effects. After 16 days (early/middle stage of inflammation), DSS treatment elevated MPO activity, TBARS, pro-inflammatory cytokines and proapoptosis-related proteins levels in the colon mucosa compared to the blank, which were lowered by dietary EtnGpl with ascidian muscle group showing higher suppression. Furthermore, ascidian muscle compared to porcine liver group led to higher levels of plasmalogens in the colon mucosa and plasma. Taken together, these results indicate that diets with abundant PlsEtn exert more anti-colitis effects by modulating apoptosis and inflammatory mediators in the colon mucosa.

4.2. INTRODUCTION

Inflammatory bowel disease (IBD), categorized as either ulcerative colitis (UC) or Crohn's disease (CD), are intestinal disorders that involve prolonged inflammation (Perše and Cerar, 2012). UC is an IBD limited to the colonic mucosa, which causes colon epithelial dysfunction and increases mucosal permeability, which are inflammation-mediated, leading to abdominal pain, diarrhea, rectal bleeding, and weight loss (GBD 2017, 2020). The inflammation-mediation results from greatly increased colon activities of infiltrating neutrophils, lymphocytes, monocytes, or macrophages, and plasma cells, which is accompanied by the overproduction of reactive oxygen species (ROS), pro-inflammatory mediators, and apoptosis signals, ultimately leading to ulceration (Bouma and Strober, 2003; Jena et al., 2012; Carvalho and Cotter, 2017). Recent statistics indicate a global increase in UC incidences and prevalence in both developed and developing countries (Kaplan and Ng, 2017; Richardson et al., 2018). The etiology of UC is not fully understood, but both genetic predisposition and environmental factors contribute to its onset by initiating inappropriate aggressive inflammatory response, which

elicits the risk of colon cancer, the third most common malignancy in humans globally (Seril et al., 2003; Jena et al., 2012; Eichele and Kharbanda, 2017).

Dextran sodium sulfate (DSS)-induce colitis is the most common experimental model of mouse colitis and has many similarities with clinical and histological characteristics of human UC (Seril et al., 2003). DSS-induced colitis in mouse has been used to study changes in epithelial permeability, myeloperoxidase (MPO), and pro-inflammatory cytokines (Cho et al., 2007; Lavi et al., 2010; Woo et al., 2016; Han et al., 2019; Kim et al., 2020). In DSS-induced colitis, M1 type macrophages are increased and promote the secretion of pro-inflammatory cytokines such as tumor necrosis factor (TNF)- α , interleukin (IL)-6, and IL-1 β , which induce colonic cells ulceration resulting into tissue damage (Gordon and Martinez, 2010; Zhu et al., 2014). This indicates that the modulation of pro-inflammatory cytokine secretion is critical during colitis remission therapy.

Apoptosis is programmed cell death that maintains a balance between cell death and survival. The colon epithelial layer serves as the barrier between the bowel wall and the potentially hazardous gastrointestinal tract contents, underlining the importance of cellular viability (Edelblum et al., 2006; Günther et al., 2013). Several studies have reported that apoptosis in intestinal epithelial cells is associated with chronic inflammation in UC patients due to increased cytokine activity such as TNF, IL, and IFN family members (Günther et al., 2013). Increased apoptosis in UC disrupts the intestinal mucosal integrity and barrier functions, which exuberates inflammation and consequently ulceration (Edelblum et al., 2006). Inhibition of epithelial cell induced apoptosis and repair of mucosal integrity is therefore, a promising therapy of UC.

Environmental risk factors such as diet, cigarette smoking, appendectomy, stress and depression, vitamin D and hormonal imbalance play an important role in the development of IBD (Ananthakrishnan, 2015). Notably, dietary fat has been associated with the risk of UC (Hou et al., 2011). Dietary intake of n-3 polyunsaturated fatty acids (PUFA) has been associated with a tendency to reduce the risk of UC (Ananthakrishnan et al., 2014). Moreover, cohort studies have shown the intake of total dietary n-3 PUFA, eicosapentaenoic acid (EPA 20:5n-3), and especially docosahexaenoic acid (DHA 22:6n-3) from fish oil are associated with protection from UC (John et al., 2010; Scaiola et al., 2017). On contrary, the intake of n-6 PUFA, that is linoleic acid and arachidonic acid (ARA 20:4n-6) are reported to increase the risk of UC (IBD in EPIC Study Investigators et al., 2009; De Silva et al., 2010, 2014). Therefore, dietary fat composition has the potential to prevent UC risk or reduce its symptoms.

PlsEtn is a sub-type of ethanolamine glycerophospholipids (EtnGpl) with a unique property of a vinyl ether linkage at the *sn*-1 position (Braverman and Moser, 2012). At the *sn*-2 position, PlsEtn is enriched with PUFA; EPA and DHA for marine food sources such as sea squirt muscle and ARA for land food sources such as porcine liver (Yamashita et al., 2016a; Nguma et al., 2020). The vinyl ether linkage is known to act as an antioxidant by

scavenging ROS (Leßig and Fuchs, 2009). Furthermore, PlsEtn has been reported in several studies to have the potential to prevent inflammation-related diseases such as Alzheimer's disease, Parkinson's disease, and colon cancer due the abundance of the vinyl ether linkage (Ifuku et al., 2012; Yamashita et al., 2017; Che et al., 2018a; Mawatari et al., 2020; Nguma et al., 2020). However, the possible role of dietary PlsEtn in IBD has not yet been investigated. Therefore, the aim of the present study was to investigate the functional role of dietary PlsEtn on the development of DSS-induced colitis *in vivo* and the underlying mechanisms.

4.3. MATERIAL AND METHODS

4.3.1 Materials

Freeze-dried ascidian muscle was provided by Yaizu Suisankagaku Industry Co., Ltd. (Shizuoka, Japan) while the porcine liver was purchased from local meatpackers in Hokkaido, Japan. Fish oil from Japanese pilchard, *Sardinops melanostictus* (Schlegel, 1846) was provided by Nippon Suisan Kaisha Ltd. (Tokyo, Japan). Standard phospholipid species was purchased from Avanti Polar Lipids, Inc. (Alabaster, AL, USA) and PlsEtn-18:0/20:5 was purified according to our previously reported method (Yamashita et al., 2014b).

4.3.2. Preparation of purified EtnGpl (ascidian muscle and porcine liver) and experimental diets

Purified EtnGpl and experimental diets were prepared as reported in [Chapter 2](#). Porcine liver EtnGpl contained low PlsEtn level (7.7 mol% PlsEtn in EtnGpl) while ascidian muscle EtnGpl contained high PlsEtn (86.2 mol% PlsEtn in EtnGpl). For experimental diets, AIN-93G diet was slightly modified by reducing soy oil content to 6% and supplemented with 1% fish oil (10 g/kg diet) to form the basal diet (Table 4.1). Ascidian muscle and porcine liver EtnGpl diets were prepared by adding 0.1% purified ascidian muscle and porcine liver EtnGpl (1 g/kg diet), respectively, to the basal diet. One percent fish oil was added to the three experimental diets to attain relatively similar n-3/n-6 ratios. Intake of fish oil with high n-3 PUFA has been shown to have protective role to the risk of UC (John et al., 2010). Moreover, the World Health Organization (WHO) recommends a n-3/n-6 ratio of 5:1 to 10:1 (World Health Organization Fat and Oils in human Nutrition, 1994).

4.3.3. Animals

Female four weeks old BALB/c mice, weighing 17-19 g were obtained from Japan SLC, Inc (Shizuoka, Japan) and housed in pathogen-free condition in micro-isolator cages at 22 ± 1 °C under a 12 h light/dark cycle. The mice had access to CE-2 diet (CLEA Japan, Inc, Tokyo, Japan) and water *ad libitum* for one week.

4.3.4. Experimental design and induction of colitis

After one week of acclimation, the mice were randomized into four experimental groups (n = 10). Experimental diets were prepared as described in [Chapter 2](#) with a slight modification by using fish oil from Japanese pilchard (*S. melanostictus*). The mice were fed with the respective experimental diet *ad lib.* and received normal drinking water for 10 days. After the 10 days of experimental diet adaptive feeding, the blank group was orally fed with the basal diet and continued receiving normal drinking water. Colitis was induced in the control, porcine liver and ascidian muscle group by 1.5% (w/v) dextran sodium sulfate (DSS; molecular weight 36-50 kDa, MP Biomedicals LLC, CA, USA) added to the drinking water (Yamashita et al., 2020a). The control group was orally fed with the basal diet and received 1.5% DSS in drinking water. The porcine liver group was orally fed with porcine liver EtnGpl diet and received 1.5% DSS in drinking water. Lastly, the ascidian muscle group was orally fed with ascidian muscle EtnGpl diet and received 1.5% DSS in drinking water. Moreover, the four experimental groups were divided into two categories; the first category was used to determine early/middle stage of inflammation biomarkers, apoptosis-related proteins and lipid assay in the colon mucosa (n = 5) and the second category was used for histological evaluation in the late stage of inflammation (n = 5). The inflammation biomarkers (MPO, pro-inflammatory cytokines, and TBARS) and apoptosis related proteins were determined at the early/late of inflammation as indicators of inflammation initiation and more so due to the absence of blood in the feces at this stage (Yamashita et al., 2020a). During the experimental period, body weight was monitored and recorded after every two days while the diet was changed and recorded daily (Figure 4.1). All animal experiment protocols were approved by the Animal Care and Use Committee and were performed according to Obihiro University Guidelines (Permit Number 18-149).

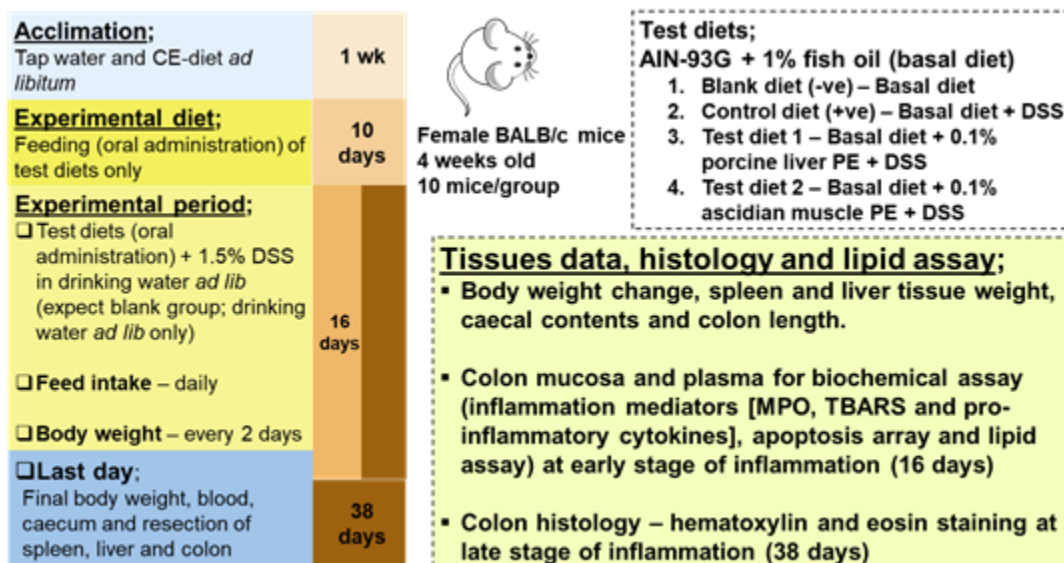


Figure 4.1 Experimental design of DSS-induced colitis in mice.

After 1 week of acclimation with chow diet *ad lib*, the experimental diets were introduced and changed everyday (about 5 g/mice/day). After 10 days of experimental diets adaptive feeding, the mice were treated with 1.5% DSS in drinking water except the blank group for 16 days (n = 5 per group) and 38 days (n = 5 per group). Diet intake was recorded everyday and body weight recorded after every two days. Day 16 was designated as the early/middle stage of inflammation and used to determine inflammatory mediators and lipid assay during initiation of inflammation. Day 38 was designated as the late stage of inflammation and used to evaluate histological damage of the colon. Body weight, colon length, spleen and liver weight were recorded for all mice.

4.3.5. Blood, Tissue and colon mucosa preparation

After 18 days, the first category of mice (early/middle stage of inflammation) were euthanized with a modified mixture of three anesthetic agents; domitor (0.3 mL), dormicum (0.8 mL), and vetorphate (1 mL) in 2.9 mL of saline. Plasma was prepared from freshly collected blood samples from the heart as previously described (Nguma et al., 2020). Liver, spleen, and caecum contents weights were determined immediately, the samples frozen in dry-ice and then kept at -80 °C. Colon length was also determined immediately followed by rinsing the colon with ice-cold saline. Colon mucosa was scraped and homogenized with 600 µl of PBS containing Protease inhibitor cocktail set III (Fujifilm Wako Pure Chemicals Corp., Gunam, Japan) and then Triton X-100 was added followed by aliquot of the homogenate and kept at -80 °C.

After 38 days, the second category of mice (late stage of inflammation) were euthanized. Plasma, liver, spleen, caecum contents, and colon were treated as described above. The colon was then opened longitudinally, Swiss rolled on a toothpick and fixed in 10% formalin.

4.3.6. Histopathological evaluation

Formalin-fixed colon tissues shall be processed for paraffin-embedding, sectioned (4-5 µm), and de-paraffinized followed by hematoxylin and eosin (H&E) staining according to the standard procedures for histological analysis. The sections shall be examined and images acquired with a light microscope (BX-51; Olympus, Tokyo, Japan).

4.3.7. Myeloperoxidase (MPO) activity in colon mucosa

MPO activity was analyzed for each mouse from samples of the colon mucosa homogenate (from the caecum to the rectum) (n = 5 per group) during the early/middle stage and late stage of inflammation. To estimate the MPO activity, the colon mucosa homogenates were thawed and homogenized with 1 mL of ice-cold 0.1M phosphate buffer (pH 6) containing 0.5% (w/v) hexadecyltrimethylammonium bromide. The homogenates were freeze-thawed three times, and centrifuged at 12,000 rpm for 15 min at 4 °C. The supernatant was analyzed using MPO

chlorination activity assay kit to detect MPO activity, according to the manufacturer's instruction (Cell Biolabs, Inc., San Diego, CA, USA).

4.3.8. Cytokines quantification and apoptosis assay

TNF- α and IFN- γ levels in the colon mucosa and plasma were quantified using a Mouse TNF- α and IFN- γ ELISA kit (FUJIFILM Wako Shibayagi Corp., Gunma, Japan). Levels of apoptosis-related proteins in the colon mucosa were determined using a Mouse Apoptosis Array Kit (R&D Systems, Minneapolis, MN, USA). After freezing and thawing the colon mucosa homogenates, the proteins were detected according to the manufacturer's protocol. The detected apoptosis-related proteins were: B-cell lymphoma 2 (Bcl-2), Bcl/leukemia x (Bcl-x), catalase, claspin, MCL-1, p27 cyclin-dependent kinase 4 inhibitor 1B (p27/Kip1), X-linked inhibitor of apoptosis (XIAP), Bcl-xL/Bcl-2 associated death promoter (Bad), cytochrome c, second mitochondria-derived activator of caspase/direct inhibitor of apoptosis-binding protein with low pI (SMAC/Diablo), fibroblast-associated (Fas), TNF receptor 1 (TNF R1), TNF-related apoptosis-inducing ligand receptor 2 (TRAIL R2), cleaved caspase-3, p53, hypoxia-inducible transcription factor (HIF)-1 α , heme oxygenase (HO)-1, HO-2, heat shock protein (HSP)27, HSP60, and HSP70.

4.3.9. Lipid assay in colon mucosa, and plasma

The phospholipid fractions from plasma and colon mucosa homogenates were extracted according to our previous report (Otoki et al., 2017). Phospholipid species were analyzed using liquid chromatography-tandem mass spectrometry (LC-MS/MS) operated in the multiple reaction monitoring (MRM) mode. Fatty acid methyl esters (FAME) and dimethyl acetals (DMA) were prepared from lipid extracts and analyzed by gas chromatography (Yamashita et al., 2019).

4.3.10. Other assays

Thiobarbituric acid-reactive substances (TBARS) levels of the diets, and the colon mucosa were determined according to the method by Ohkawa et al.,(1979). The protein levels of the samples were measured using the DC Protein Assay kit (Bio-Rad, Hercules, CA, USA).

4.3.11. Statistical analysis

The results are represented as means \pm SEM. All data were subjected to analysis of variance using SPSS software (version 17.0; SPSS Inc., Chicago, IL, USA). Differences between the means were tested using one-way ANOVA followed by Tukey's post-hoc test. Values of $P < 0.05$ were considered statistically significant.

4.4. RESULTS

4.4.1. EtnGpl Fractions from Porcine Liver and Ascidian Muscle

The alkenyl moieties in porcine liver EtnGpl mainly consisted of 18:0ol and 16:0ol, and the prominent acyl moieties were ARA and 18:0 (Table 4.1A), while the main phospholipid species was PtdEtn-18:0/20:4 (Table 4.1B). The alkenyl moieties in ascidian muscle mainly comprised of 18:0ol, and the prominent acyl moieties were EPA, and DHA (Table 4.1A), while the main phospholipid species were PlsEtn-18:0/20:5, PlsEtn-18:0/22:6, and PtdEtn-18:0/22:6 (Table 4.1B). The PlsEtn level in porcine liver EtnGpl (7.7 mol% in EtnGpl) was lower compared to that of ascidian muscle EtnGpl (86.2 mol% in EtnGpl). Furthermore, the ratio of n-3/n-6 and (EPA + DHA)/ARA in porcine liver EtnGpl was lower compared to ascidian muscle EtnGpl.

Table 4.1 Composition of acyl and alkenyl chains (A), and phospholipid species (B) of prepared EtnGpl (mol%)

| A | Porcine liver EtnGpl | Ascidian muscle EtnGpl | B | Porcine liver EtnGpl | Ascidian muscle EtnGpl |
|----------------|-------------------------|---------------------------|---|-------------------------|---------------------------|
| Acyl (mol%) | | | Species <i>sn</i> -1/ <i>sn</i> -2 (mol%) | | |
| 16:0 | 6.8 | 1.3 | PlsEtn-18:0/18:1 | 0.4 | 2.2 |
| 18:0 | 36.8 | 3.8 | PlsEtn-18:0/20:4 | 2.1 | 3.5 |
| 18:1n-9 | 4.3 | 2.0 | PlsEtn-18:0/20:5 | Traces | 53.1 |
| 18:2n-6 | 7.0 | nd | PlsEtn-18:0/22:6 | 0.2 | 12.4 |
| 18:3n-6 | 0.1 | 0.9 | PlsCho-18:0/18:1 | nd | Traces |
| 20:3n-6 | 0.4 | nd | PlsCho-18:0/20:4 | nd | nd |
| 20:4n-6 | 30.6 | 1.8 | PlsCho-18:0/22:6 | nd | nd |
| 20:5n-3 | 0.6 | 33.7 | PtdEtn-18:0/18:1 | 5.6 | 0.8 |
| 22:5n-3 | 2.0 | 0.4 | PtdEtn-18:0/20:4 | 69.2 | 0.5 |
| 22:6n-3 | 4.8 | 10.0 | PtdEtn-18:0/22:6 | 5.5 | 7.4 |
| n-3/n-6 | 0.2 | 23.2 | PtdCho-18:0/18:1 | Traces | Traces |
| (EPA+DHA)/ARA | 0.2 | 24.1 | PtdCho-18:0/20:4 | Traces | Traces |
| Alkenyl (mol%) | | | PtdCho-18:0/22:6 | Traces | Traces |
| 16:0ol | 1.5 | 4.7 | LysoPlsEtn-16:0 | Traces | Traces |
| 18:0ol | 2.0 | 36.0 | LysoPlsEtn-18:0 | Traces | 0.5 |
| 18:1ol | 0.4 | 2.4 | LysoPlsCho-16:0 | nd | nd |
| Total | 3.9 | 43.1 | LysoPlsCho-18:0 | nd | nd |
| | | | LysoPtdEtn-16:0 | 0.1 | Traces |
| | | | LysoPtdEtn-18:0 | 0.3 | 0.1 |

EtnGpl ethanolamine glycerophospholipids, *DHA* docosahexaenoic acid (22:6n-3), *ARA* arachidonic acid (20:4n-6), *PlsEtn/Cho* ethanolamine/choline plasmalogen, *PtdEtn/Cho* phosphatidylethanolamine/choline, *Lyso-PtdEtn/Cho* Lysophosphatidylethanolamine/choline, *Lyso-PlsEtn/Cho* Lysoethanolamine/choline plasmalogen, *nd* not detected.

4.4.2. Fish and Soy Oil Acyl and Alkenyl Chains

The acyl and alkenyl chains of fish and soy oil are as shown in Table 4.2. The fish oil contained 31.2 mol% EPA (20:5n-3) and 12.0 mol% DHA (22:6n-3). The major saturated (SFA) and monounsaturated fatty acid were

palmitic acid (16:0, 10.7 mol%), and palmitoleic acid (16:1n-9, 12.7 mol%), and oleic acid (18:1n-9, 6.7 mol%). The major n-3 PUFA, DHA and EPA had the highest proportion (43.2 mol%) while n-6 ARA was 1.4 mol%. This led to the high ratio of n-3/n-6 and (EPA+DHA)/ARA. Soy oil used is as described in [Chapter 2](#).

Table 4.2 Composition of acyl and alkenyl chains (mol%) in fish and soy oil

| | Fish oil (Japanese pilchard) | Soy oil |
|--------------------|---------------------------------|---------|
| Acyl chains (mol%) | | |
| 16:0 | 10.7 | 11.5 |
| 16:1n-7 | 12.7 | 0.1 |
| 18:0 | 2.7 | 4.2 |
| 18:1n-9 | 6.7 | 23.5 |
| 18:2n-6 | 1.2 | 54.2 |
| 18:3n-6 | 0.4 | nd |
| 18:3n-3 | 0.7 | 6.6 |
| 20:4n-6 | 1.4 | nd |
| 20:5n-3 | 31.2 | nd |
| 22:5n-3 | 2.6 | nd |
| 22:6n-3 | 12.0 | nd |
| ΣSFA | 23.3 | 15.7 |
| ΣMUFA | 26.0 | 23.6 |
| ΣPUFA | 54.4 | 60.7 |
| Σn-3 | 46.5 | 6.6 |
| Σn-6 | 4.0 | 54.2 |
| EPA + DHA | 43.2 | 0.0 |
| PUFA/SFA | 2.3 | 3.9 |
| n-3/n-6 | 11.5 | 0.1 |
| DHA/AA | 8.3 | 0.0 |
| (EPA + DHA)/ARA | 29.9 | 0.0 |

Fish oil from Japanese pilchard, *S. melanostictus* (Schlegel, 1846); *nd* not detected.

4.4.3. Diet Lipid Composition

The main acyl chains in the diets were palmitic acid, oleic acid, linoleic acid, EPA, and DHA (Table 4.3). The ratio of (EPA+DHA)/ARA in the porcine liver EtnGpl diet was lower than that of basal and ascidian muscle EtnGpl diets due to the slightly higher levels of ARA in porcine liver EtnGpl. All the other acyl chains levels were relatively the same among the diets resulting in a similar n-3/n-6 ratio. Importantly, ascidian muscle EtnGpl diet had a higher abundance of alkenyl chains i.e. plasmalogens than porcine liver EtnGpl and basal diets.

Table 4.3 Composition of acyl and alkenyl chains ($\mu\text{mol}/100\text{g}$) in the experimental diet

| | Basal diet | Porcine liver EtnGpl diet | Ascidian muscle EtnGpl diet |
|---|------------|---------------------------|-----------------------------|
| Acyl ($\mu\text{mol}/100\text{g}$) | | | |
| 16:0 | 4704.2 | 4735.8 | 4708.2 |
| 18:0 | 1415.3 | 1587.0 | 1427.4 |
| 18:1n-9 | 5913.9 | 5933.9 | 5920.3 |
| 18:1n-7 | 691.2 | 698.5 | 693.4 |
| 18:2 n-6 | 10159.2 | 10191.9 | 10159.7 |
| 18:3 n-3 | 1297.3 | 1297.6 | 1300.2 |
| 18:3 n-6 | 178.9 | 180.8 | 179.0 |
| 20:3 n-6 | 11.2 | 12.0 | 11.4 |
| 20:4 n-6 | 353.1 | 495.9 | 358.8 |
| 20:5 n-3 | 7622.7 | 7625.7 | 7729.0 |
| 22:4 n-6 | 236.8 | 241.5 | 236.8 |
| 22:5 n-3 | 629.1 | 638.2 | 630.5 |
| 22:6 n-3 | 2937.2 | 2959.4 | 2968.6 |
| n-3/n-6 | 0.9 | 0.9 | 0.9 |
| (EPA + DHA)/ARA | 29.9 | 21.3 | 29.8 |
| Alkenyl ($\mu\text{mol}/100\text{g}$) | | | |
| 16:0ol | nd | 6.8 | 14.9 |
| 18:0ol | nd | 9.5 | 113.8 |
| 18:1ol | nd | 1.7 | 7.6 |
| Total | - | 18.0 | 136.3 |

4.4.4. Dietary EtnGpl suppresses the progression of DSS-induced colitis

During the DSS treatment, significant body weight change among the four mouse groups was observed from day 34 as shown in Figure 4.2a. At day 38, the blank group has significantly higher body weight compared to control group ($P < 0.05$). The ascidian muscle group showed an increased body weight compared to the control group, while no change in body weight was observed between the porcine liver group and the control group.

After 16 days of DSS treatment (early/middle stage of inflammation), the mice ($n = 5$) were sacrificed and the colon length and spleen weights were determined. The colon length was significantly longer in the blank group compared to the control group, while no change in colon length was observed among EtnGpl groups and the control group (Figure 4.2b). The spleen weight was significantly increased in control group compared to the blank, while there was a weight decrease in EtnGpl groups compared to the control group (Figure 4.2c).

After 38 days of DSS treatment (late stage of inflammation), the mice (n = 5) were sacrificed and the colon length and spleen weights were determined. The colon length was significantly longer in the blank group compared to the control group, while ascidian muscle group showed significant increase in colon length compared to porcine liver and control groups (Figure 4.2b) ($P < 0.05$). The spleen weight change had a similar trend as observed in early/middle stage of inflammation.

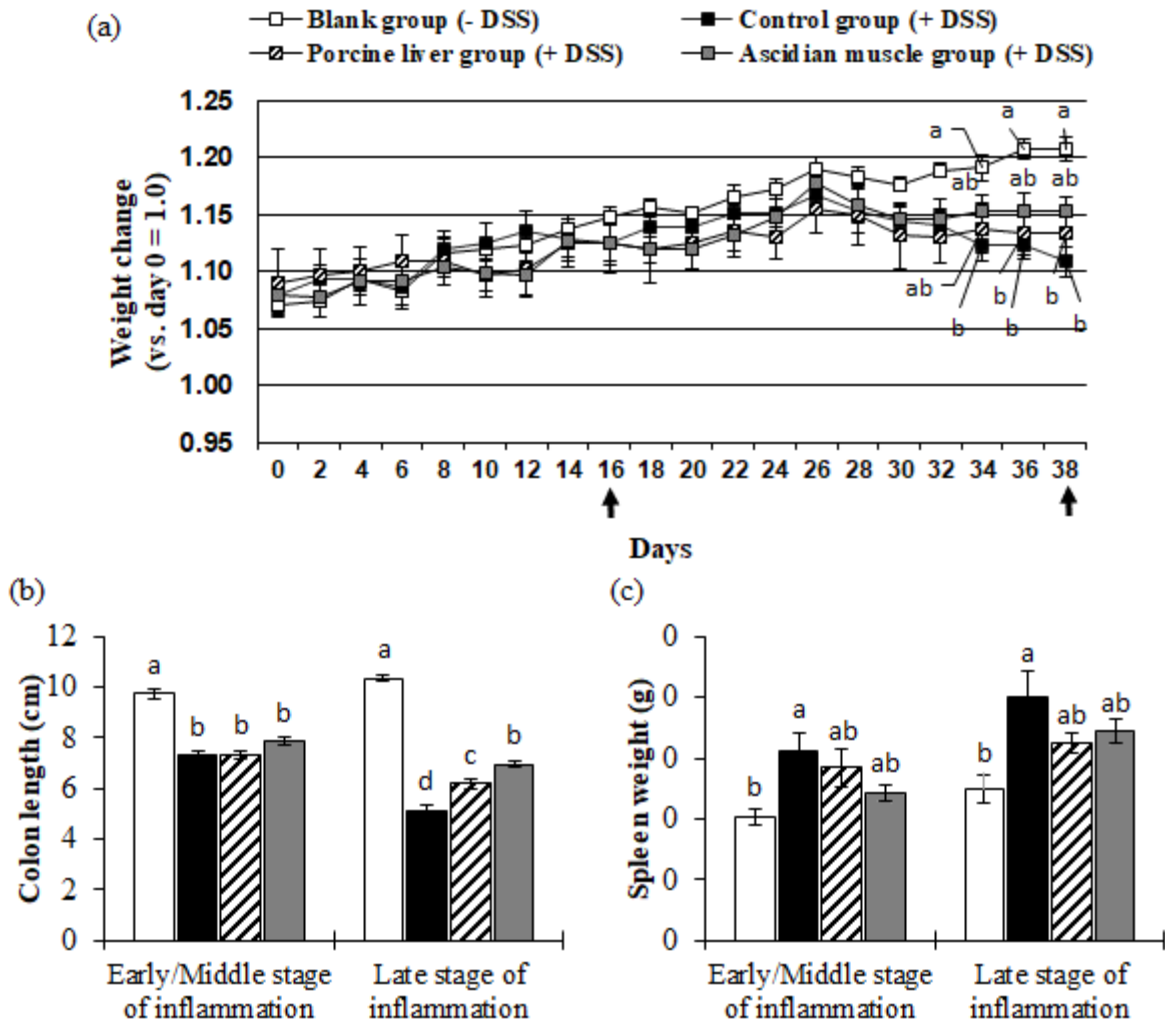


Figure 4.2 General evaluation of effects of dietary EtnGpl on DSS-induced colitis in mice

(a) Body weight change; (b) colon length; and (c) spleen weight. Body weight change was calculated as a fold change compared to the original body weight (day 0).

↑ : Day of dissection; first for inflammation biomarkers (early/middle stage of inflammation); second for other analyses (late stage of inflammation). The values are expressed as the mean \pm SEM (n = 5). Different letters indicate significant differences at $P < 0.05$, determined by ANOVA (Tukey's test).

4.4.5. Dietary EtnGpl attenuates inflammatory mediators in the colon mucosa

To confirm the inflammatory destruction of the colon epithelial layer by potentially elevated neutrophils infiltration, we quantified MPO activity in the colon mucosa. The MPO activity was significantly increased in the control group compared to the blank group ($P < 0.05$) (Figure 4.3a). The elevated MPO activity in DSS treated control group was significantly reduced by dietary ascidian muscle EtnGpl with high PlsEtn levels (ascidian muscle group) ($P < 0.05$), whereas porcine liver EtnGpl with low PlsEtn levels (porcine liver group) showed a downward trend of MPO activity levels. Moreover, a similar trend was observed with the levels of TBARS in the colon mucosa as a measure of lipid peroxidation. DSS treatment significantly increased TBARS levels, which were significantly reduced in porcine liver and ascidian muscle groups ($P < 0.05$) (Figure 4.3b).

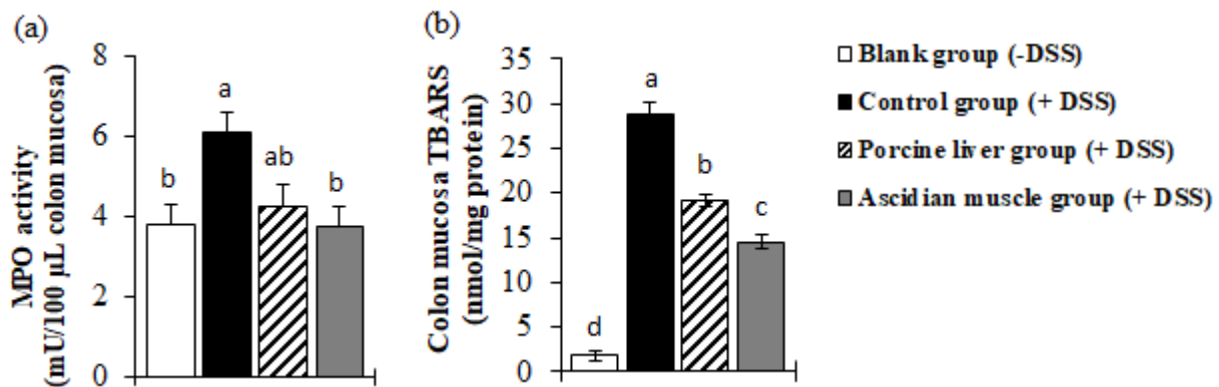


Figure 4.3 Dietary EtnGpl is associated with decreased inflammatory mediators in the colon mucosa of DSS-induced colitis in mice

Inflammatory mediators were analyzed in the colon mucosa; (a) myeloperoxidase (MPO) activity, and (b) thiobarbituric acid-reactive substances (TBARS). The values are expressed as the mean \pm SEM ($n = 5$). Different letters indicate significant differences at $P < 0.05$, determined by ANOVA (Tukey's test).

The effect of dietary EtnGpl with high and low PlsEtn levels on colon mucosa and circulating pro-inflammatory cytokines were analyzed using ELISA. In the colon mucosa, TNF- α was not significantly affected among the four mouse groups, however DSS treated control group showed a tendency to increase TNF- α levels by 33% compared to the blank group, which was slightly decreased in porcine liver and ascidian muscle groups by 16% and 24%, respectively. (Figure 4.4a). Similarly, DSS treated control group showed an upward trend in IFN- γ levels in the colon mucosa compared to the blank group. Porcine liver group showed a decrease in the overregulated IFN- γ levels by DSS treatment, while ascidian muscle group showed a significant downregulation of the elevated IFN- γ levels by DSS treatment ($P < 0.05$) (Figure 4.4b).

In addition, DSS treatment showed an upward trend in circulating TNF- α and IFN- γ levels compared to the blank group (Figure 4.4c and d). Porcine liver group with low levels of dietary PlsEtn showed a downward trend in plasma TNF- α and IFN- γ levels while ascidian muscle group with high levels of dietary PlsEtn significantly downregulated TNF- α and IFN- γ levels compared to the DSS treated mice ($P < 0.05$).

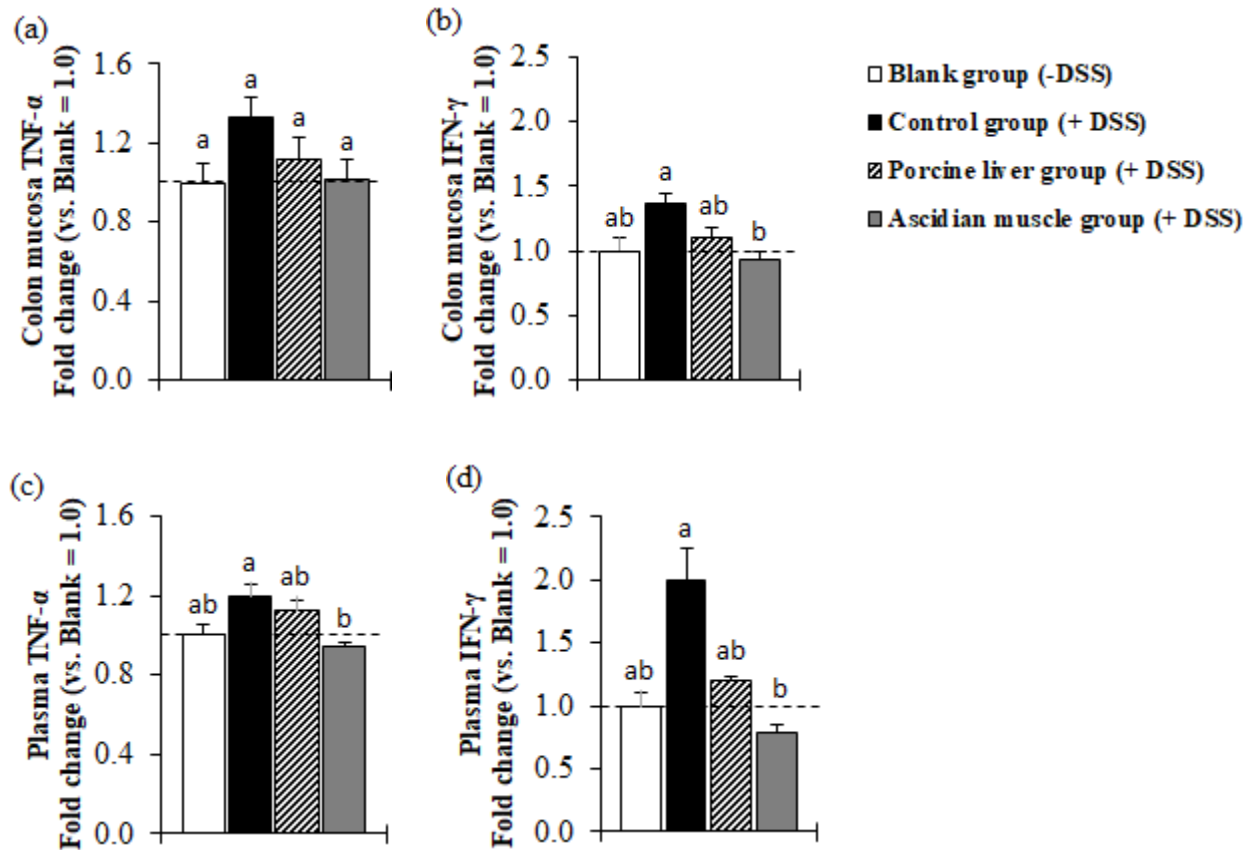


Figure 4.4 Effect of dietary EtnGpl on pro-inflammatory mediators in the colon tissue and plasma of DSS-induced colitis in mice

(a and b) Colon mucosa tumor necrosis factor (TNF)- α and interferon (IFN)- γ , and (c and d) plasma TNF- α and IFN- γ levels analyzed by ELISA. The values are expressed as the mean \pm SEM ($n = 5$). Different letters indicate significant differences at $P < 0.05$, determined by ANOVA (Tukey's test).

4.4.6. Dietary EtnGpl modulates apoptosis-related proteins in the colon mucosa

Next, we sought to determine whether oral administration of EtnGpl with high and low PlsEtn levels modulated apoptosis-related proteins in the colon mucosa of DSS-induced colitis in mice (Figure 4.5). DSS treated mice showed an upward trend in proapoptotic Bad, cytochrome c and p53 proteins compared to the blank group (Figure 4.5a). Moreover, DSS treatment in control group upregulated the relative levels of Bcl-2 and p27 antiapoptotic proteins, cleaved caspase-3 apoptosis executioner protein, and TNF R1 death receptor protein

compared to the blank group ($P < 0.05$). On the other hand, porcine liver group showed a downward trend in the relative levels of proapoptotic cytochrome c protein, apoptosis executioner cleaved caspase-3 protein, and antiapoptotic Bcl-2, and Bcl-x proteins compared to DSS treated mice. Notably, ascidian muscle group showed a significant downregulation of the relative levels of proapoptotic Bad, cytochrome c, SMAC/Diablo proteins, antiapoptotic Bcl-x protein, apoptosis executioner cleaved caspase-3 protein, and TNF R1 and TRAIL R2 death receptor proteins compared to the DSS treated mice ($P < 0.05$).

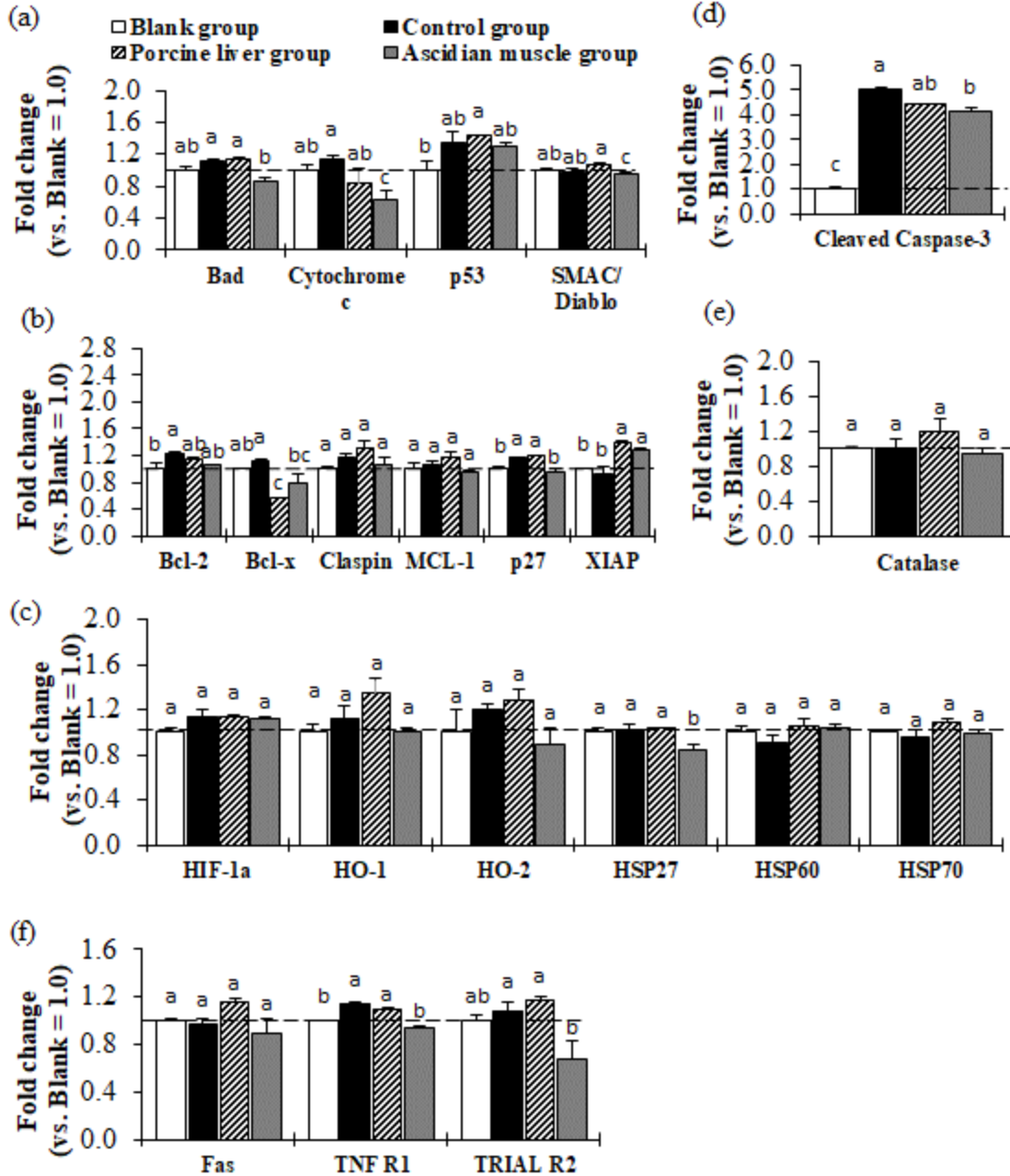


Figure 4.5 Effect of dietary EtnGpl on relative levels of apoptosis-related proteins (fold change vs. blank) in DSS-induced colitis in mice.

(a) Proapoptotic proteins. (b) Antiapoptotic proteins. (c) Cysteine proteases. (d) Other apoptosis-related proteins. (e) Death receptors. (f) Antibody proteins. The dashed line indicates the blank group = 1.0. Different letters indicate significant differences at $P < 0.05$, determined by ANOVA (Tukey's test).

4.4.7. Dietary EtnGpl alters tissues lipid composition

After 16 days of DSS treatment (early/middle stage of inflammation), acyl and alkenyl chains in the phospholipid fraction of the mice colon mucosa and plasma were analyzed. In the colon mucosa, DSS treatment in the control group did not alter the composition of acyl chains compared to the blank group (Table 4.4). Similarly, the composition of acyl chains in porcine liver and ascidian muscle group were not altered compared to the control group. Moreover, the n-3/n-6 ratio remained relatively the same among the four mice groups. Notably, DSS treatment in the control group significantly lowered the 18:0ol alkenyl chain ratio and total plasmalogens (alkenyl chains) compared with the blank group. Despite of the observed decrease, the porcine liver and ascidian muscle groups showed significantly increased 18:0ol alkenyl chain ratio and total alkenyl chains compared to the control group, with ascidian muscle group showing significantly the highest levels ($P < 0.05$).

Table 4.4 Composition of acyl and alkenyl chains (mol%) in colon mucosa phospholipid fraction after 16 days of DSS-induced colitis (early/middle stage of inflammation)

| | Blank group | Control group | Porcine liver group | Ascidian muscle group |
|-----------------------|-------------|---------------|---------------------|-----------------------|
| DSS | - | + | + | + |
| Acyl (mol%) | | | | |
| 16:0 | 43.2 ± 8.7a | 50.3 ± 12.2a | 36.7 ± 1.3a | 46.4 ± 3.4a |
| 18:0 | 12.1 ± 5.0a | 10.8 ± 0.3a | 12.3 ± 0.9a | 17.1 ± 2.2a |
| 18:1n-9 | 19.6 ± 5.7a | 22.5 ± 7.9a | 25.7 ± 0.9a | 17.8 ± 2.8a |
| 18:2n-6 | 13.8 ± 6.0a | 9.0 ± 3.3a | 15.0 ± 1.2a | 8.8 ± 2.3a |
| 18:3n-3 | 0.5 ± 0.2a | 0.5 ± 0.1a | 0.6 ± 0.1a | 0.7 ± 0.1a |
| 20:4n-6 | 1.1 ± 0.2a | 0.8 ± 0.2a | 1.7 ± 0.1a | 1.2 ± 0.3a |
| 20:5n-3 | 0.8 ± 0.1a | 0.3 ± 0.1a | 0.5 ± 0.0a | 0.4 ± 0.1a |
| 22:5n-3 | 0.2 ± 0.0a | 0.1 ± 0.0a | 0.1 ± 0.0a | 0.2 ± 0.0a |
| 22:6n-3 | 0.5 ± 0.1a | 0.3 ± 0.1a | 0.6 ± 0.1a | 0.5 ± 0.1a |
| n-3/n-6 | 0.4 ± 0.3a | 0.2 ± 0.1a | 0.1 ± 0.0a | 0.2 ± 0.0a |
| (EPA + DHA)/ARA | 1.3 ± 0.2a | 0.8 ± 0.0ab | 0.6 ± 0.0b | 0.7 ± 0.0b |
| Alkenyl (mol%) | | | | |
| 16:0ol | 0.2 ± 0.1a | nd | 0.1 ± 0.0a | 0.2 ± 0.0a |
| 18:0ol | 0.7 ± 0.3b | 0.5 ± 0.0c | 0.7 ± 0.0b | 1.3 ± 0.3a |
| 18:1ol | nd | nd | 0.2 ± 0.1a | 0.1 ± 0.0ab |
| Total | 0.9 ± 0.2b | 0.5 ± 0.2c | 1.0 ± 0.0b | 1.7 ± 0.3a |

Means ± SEM, n = 5

Different letters indicate significant difference at $P < 0.05$ determined by ANOVA (Tukey's test).

In the plasma, we observed alteration of several acyl chains in the control group compared to the blank group as well as in porcine liver and ascidian muscle groups compared to the control, however the n-3/n-6 ratio was relatively the same among the four mice groups (Table 4.5). Importantly, DSS treatment in the control group showed lower 18:0ol alkenyl chain ratio and total plasmalogens (alkenyl chains) compared with the blank group. Despite of the observed decreasing trend, the porcine liver and ascidian muscle groups showed significantly increased 18:0ol alkenyl chain ratio and total alkenyl chains compared to the control group, with ascidian muscle group showing significantly the highest levels ($P < 0.05$).

Table 4.5 Composition of acyl and alkenyl chains (mol%) in plasma phospholipid fraction after 16 days of DSS-induced colitis (early/middle stage of inflammation)

| | Blank group | Control group | Porcine liver group | Ascidian muscle group |
|-----------------------|-------------|---------------|---------------------|-----------------------|
| DSS | - | + | + | + |
| Acyl (mol%) | | | | |
| 16:0 | 24.0 ± 0.4a | 23.8 ± 0.6a | 24.5 ± 0.3a | 25.0 ± 0.4a |
| 18:0 | 10.3 ± 0.3b | 12.0 ± 0.3a | 12.2 ± 0.6a | 11.3 ± 0.0a |
| 18:1n-9 | 14.5 ± 0.6a | 10.6 ± 0.5b | 11.0 ± 0.2b | 12.1 ± 0.2b |
| 18:2n-6 | 23.8 ± 0.2a | 23.2 ± 0.2a | 23.6 ± 1.0a | 23.8 ± 0.2a |
| 18:3n-3 | 0.4 ± 0.0c | 0.4 ± 0.0b | 0.5 ± 0.0a | 0.5 ± 0.0ab |
| 20:4n-6 | 10.4 ± 0.5b | 14.1 ± 0.7a | 13.2 ± 0.3a | 11.2 ± 0.1b |
| 20:5n-3 | 2.5 ± 0.1a | 2.0 ± 0.0b | 1.5 ± 0.1c | 2.2 ± 0.1ab |
| 22:5n-3 | 0.5 ± 0.0a | 0.4 ± 0.0b | 0.4 ± 0.0b | 0.5 ± 0.0a |
| 22:6n-3 | 7.2 ± 0.1a | 8.2 ± 0.4a | 7.8 ± 0.4a | 7.8 ± 0.3a |
| n-3/n-6 | 0.4 ± 0.0a | 0.3 ± 0.0a | 0.3 ± 0.0a | 0.4 ± 0.0a |
| (EPA + DHA)/ARA | 0.9 ± 0.1a | 0.7 ± 0.0b | 0.7 ± 0.0b | 0.9 ± 0.0a |
| Alkenyl (mol%) | | | | |
| 16:0ol | 0.1 ± 0.0a | 0.1 ± 0.0a | 0.1 ± 0.0a | 0.1 ± 0.0a |
| 18:0ol | 0.2 ± 0.0bc | 0.1 ± 0.0c | 0.3 ± 0.0b | 0.6 ± 0.0a |
| 18:1ol | 0.1 ± 0.0 | nd | nd | nd |
| Total | 0.4 ± 0.0bc | 0.2 ± 0.0c | 0.4 ± 0.0b | 0.7 ± 0.0a |

Means ± SEM, n = 5

Different letters indicate significant difference at P < 0.05 determined by ANOVA (Tukey's test).

4.5. DISCUSSION

In the present study, we demonstrate that dietary intake of EntGpl with high PlsEtn levels might be utilized as a functional food with possible preventive strategy against IBD, especially UC. Our results show that diet with high PlsEtn levels might regulate intestinal inflammation in DSS-induced colitis by improving reduction in body weight, shortening of colon length, and increasing of spleen weight.. Our study also confirmed the potential of dietary PlsEtn to downregulate colon mucosa pro-inflammatory cytokines and apoptosis-related protein levels, which are indicators of colitis progression. Notably, dietary PlsEtn elevated the levels of total alkenyl chains (i.e. plasmalogens) in the colon mucosa and the plasma. This suggest that dietary EtnGpl containing high PlsEtn ratio alleviated syndromes of DSS-induce colitis. To our knowledge, this is the first study to show the functional role of dietary PlsEtn in suppressing DSS-induced experimental colitis and partly the underlying mechanisms.

Mice treated with DSS for 32 days have severe illness as indicated by higher disease activity index, that is, significant weight loss, rectal bleeding, and diarrhea compared to the healthy control groups (Cai et al., 2019). Moreover, it is generally accepted that colon length is shortened while spleen weight increases with the severity of DSS-induced colitis (Oh et al., 2014). Furthermore, the shortening of colon length is hypothesized to occur due to thickening of the mucosal layers due to inflammation, edema, and muscular hypertrophy (Kraft and Kirsner, 1971). In the present study, the dramatic weight loss, shortening of colon length and increase in the spleen weight in control group compared to the blank group confirmed induction of inflammatory process in DSS-treated mice ([Figure 4.2](#)). Markedly, oral administration of EtnGpl with high PlsEtn level compared to low PlsEtn level significantly diminished the progression of inflammatory process caused by DSS. Therefore, the present findings indicate that diets with high PlsEtn ratio have the potential to effectively prevent the advancement of colitis in DSS-treated mice.

Patients with IBD have increased infiltration of immune cells, which is similar to the situation in DSS-induced colitis in mice (Hu et al., 2019). It has been shown that DSS-induced colitis is characterized by infiltration of inflammatory cells in the colon epithelial layers, which leads to the deterioration of the mucosal layers and damage of colon crypts (Lu et al., 2003; Woo et al., 2016). MPO activity is widely recognized as a colon inflammatory mediator indicator, and it also correlates with neutrophil infiltration (Krawisz et al., 1984). Moreover, the infiltration of neutrophils has been reported in DSS-treated mice, accompanied by oxidative stress (Alex et al., 2009). Oxidative stress accentuates the severity of colon inflammation by sustaining an overproduction of ROS and acute lipid peroxidation (Grisham and Granger, 1988; Medicherla et al., 2015). In the present study, DSS treatment significantly elevated MPO activity in the colon mucosa, which was significantly lowered by diet with high PlsEtn ratio as compared to diet with low PlsEtn ratio. Moreover, dietary PlsEtn similarly, significantly lowered the increased levels of TBARS in DSS treated mice ([Figure 4.3a and b](#)). Food compounds with antioxidants have been found to be effective in attenuating colitis (Han et al., 2019), suggesting that the DSS-induced neutrophil infiltration and tissue damage due to lipid peroxidation in the colon mucosa and were suppressed by dietary PlsEtn.

Uncontrolled upregulation of colon mucosa and circulating pro-inflammatory cytokines is a biomarker of inflammation in IBD (Andoh et al., 2008; Sanchez-muñoz et al., 2008). DSS-treated mice have drastic enhanced secretion of pro-inflammatory cytokines in the colon mucosa such as TNF- α , IFN- γ , and IL-1 β compared to untreated mice (Han et al., 2019). In this study, we observed TNF- α levels in the colon mucosa of dietary PlsEtn-administered groups had a downward trend and a significant downregulation of IFN- γ level in colon mucosa and circulating TNF- α and IFN- γ levels ([Figure 4.4](#)). Cytokine-induced elevated MPO levels and also leads to ROS generation (Jena et al., 2012). Moreover, immune cells are the major producers of the various cytokines.

Considering that dietary PlsEtn lowered the infiltration of neutrophils and pro-inflammatory cytokines, our findings suggest that PlsEtn in the colon mucosa and plasma partly contributed in normalizing the cellular processes in the colon mucosa by inhibiting immune cell influx and overproduction of pro-inflammatory cytokines.

Colon mucosa oxidative stress as a result of pro-inflammatory cytokines accentuates ROS metabolism and excessive activation of apoptosis. This creates an increased pro-inflammatory cellular microenvironment that further heightens oxidative stress, leading to colon mucosa epithelial cells damage and destruction of intestinal barrier integrity (Shi et al., 2019). In our study, we observed an increase in Bad, cytochrome c, and p53 proapoptotic proteins, Bcl-2, and Bcl-x antiapoptotic proteins, TNF R1 and TRAIL R2 death receptor proteins and importantly apoptosis executioner cleaved caspase-3 in DSS-treated mice, which were significantly downregulated by diet with high PlsEtn level ([Figure 4.5](#)). This indicates that dietary PlsEtn regulated apoptosis in the colon mucosa by modulating apoptosis-related proteins; therefore, dietary PlsEtn might be beneficial for treating IBD. Considering TBARS levels as an indicator of lipid peroxidation due to oxidative stress was decreased in dietary PlsEtn-administered groups, further confirms the suppression of apoptosis by dietary PlsEtn. Moreover, this provides evidence on the functional role of dietary PlsEtn in suppressing tissue damage during DSS-induced colitis in mice. Additionally, the observed downward trend of TNF- α level by dietary PlsEtn explains the downregulation of TNF R1 death receptor protein in the colon mucosa. Taken together, these suggest PlsEtn inhibited apoptosis in the colon mucosa of DSS-induced colitis via mitochondria-dependent and death receptor-dependent apoptosis pathways.

Absorption of dietary PlsEtn begins with hydrolysis by pancreatic phospholipase A2 (PLA2) at the *sn*-2 position to yield lysoPlsEtn and fatty acids, which are taken up into the enterocytes, re-esterified, and then form chylomicrons that move to the lymphatic system and then enter the circulation (Zhang et al., 2019). Our results show that DSS-treatment decreased plasmalogens (alkenyl chains) in the colon mucosa and in the circulation compared to the blank group ([Table 4.4 and 4.5](#)). This might be a result of increase in utilization of PlsEtn to protect mucosal cells from the induced oxidative stress during DSS-treatment and/or the initiation of apoptosis and tissue damage during the early/middle stage of inflammation. We have previously shown that dietary absorption of EtnGpl with high PlsEtn levels increases the levels of PlsEtn, PlsChom PtdCho, and lysoPtdEtn species in the colon mucosa during colon carcinogenesis (Nguma et al., 2020). The anti-oxidant effect of PlsEtn is associated with the vinyl ether linkage, which makes PlsEtn a scavenger of oxygen free radicals in biological membranes (Hahnel et al., 1999). In our present study, dietary PlsEtn increased the levels of plasmalogens (alkenyl chains) in the colon mucosa and in the circulation of DSS-treated mice compared to the control group. Notably, diet with high levels of PlsEtn led to significantly higher tissue plasmalogens than diet with low PlsEtn.

Similarly, diet with high PlsEtn levels achieved better progression of DSS-induced symptoms, decreased mucosal inflammatory mediators, and apoptosis. Moreover, the superiority of PlsEtn to inhibit oxidative stress, neuronal injury, apoptosis and neuro-inflammation has been demonstrated (Che et al., 2018a); therefore, the consistency in our observed results strongly suggest that the abundance of vinyl ether linkages in the diet significantly contributed to the observed alleviation of DSS-induced colitis characteristics.

4.6. CONCLUSION

Based on our results, we demonstrated for the first time the protective effect of dietary PlsEtn against the progression of colon inflammation in DSS-induced colitis in mice. The amelioration of DSS-induced colitis was strongly associated with normalization of colon mucosa functions by dietary PlsEtn as a result of reduction in immune cell infiltration, pro-inflammatory cytokines, and oxidative stress in the colon mucosa. The observed effects of dietary PlsEtn are thought to be from the increased levels of PlsEtn in the colon mucosa of DSS-treated mice. Notably, the diet with high PlsEtn level showed superior effects in alleviating DSS-induced colitis compared to the diet with low PlsEtn levels. Overall, our findings provide a strong correlation of dietary PlsEtn and amelioration of DSS-induced colitis in mice. This highlights the potential of utilizing food sources rich in PlsEtn for the prevention of chronic colon inflammation, a risk of colon cancer development.

5. GENERAL DISCUSSION

Dietary glycerophospholipids with specific lipid composition have the potential to alter cellular membrane composition, leading to the modulation of cells functionality like signaling, transport and adaption to cellular environmental factors like oxidative stress (Küllenberg et al., 2012). Furthermore, alteration of lipid metabolism can cause the development and progression of many diseases such as inflammation, diabetes, neurological disorders, and cancer (Huang and Freter, 2015). Therefore, careful selection of dietary lipids depending on their lipid composition can play a crucial role in human health. Ethanolamine plasmalogen (PlsEtn) was selected in this study due to its reported anti-oxidant potential from the vinyl ether linkage at the *sn*-1 position (Braverman and Moser, 2012). In addition, the vinyl ether linkage has been suggested to inhibit oxidative stress, neuronal injury, apoptosis, and neuro-inflammation (Ifuku et al., 2012; Yamashita et al., 2015; Che et al., 2018a). Moreover PlsEtn as well as fish oil, are enriched with eicosapentaenoic acid (EPA, 20:5n-3) and docosahexaenoic acid (DHA, 22:6n-3), which are metabolized into eicosanoids and docosanoids with anti-inflammatory effects (Gil, 2002; Yamashita et al., 2016a). However, the functional role and metabolism of PlsEtn during colon-inflammation disorders such as inflammatory bowel diseases (IBD) and colon cancer has not been fully characterized. Notably, chronic inflammation in the colon is closely associated with inflammatory bowel disease (IBD), which is a risk for colon cancer development (Coussens and Werb, 2002; Bartsch and Nair, 2006). Here we therefore aimed at investigating how dietary PlsEtn can suppress colon chronic inflammation and the associated IBD, and carcinogenic states using suitable *in vivo* and *in vitro* experimental models. This thesis represents the first step in understanding the functional role of dietary PlsEtn during colon pathophysiological state and the underlying mechanisms.

We have observed in Chapter 2 that induction of colon carcinogenesis by i.p. administration of DMH not only increased colon ACF formation, but also increased the levels of TBARS, TNF- α , cleaved caspase 3, and catalase in the colon mucosa. Moreover, DMH administration reduced the levels of PlsEtn molecular species in the colon mucosa, which suggested chronic inflammation induced by DMH utilized PlsEtn possibly as a way of protecting colon mucosa cell. Interestingly, oral administration of diet with EtnGpl, especially from ascidian muscle with high PlsEtn levels remarkably suppressed colon ACF formation and reduced the levels of TBARS, TNF- α , cleaved caspase 3, and catalase in the colon mucosa ($P < 0.05$). Importantly, orally administered EtnGpl diets, particularly ascidian muscle increased the levels of PlsEtn in the colon mucosa. In parallel, there was no change observed in the acyl chains in colon mucosa of the blank, control, porcine liver and ascidian muscle groups) due to the relatively similar of n-3/n-6 ratio in the diets as a result of incorporating 1% fish oil. Therefore, it is plausible to say that the increase in PlsEtn species in the colon mucosa contributed to the inhibition of oxidative stress and lipid peroxidation from DMH-induced carcinogenesis, hence a reduction in the intestinal

impairment observed in the mice fed with EtnGpl diets. This can be attributed to the anti-oxidant potential of vinyl ether linkage in PlsEtn (Reiss et al., 1997; Hahnel et al., 1999).

The study in Chapter 3 further elaborates the uptake of PlsEtn and its functional role during intestinal chronic inflammation state. Inflammatory stress and cell injury was induced in differentiated Caco-2 cells (exhibit similar properties to normal human colon epithelial cells) by use of LPS. LPS treated differentiated Caco-2 cells for 48 h had increased apoptotic cells and decrease in cell viability. This was attributed to the upregulation of TNF- α , proapoptotic-related proteins (Bad and cytochrome c) and apoptosis executioner proteins (pro-caspase 3 and cleaved caspase 3). Differentiated Caco-2 cells treated with LPS have been shown to enhance proapoptotic response (Jutanom et al., 2020), which was in agreement with our study. Interestingly, co-treatment of the cells with extrinsic EtnGpl from ascidian muscle with high PlsEtn, EPA and DHA compared to porcine liver EtnGpl with low PlsEtn and high ARA resulted in higher downregulation of TNF- α , Bad and cytochrome c proapoptotic-related proteins and apoptosis executioner proteins pro-caspase 3 and cleaved caspase 3 (ascidian muscle > porcine liver EtnGpl treatment). The release of cytochrome c activates initiator caspase 9, which, in turn, activates the apoptosis executioner caspase 3 resulting in apoptosis of cells (Yang et al., 2009). This explains the higher cell viability and suppression of apoptotic cells by ascidian muscle EtnGpl compared to porcine liver EtnGpl. Similar to Chapter 2, treatment of the cells with extrinsic ascidian muscle EtnGpl resulted in higher levels of intracellular PlsEtn species, EPA and DHA compared to porcine liver EtnGpl. This indicate that the increase in PlsEtn contributed to the anti-apoptotic effect observed in the human intestinal tract cell *in vitro*. Therefore, our results confirmed the anti-apoptotic potential of PlsEtn during chronic colon inflammation state and further provided the evidence that the abundance of the vinyl ether linkages provides superior anti-apoptotic effect.

In Chapter 4, ulcerative colitis, which is a form of IBD in the colon was induced by administering 1.5% DSS to mice. Mice administered with DSS for 38 days had decreased body weight, shorter colon length, and increased spleen weight. Moreover, at 16 days, which was identified as the early/middle stage of inflammation, the mice showed elevated levels of MPO, TBARS, pro-inflammatory cytokines (TNF- α and IFN- γ) and apoptosis-related proteins in the colon mucosa. Similar colitis symptoms have been reported in DSS-treated mice (Oh et al., 2014). MPO activity in DSS-treated mice is accompanied by oxidative stress, which increases the severity of colon inflammation by maintaining an overproduction of ROS and acute lipid peroxidation (Alex et al., 2009; Medicherla et al., 2015). Notably, oral intake of ascidian muscle EtnGpl diet with high PlsEtn levels diminished the progression of inflammation process by downregulating inflammatory mediators and in turn suppressed apoptosis compared to porcine liver EtnGpl diet with low PlsEtn levels and the DSS-treated mice. This observed alleviation of DSS-induced colitis symptoms was in accordance with the increased levels of colon mucosa

alkenyl chains composition (ascidian muscle > porcine liver EtnGpl). These findings provide evidence of anti-colitis effect of dietary PlsEtn, particularly PlsEtn with abundant vinyl ether linkages.

6. GENERAL CONCLUSIONS AND FUTURE PERSPECTIVES

This study has contributed knowledge on the health benefits of dietary PlsEtn in colon inflammation-associated disorders by highlighting its functional role and metabolism. Specifically, we have shown the levels of PlsEtn in the colon mucosa were decreased during induced-carcinogenesis and colitis, which are closely associated with colon chronic inflammation. Importantly, dietary and extrinsic EtnGpl increased colon mucosa and intracellular PlsEtn levels, respectively, with ascidian muscle EtnGpl containing high PlsEtn ratio showing higher levels than porcine liver EtnGpl with low PlsEtn ratio. The increase in colon mucosa and intercellular PlsEtn levels is suggested to have contributed to the anti-carcinogenic, anti-apoptotic and anti-colitis effects observed in the three studies by minimizing oxidative stress and apoptosis via downregulating inflammatory mediators and modulating apoptosis-related proteins (Figure 6.1). Our study indicates that selection of dietary lipids with specific lipid composition is crucial in alleviating intestinal inflammation-related diseases. Therefore, based on the findings in our studies, PlsEtn with abundant vinyl ether linkages can potentially be used as a strategic dietary therapy for colon inflammation-related disorders such as IBD and colon cancer.

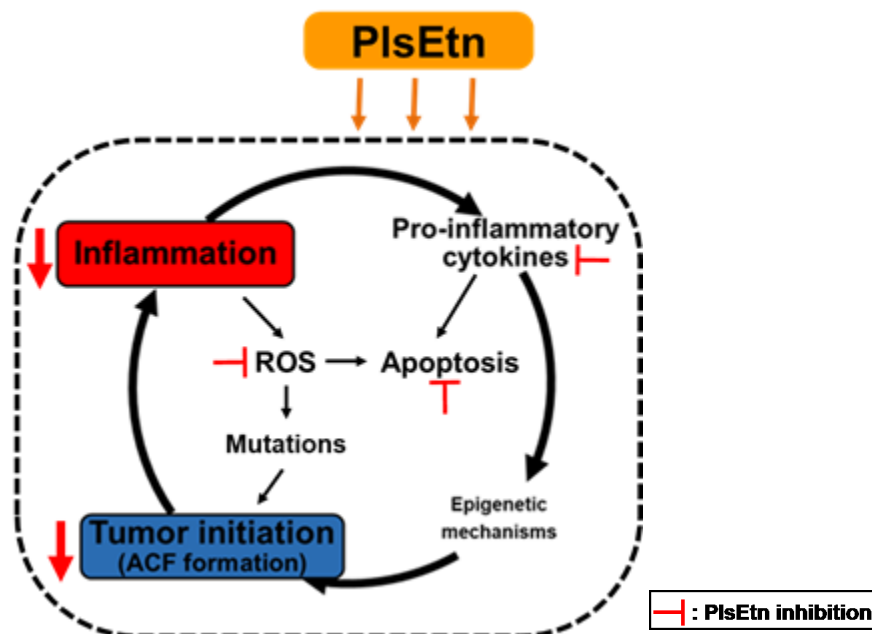


Figure 6.1 Schematic illustration of anti-carcinogenic, anti-apoptotic and anti-colitis effect of dietary

PlsEtn

ROS; Reactive oxygen species, ACF; Aberrant crypt foci

From our results, we speculate that PlsEtn metabolites, especially lyso-PlsEtn might contribute partly to the overall modulation of inflammatory mediators, and apoptosis related proteins during colon inflammation, induced-colitis and carcinogenesis. This presents an opportunity for future *in vivo* and *in vitro* studies to provide evidence. Moreover, there is limited research on the absorption of PlsEtn metabolites. We have recently demonstrated that lyoEtnGpl improves the absorption kinetics of PlsEtn *in vivo* in the plasma of mice via re-esterification (Yamashita et al., 2020b). The use of *ex vivo* model can be utilized to elucidate the absorption of lysoEtnGpl due to its simplicity and less time required as previously demonstrated (Takahashi et al., 2020). Changes in gut microbiota and the resulting microbiota metabolites have been demonstrated to be directly involved in chronic intestinal inflammation and development of colonic neoplasia (Tlakalova-Hogenova et al., 2011). Dietary PlsEtn has been shown to alleviate atherosclerosis by possibly remodeling the gut microbiota, which results in regulation of bile acid metabolism in LDLR^{-/-} mice. Therefore, it would be interesting to establish the effects dietary PlsEtn and its metabolites on colon microbiota and the resulting microbiota metabolites during induce-colitis and colon carcinogenesis.

7. REFERENCES

- Al-Abrash, A.S., Al-Quobaili, F.A., & Al-Akhras, G.N. 2000 Catalase evaluation in different human diseases associated with oxidative stress. *Saudi Medical Journal*, **9**:826–830
- Alex, P., Zachos, N., Nguyen, T., Gonzales, L., Chen, T., Conklin, L., Centola, M., & Li, X. 2009 Distinct cytokine patterns identified from multiplex profiles of murine DSS and TNBS-induced colitis. *Inflammatory Bowel Diseases*, **15**:341–352. <https://doi.org/10.1002/ibd.20753>
- Ananthakrishnan, A.N. 2015 Environmental risk factors for inflammatory bowel diseases: A review. *Digestive Diseases and Sciences*, **60**:290–298. <https://doi.org/10.1007/s10620-014-3350-9>
- Ananthakrishnan, A.N., Khalili, H., Konijeti, G.G., Higuchi, L.M., De Silva, P., Fuchs, C.S., Willett, W.C., Richter, J.M., & Chan, A.T. 2014 Long-term intake of dietary fat and risk of ulcerative colitis and Crohn's disease. *Gut*, **63**:776–784. <https://doi.org/10.1136/gutjnl-2013-305304>
- Andoh, A., Yagi, Y., Shioya, M., Nishida, A., Tsujikawa, T., & Fujiyama, Y. 2008 Mucosal cytokine network in inflammatory bowel disease **14**:5154–5161. <https://doi.org/10.3748/wjg.14.5154>
- Arai, K., Yamazaki, T., Tokuji, Y., Kawahara, M., Ohba, K., Hironaka, K., Kinoshita, M., & Ohnishi, M. 2013 Effects of chinese yam storage protein on formation of aberrant crypt foci in 1,2-dimethylhydrazine-treated mice. *Journal of Food and Nutrition Research*, **52**:139–145
- Axelrad, J.E., Lichtiger, S., & Yajnik, V. 2016 Inflammatory bowel disease and cancer: The role of inflammation, immunosuppression, and cancer treatment. *World Journal of Gastroenterology*, **22**:4794–4801. <https://doi.org/10.3748/wjg.v22.i20.4794>
- Bartsch, H., & Nair, J. 2006 Chronic inflammation and oxidative stress in the genesis and perpetuation of cancer: Role of lipid peroxidation, DNA damage, and repair. *Langenbeck's Archives of Surgery*, **391**:499–510. <https://doi.org/10.1007/s00423-006-0073-1>
- Beutler, B., Du, X., & Poltorak, A. 2001 Identification of Toll-like receptor 4 (TLR4) as the sole conduit for LPS signal transduction: genetic and evolutionary studies. *Journal of Endotoxin Research*, **7**:277–280
- Bird, R.P. 1995 Role of aberrant crypt foci in understanding the pathogenesis of colon cancer. *Cancer letters*, **93**:55–71. [https://doi.org/10.1016/0304-3835\(95\)03788-X](https://doi.org/10.1016/0304-3835(95)03788-X)
- Blander, J.M. 2016 Death in the intestinal epithelium — basic biology and implications for inflammatory bowel disease 1–11. <https://doi.org/10.1111/febs.13771>
- Bouma, G., & Strober, W. 2003 The immunological and genetic basis of inflammatory bowel disease. *Nature Reviews Immunology*, **3**:521–533. <https://doi.org/10.1038/nri1132>
- Braverman, N.E., & Moser, A.B. 2012 Functions of plasmalogen lipids in health and disease. *BBA - Molecular Basis of Disease*, **1822**:1442–1452. <https://doi.org/10.1016/j.bbadis.2012.05.008>
- Bray, F., Ferlay, J., Soerjomataram, I., Siegel, R., Torre, L., & Jemal, A. 2018 Global cancer statistics 2018: GLOBOCAN estimates of incidence and mortality worldwide for 36 cancers in 185 countries. *CA: Cancer Journal for Clinicians*, **68**:394–424. <https://doi.org/10.3322/caac.21492>
- Brites, P., Waterham, H.R., & Wanders, R.J.A. 2004 Functions and biosynthesis of plasmalogens in health and disease. *Biochimica et Biophysica Acta*, **1636**:219–231. <https://doi.org/10.1016/j.bbalip.2003.12.010>
- Bruce, W.R., & Corpet, D.E. 1996 The colonic protein fermentation and insulin resistance hypotheses for colon cancer etiology: Experimental tests using precursor lesions. *European Journal of Cancer Prevention*, **5**:41–47. <https://doi.org/10.1097/00008469-199612002-00007>
- Byers, T. 1996 Nutrition and cancer among American Indians and Alaska natives. *Cancer*, **78**:1612–1616
- Cai, X., Han, Y., Gu, M., Song, M., Wu, X., Li, Z., Li, F., Goulette, T., & Xiao, H. 2019 Dietary cranberry

- suppressed colonic inflammation and alleviated gut microbiota dysbiosis in dextran sodium sulfate-treated mice. *Food and Function*, **10**:6331–6341. <https://doi.org/10.1039/c9fo01537j>
- Calder, P.C. 2015 Marine omega-3 fatty acids and inflammatory processes: Effects, mechanisms and clinical relevance. *BBA - Molecular and Cell Biology of Lipids*, **1851**:469–484. <https://doi.org/10.1016/j.bbalip.2014.08.010>
- Calviello, G., Serini, S., & Piccioni, E. 2007 n-3 Polyunsaturated fatty acids and the prevention of colorectal cancer: molecular mechanisms involved. *Current Medicinal Chemistry*, **14**:3059–3069. <https://doi.org/10.2174/092986707782793934>
- Cario, E., & Podolsky, D.K. 2000 Differential alteration in intestinal epithelial cell expression of Toll-like receptor 3 (TLR3) and TLR4 in inflammatory bowel disease. *Infection and Immunity*, **68**:7010–7017. <https://doi.org/https://doi.org/10.1128/iai.68.12.7010-7017.2000>
- Carvalho, P.B., & Cotter, J. 2017 Mucosal healing in ulcerative colitis: A comprehensive review. *Drugs*, **77**:159–173. <https://doi.org/10.1007/s40265-016-0676-y>
- Cas, M.D., Roda, G., Li, F., & Secundo, F. 2020 Functional lipids in autoimmune inflammatory diseases. *International Journal of Molecular Sciences*, **21**:1–19. <https://doi.org/https://doi.org/10.3390/ijms21093074>
- Castelló, A., Amiano, P., Larrea, N.F. De, Martín, V., Alonso, M., Castano-Vinyals, G., Pere-Gomez, B., Olmedo-Requena, R., Guevara, M., Fernandez-Tardon, G., Fernandez-Villa, T., Jesus, C., Jimenez-Moleon, J., Moreno, V., Davila-Batista, V., Kogevina, M., Aragones, N., & Pollan, M. 2019 Low adherence to the western and high adherence to the mediterranean dietary patterns could prevent colorectal cancer. *European Journal of Nutrition*, **58**:1495–1505. <https://doi.org/10.1007/s00394-018-1674-5>
- Chassing, B., Aitken, J.D., Malleshappa, M., & Vijay-Kumar, M. 2015 Dextran sulfate sodium (DSS)-induced colitis in mice. *Current Protocal in Immunology*, **104**:15.25.1-15.25.14. <https://doi.org/10.1002/0471142735.im1525s104>
- Che, H., Li, Q., Zhang, T., Ding, L., Zhang, L., Shi, H., Yanagita, T., Xue, C., Chang, Y., & Wang, Y. 2018a Comparative study of EPA-enriched ethanolamine plasmalogen and EPA-enriched phosphatidylethanolamine on A β 42 induced cognitive deficiency in a rat model of Alzheimer's disease. *Food and Function*, **9**:3008–3017. <https://doi.org/10.1039/C8FO00643A>
- Che, H., Zhou, M., Zhang, T., Zhang, L., Ding, L., Yanagita, T., Xu, J., Xue, C., & Wang, Y. 2018b EPA enriched ethanolamine plasmalogens significantly improve cognition of Alzheimer's disease mouse model by suppressing β -amyloid generation. *Journal of Functional Foods*, **41**:9–18. <https://doi.org/10.1016/j.jff.2017.12.016>
- Cheng, L., & Lai, M. De 2003 Aberrant crypt foci as microscopic precursors of colorectal cancer. *World Journal of Gastroenterology*, **9**:2642–2649. <https://doi.org/10.3748/wjg.v9.i12.2642>
- Cho, J.Y., Chang, H.J., Lee, S.K., Kim, H.J., Hwang, J.K., & Chun, H.S. 2007 Amelioration of dextran sulfate sodium-induced colitis in mice by oral administration of β -caryophyllene, a sesquiterpene. *Life Sciences*, **80**:932–939. <https://doi.org/10.1016/j.lfs.2006.11.038>
- Cohn, J.S., Kamili, A., Wat, E., Chung, R.W.S., & Tandy, S. 2010 Dietary phospholipids and intestinal cholesterol absorption. *Nutrients*, **2**:116–127. <https://doi.org/10.3390/nu2020116>
- Corpet, D.E., Tache, S., Corpet, D.E., & Taché, S. 2009 Most effective colon cancer chemopreventive agents in rats: A systematic review of aberrant crypt foci and tumor data, ranked by potency. *Nutrition and Cancer*, **43**:1–21. <https://doi.org/10.1207/S15327914NC431>
- Coussens, L.M., & Werb, Z. 2002 Inflammation and cancer. *Nature*, **420**:860–867
- De Silva, P.S.A., Luben, R., Shrestha, S.S., Khaw, K.T., & Hart, A.R. 2014 Dietary arachidonic and oleic acid intake in ulcerative colitis etiology: A prospective cohort study using 7-day food diaries. *European Journal of*

- Gastroenterology and Hepatology*, **26**:11–18. <https://doi.org/10.1097/MEG.0b013e328365c372>
- De Silva, P.S.A., Olsen, A., Christensen, J., Schmidt, E.B., Overvaad, K., Tjønneland, A., & Hart, A.R. 2010 An association between dietary arachidonic acid, measured in adipose tissue, and ulcerative colitis. *Gastroenterology*, **139**:1912–1917. <https://doi.org/10.1053/j.gastro.2010.07.065>
- Ding, L., Zhang, L., Shi, H., Xue, C., Yanagita, T., & Zhang, T. 2020 EPA-enriched ethanolamine plasmalogen alleviates atherosclerosis via mediating bile acids metabolism. *Journal of Functional Foods*, **66**:103824. <https://doi.org/10.1016/j.jff.2020.103824>
- Djuric, Z., Aslam, M.N., Simon, B.R., Sen, A., Jiang, Y., Ren, J., Chan, R., Soni, T., Rajendiran, T.M., Smith, W.L., & Brenner, D.E. 2017 Effects of fish oil supplementation on prostaglandins in normal and tumor colon tissue: modulation by the lipogenic phenotype of colon tumors. *The Journal of Nutritional Biochemistry*, **46**:90–99. <https://doi.org/10.1016/j.jnutbio.2017.04.013>
- Dorninger, F., Brodde, A., Braverman, N.E., Moser, A.B., Just, W.W., Forss-Petter, S., Brügger, B., & Berger, J. 2015 Homeostasis of phospholipids — The level of phosphatidylethanolamine tightly adapts to changes in ethanolamine plasmalogens. *BBA - Molecular and Cell Biology of Lipids*, **1851**:117–128. <https://doi.org/10.1016/j.bbalip.2014.11.005>
- Dragonas, C., Bertsch, T., Sieber, C.C., & Brosche, T. 2009 Plasmalogens as a marker of elevated systemic oxidative stress in Parkinson's disease. *Clinical Chemistry and Laboratory Medicine*, **47**:894–897. <https://doi.org/10.1515/CCLM.2009.205>
- Dueck, D., Chan, M., Tran, K., Wong, J.T., Jay, T., Littman, C., Stimpson, R., & Choy, P.C. 1996 The modulation of choline phosphoglyceride metabolism in human colon cancer. *Molecular and Cellular Biochemistry*, **162**:97–103
- Dwivedi, C., Muller, L.A., Goetz-Parten, D.E., Kasperson, K., & Mistry, V. V. 2003 Chemopreventive effects of dietary mustard oil on colon tumor development. *Cancer Letters*, **196**:29–34. [https://doi.org/10.1016/S0304-3835\(03\)00211-8](https://doi.org/10.1016/S0304-3835(03)00211-8)
- Edelblum, K.L., Yan, F., Yamaoka, T., & Polk, D.B. 2006 Regulation of apoptosis during homeostasis and disease in the intestinal epithelium. *Inflammatory Bowel Diseases*, **12**:413–424. <https://doi.org/10.1097/01.MIB.0000217334.30689.3e>
- Eichele, D.D., & Kharbanda, K.K. 2017 Dextran sodium sulfate colitis murine model : An indispensable tool for advancing our understanding of inflammatory bowel diseases pathogenesis **23**:6016–6029. <https://doi.org/10.3748/wjg.v23.i33.6016>
- Empey, L.R., Jewell, L.D., Garg, M.L., Thomson, A.B.R., Clandinin, M.T., & Fedorak, R.N. 1991 Fish oil-enriched diet is mucosal protective against acetic acid-induced colitis in rats. *Canadian Journal of Physiology and Pharmacology*, **69**:480–487. <https://doi.org/10.1139/y91-072>
- Fan, F., Mundra, P.A., Fang, L., Galvin, A., Moore, X.L., Weir, J.M., Wong, G., White, D.A., Chin-dusting, J., Sparrow, M.P., Meikle, P.J., & Dart, A.M. 2015 Lipidomic profiling in inflammatory bowel disease: comparison between ulcerative colitis and crohn's disease. *Inflammatory Bowel Disease*, **21**:1511–1518. <https://doi.org/10.1097/MIB.0000000000000394>
- Farooqui, A.A. 2010 Studies on plasmalogen-selective phospholipase A2 in brain. *Molecular Neurobiology*, **41**:267–273. <https://doi.org/10.1007/s12035-009-8091-y>
- Femia, A.P., Luceri, C., Toti, S., Giannini, A., Dolara, P., & Caderni, G. 2010 Gene expression profile and genomic alterations in colonic tumours induced by 1,2-dimethylhydrazine (DMH) in rats. *BMC Cancer*, **10**. <https://doi.org/10.1186/1471-2407-10-194>
- Fiala, E.S., & Stathopoulos, C. 1984 Metabolism of methylazoxymethanol acetate in the F344 rat and strain-2 guinea pig and its inhibition by pyrazole and disulfiram. *Journal of Cancer Research Clinical Oncology*,

- Folch, J., Lees, M., & Stanley, G.H. 1957 A simple method for the isolation and purification of total lipids from animal tissues. *J. Biol. Chem.*, **226**:497–509
- Fulda, S., Gorman, A.M., Hori, O., & Samali, A. 2010 Cellular stress responses: cell survival and cell death. *International Journal of Cell Biology*, **2010**:1–23. <https://doi.org/10.1155/2010/214074>
- GBD 2017, I.B.D.C. 2020 The global, regional, and national burden of inflammatory bowel disease in 195 countries and territories, 1990-2017: a systematic analysis for the global burden of disease study 2017. *The Lancet Gastroenterology and Hepatology*, **5**:17–30. [https://doi.org/https://doi.org/10.1016/S2468-1253\(19\)30333-4](https://doi.org/https://doi.org/10.1016/S2468-1253(19)30333-4)
- Gil, Á. 2002 Polyunsaturated fatty acids and inflammatory diseases. *Biomedicine & Pharmacotherapy*, **56**:388–396
- Ginsberg, L., Rafique, S., Xuereb, J.H., Rapoport, S.I., & Gershfeld, N.L. 1995 Disease and anatomic specificity of ethanolamine plasmalogen deficiency in Alzheimer's disease brain. *Brain Research*, **698**:223–226. [https://doi.org/10.1016/0006-8993\(95\)00931-F](https://doi.org/10.1016/0006-8993(95)00931-F)
- Gordon, S., & Martinez, F.O. 2010 Alternative activation of macrophages: Mechanism and functions. *Immunity*, **32**:593–604. <https://doi.org/10.1016/j.immuni.2010.05.007>
- Grisham, M.B., & Granger, D.N. 1988 Neutrophil-mediated mucosal injury - Role of reactive oxygen metabolites. *Digestive Diseases and Sciences*, **33**:6S-15S. <https://doi.org/10.1007/BF01538126>
- Günther, C., Neumann, H., Neurath, M.F., & Becker, C. 2013 Apoptosis, necrosis and necroptosis: Cell death regulation in the intestinal epithelium. *Gut*, **62**:1062–1071. <https://doi.org/10.1136/gutjnl-2011-301364>
- Hahnel, D., Beyer, K., & Engelmann, B. 1999 Inhibition of peroxy radical-mediated lipid oxidation by plasmalogen phospholipid and alpha-tocopherol. *Free Radical Biology & Medicine*, **27**:1087–1094. [https://doi.org/https://doi.org/10.1016/S0891-5849\(99\)00142-2](https://doi.org/https://doi.org/10.1016/S0891-5849(99)00142-2)
- Han, Y., Song, M., Gu, M., Ren, D., Zhu, X., Cao, X., Li, F., Wang, W., Cai, X., Yuan, B., Goulette, T., Zhang, G., & Xiao, H. 2019 Dietary intake of whole strawberry inhibited colonic inflammation in dextran sulfate sodium-treated mice via restoring immune homeostasis and alleviating gut microbiota dysbiosis. *Journal of Agricultural and Food Chemistry*, **67**:9168–9177. <https://doi.org/10.1021/acs.jafc.8b05581>
- Hara, S., Sone, T., & Totani, Y. 2000 Antioxidative activity of nitrogen-containing phospholipids towards emulsified fish oil. *Journal of Japan Oil Chemists' Society*, **49**:937–974
- Harada-Shiba, M., Kinoshita, M., & Shimokado, K. 1998 Oxidized low density lipoprotein induces apoptosis in cultured human umbilical vein endothelial cells by common and unique mechanisms. *Journal of Biological Chemistry*, **273**:9681–9687. <https://doi.org/10.1074/jbc.273.16.9681>
- Hofmanová, J., Straková, N., Vaculová, A.H., Tylichová, Z., Šafa, B., Skender, B., & Kozubík, A. 2014 Interaction of dietary fatty acids with tumour necrosis factor family cytokines during colon inflammation and cancer. *Mediators of Inflammation*, **2014**:1–17. <https://doi.org/http://dx.doi.org/10.1155/2014/848632>
- Honsho, M., Abe, Y., & Fujiki, Y. 2017 Plasmalogen biosynthesis is spatiotemporally regulated by sensing plasmalogens in the inner leaflet of plasma membranes. *Scientific Reports*, **7**:43936. <https://doi.org/10.1038/srep43936>
- Honsho, M., Abe, Y., & Fujiki, Y. 2015 Dysregulation of plasmalogen homeostasis impairs cholesterol biosynthesis. *Journal of Biological Chemistry*, **290**:28822–28833. <https://doi.org/10.1074/jbc.M115.656983>
- Honsho, M., & Fujiki, Y. 2017 Plasmalogen homeostasis – regulation of plasmalogen biosynthesis and its physiological consequence in mammals. *FEBS Letters*, **591**:2720–2729. <https://doi.org/10.1002/1873-3468.12743>
- Hossain, Z., Hosokawa, M., & Takahashi, K. 2009 Growth inhibition and induction of apoptosis of colon cancer cell

- lines by applying marine phospholipid. *Nutrition and Cancer*, **61**:123–130. <https://doi.org/10.1080/01635580802395725>
- Hou, J.K., Abraham, B., & El-Serag, H. 2011 Dietary intake and risk of developing inflammatory bowel disease: A systematic review of the literature. *American Journal of Gastroenterology*, **106**:563–573. <https://doi.org/10.1038/ajg.2011.44>
- Hu, Q., Yuan, B., Wu, X., Du, H., Gu, M., Han, Y., Yang, W., Song, M., & Xiao, H. 2019 Dietary Intake of *Pleurotus eryngii* Ameliorated Dextran-Sodium-Sulfate-Induced Colitis in Mice. *Molecular Nutrition and Food Research*, **63**:1–10. <https://doi.org/10.1002/mnfr.201801265>
- Huang, C., & Freter, C. 2015 Lipid Metabolism , Apoptosis and Cancer Therapy 924–949. <https://doi.org/10.3390/ijms16010924>
- Hung, N.D., Kim, M.R., & Sok, D.E. 2011 Oral administration of 2-docosahexaenoyl lysophosphatidylcholine displayed anti-inflammatory effects on zymosan A-induced peritonitis. *Inflammation*, **34**:147–160. <https://doi.org/10.1007/s10753-010-9218-z>
- IBD in EPIC Study Investigators, Tjonneland, A., Overvad, K., Bergmann, M.M., Nagel, G., Linseisen, J., Hallmans, G., Palmqvist, R., Sjodin, H., Häggglund, G., Berglund, G., Lindgren, S., Grip, O., Palli, D., Day, N.E., Khaw, K.T., Bingham, S., Riboli, E., Kennedy, H., & Hart, A. 2009 Linoleic acid, a dietary n-6 polyunsaturated fatty acid, and the aetiology of ulcerative colitis: A nested case-control study within a European prospective cohort study. *Gut*, **58**:1606–1611. <https://doi.org/10.1136/gut.2008.169078>
- Iborra, M., Moret, I., Rausell, F., Bastida, G., Aguas, M., Cerrillo, E., Nos, P., & Beltran, B. 2011 Role of oxidative stress and antioxidant enzymes in Crohn's disease. *Biochemical Society Transactions*, **39**:1102–1106. <https://doi.org/https://doi.org/10.1042/BST0391102>
- Ifuku, M., Katafuchi, T., Mawatari, S., Noda, M., Miake, K., Sugiyama, M., & Fujino, T. 2012 Anti-inflammatory/anti-amyloidogenic effects of plasmalogens in lipopolysaccharide-induced neuroinflammation in adult mice. *Journal of Neuroinflammation*, **9**:1–13. <https://doi.org/https://doi.org/10.1186/1742-2094-9-197>
- Jena, G., Trivedi, P.P., & Sandala, B. 2012 Oxidative stress in ulcerative colitis: An old concept but a new concern. *Free Radical Research*, **46**:1339–1345. <https://doi.org/10.3109/10715762.2012.717692>
- Jia, W., Xie, G., & Jia, W. 2018 Bile acid-microbiota crosstalk in gastrointestinal inflammation and carcinogenesis. *Nature Reviews Gastroenterology and Hepatology*, **15**:111–128. <https://doi.org/10.1038/nrgastro.2018.23>
- John, S., Luben, R., Shrestha, S.S., Welch, A., Khaw, K.T., & Hart, A.R. 2010 Dietary n-3 polyunsaturated fatty acids and the aetiology of ulcerative colitis: A UK prospective cohort study. *European Journal of Gastroenterology and Hepatology*, **22**:602–606. <https://doi.org/10.1097/MEG.0b013e3283352d05>
- Jutanom, M., Higaki, C., Yamashita, S., Nakagawa, K., Matsumoto, S., & Kinoshita, M. 2020 Effects of sphingolipid fractions from golden oyster mushroom (*Pleurotus citrinopileatus*) on apoptosis induced by inflammatory stress in an intestinal tract in vitro model. *Journal of Oleo Science*, **69**:1087–1093. <https://doi.org/10.5650/jos.ess20105>
- Kaplan, G.G., & Ng, S.C. 2017 Understanding and preventing the global increase of inflammatory bowel disease. *Gastroenterology*, **152**:313–321. <https://doi.org/10.1053/j.gastro.2016.10.020>
- Kim, E., Kim, Yerin, Lee, J., Shin, J.H., Seok, P.R., Kim, Yuri, & Yoo, S.H. 2020 Leucrose, a natural sucrose isomer, suppresses dextran sulfate sodium (DSS)-induced colitis in mice by regulating macrophage polarization via JAK1/STAT6 signaling. *Journal of Functional Foods*, **74**:104156. <https://doi.org/10.1016/j.jff.2020.104156>
- Kim, I.W., Myung, S.J., Do, M.Y., Ryu, Y.M., Kim, M.J., Do, E.J., Park, S., Yoon, S.M., Ye, B.D., Byeon, J.S., Yang, S.K., & Kim, J.H. 2010 Western-style diets induce macrophage infiltration and contribute to colitis-associated carcinogenesis. *Journal of Gastroenterology and Hepatology (Australia)*, **25**:1785–1794.

<https://doi.org/10.1111/j.1440-1746.2010.06332.x>

- Kinoshita, M., & Shimokado, K. 1999 Autocrine FGF-2 is responsible for the cell density – dependent susceptibility to apoptosis of HUVEC; A role of a calpain inhibitor – sensitive mechanism. *Arterioscler Thromb Vasc Biol.*, **19**:2323–2329
- Kraft, S.C., & Kirsner, J.B. 1971 Immunological apparatus of the gut and inflammatory bowel disease. *Gastroenterology*, **60**:922–951. [https://doi.org/10.1016/S0016-5085\(71\)80094-X](https://doi.org/10.1016/S0016-5085(71)80094-X)
- Krawisz, J.E., Sharon, P., & Stenson, W.F. 1984 Quantitative assay for acute intestinal inflammation based on myeloperoxidase activity. Assessment of inflammation in rat and hamster models. *Gastroenterology*, **87**:1344–1350. [https://doi.org/10.1016/0016-5085\(84\)90202-6](https://doi.org/10.1016/0016-5085(84)90202-6)
- Krzystek-korpaczka, M., Diakowska, D., Kapturkiewicz, B., Bebenek, M., & Gamian, A. 2013 Profiles of circulating inflammatory cytokines in colorectal cancer (CRC), high cancer risk conditions, and health are distinct. Possible implications for CRC screening and surveillance. *Cancer letters*, **337**:107–114. <https://doi.org/10.1016/j.canlet.2013.05.033>
- Küllenberg, D., Taylor, L.A., Schneider, M., & Massing, U. 2012 Health effects of dietary phospholipids. *Lipids in Health and Disease*, **11**:1–16
- Labianca, R., Beretta, G.D., Kildani, B., Milesi, L., Merlin, F., Mosconi, S., Pessi, M.A., Prochilo, T., Quadri, A., Gatta, G., de Braud, F., & Wils, J. 2010 Colon cancer. *Critical Reviews in Oncology/Hematology*, **74**:106–133. <https://doi.org/10.1016/j.critrevonc.2010.01.010>
- Lavi, I., Levinson, D., Peri, I., Nimri, L., Hadar, Y., & Schwartz, B. 2010 Orally administered glucans from the edible mushroom *Pleurotus pulmonarius* reduce acute inflammation in dextran sulfate sodium-induced experimental colitis. *British Journal of Nutrition*, **103**:393–402. <https://doi.org/10.1017/S0007114509991760>
- Lee, J.Y., Sim, T., Lee, J., Na, H., & Lee, J. 2017 Chemopreventive and Chemotherapeutic Effects of Fish Oil derived Omega-3 Polyunsaturated Fatty Acids on Colon Carcinogenesis **6**:147–160
- LeBig, J., & Fuchs, B. 2009 Plasmalogens in biological systems: Their role in oxidative processes in biological membranes, their contribution to pathological processes and aging and plasmalogen analysis. *Current Medicinal Chemistry*, **16**:2021–2041
- Liu, H., Kai, L., Du, H., Wang, X., & Wang, Y. 2019 LPS Inhibits fatty acid absorption in enterocytes through TNF- α secreted by macrophages. *Cells*, **8**:1–21. <https://doi.org/10.3390/cells8121626>
- Lohner, K. 1996 Is the high propensity of ethanolamine plasmalogens to form non-lamellar lipid structures manifested in the properties of biomembranes? *Chemistry and Physics of Lipids*, **81**:167–184. [https://doi.org/10.1016/0009-3084\(96\)02580-7](https://doi.org/10.1016/0009-3084(96)02580-7)
- Lopez, D.H., Bestard-Escalas, J., Garate, J., Maimó-barceló, A., Fernández, R., Reigada, R., Khorrani, S., Ginard, D., Okazaki, T., Fernández, J., & Barcelo-Coblijn, G. 2018 Tissue-selective alteration of ethanolamine plasmalogen metabolism in dedifferentiated colon mucosa. *BBA - Molecular and Cell Biology of Lipids*, **1863**:928–938. <https://doi.org/10.1016/j.bbalip.2018.04.017>
- Lu, J., Wang, A., Ansari, S., Hershberg, R.M., & McKay, D.M. 2003 Colonic bacterial superantigens evoke an inflammatory response and exaggerate disease in mice recovering from colitis. *Gastroenterology*, **125**:1785–1795. <https://doi.org/10.1053/j.gastro.2003.09.020>
- Maeba, R., & Ueta, N. 2003 Ethanolamine plasmalogen and cholesterol reduce the total membrane oxidizability measured by the oxygen uptake method. *Biochemical and Biophysical Research Communications*, **302**:265–270. [https://doi.org/10.1016/S0006-291X\(03\)00157-8](https://doi.org/10.1016/S0006-291X(03)00157-8)
- Mawatari, S., Ohara, S., Taniwaki, Y., Tsuboi, Y., Maruyama, T., & Fujino, T. 2020 Improvement of blood plasmalogens and clinical symptoms in Parkinson's disease by oral administration of ether phospholipids: A preliminary report. *Parkinson's Disease*, **2020**:1–7. <https://doi.org/10.1155/2020/2671070>

- McKay, D.M., Philpott, D.J., & Perdue, M.H. 1997 Review article: In vitro models in inflammatory bowel disease research - A critical review. *Alimentary Pharmacology and Therapeutics, Supplement*, **11**:70–80. <https://doi.org/10.1111/j.1365-2036.1997.tb00811.x>
- McLellan, E.A., Medline, A., & Bird, R.P. 1991 Dose response and proliferative characteristics of aberrant crypt foci: putative preneoplastic lesions in rat colon. *Carcinogenesis*, **12**:2093–2098. <https://doi.org/10.1093/carcin/12.11.2093>
- McMullen, C.A., Natarajan, V., & Smyth, S.S. 2020 Lysophospholipids and their receptors: New data and new insights into their function. *Biochimica et Biophysica Acta - Molecular and Cell Biology of Lipids*, **1865**:158697. <https://doi.org/10.1016/j.bbalip.2020.158697>
- Medicherla, K., Sahu, B.D., Kuncha, M., Kumar, J.M., Sudhakar, G., & Sistla, R. 2015 Oral administration of geraniol ameliorates acute experimental murine colitis by inhibiting pro-inflammatory cytokines and NF- κ B signaling. *Food and Function*, **6**:2984–2995. <https://doi.org/10.1039/c5fo00405e>
- Messias, M.C., Mecatti, G.C., Priolli, D.G., & Carvalho, P.O. 2018 Plasmalogen lipids: functional mechanism and their involvement in gastrointestinal cancer. *Lipids in Health and Disease*, **17**:1–12
- Moulahoum, H., Nagy, A., Djerdjouri, B., & Clichici, S. 2018 Precancerous ACF induction affects their regional distribution forsaking oxidative stress implication in 1,2-dimethylhydrazine-induced colon carcinogenesis model. *Inflammopharmacology*, **26**:457–468. <https://doi.org/10.1007/s10787-017-0377-5>
- Nadeem, M.S., Kumar, V., Al-abbasi, F.A., Amjad, M., & Anwar, F. 2019 Risk of colorectal cancer in inflammatory bowel diseases. *Seminars in Cancer Biology*, **40**:51–60. <https://doi.org/10.1016/j.semcancer.2019.05.001>
- Nagengast, F.M., Grubben, M.J.A.L., & Munster, I.P. 1995 Role of bile acids in colorectal carcinogenesis. *European Journal of Cancer*, **31**:1067–1070
- Narayanan, B.A., Narayanan, N.K., Desai, D., Pittman, B., & Reddy, B.S. 2004 Effects of a combination of docosahexaenoic acid and 1,4-phenylene bis(methylene) selenocyanate on cyclooxygenase 2, inducible nitric oxide synthase and β -catenin pathways in colon cancer cells. *Carcinogenesis*, **25**:2443–2449. <https://doi.org/10.1093/carcin/bgh252>
- Nguma, E., Tominaga, Y., Yamashita, S., Otoki, Y., Yamamoto, A., Nakagawa, K., Miyazawa, T., & Kinoshita, M. 2020 Dietary ethanolamine plasmalogen ameliorates colon mucosa inflammatory stress and pre-cancerous ACF in 1,2-DMH-induced colon carcinogenesis mice model: protective role of vinyl ether linkage. *Lipids*, **56**:In press. <https://doi.org/10.1002/lipd.12283>
- Nishimukai, M., Wakisaka, T., & Hara, H. 2003 Ingestion of plasmalogen markedly increased plasmalogen levels of blood plasma in rats. *Lipids*, **38**:1227–1235. <https://doi.org/10.1007/s11745-003-1183-9>
- Nishimukai, M., Yamashita, M., Watanabe, Y., Yamazaki, Y., Nezu, T., Maeba, R., & Hara, H. 2011 Lymphatic absorption of choline plasmalogen is much higher than that of ethanolamine plasmalogen in rats. *European Journal of Nutrition*, **50**:427–436. <https://doi.org/10.1007/s00394-010-0149-0>
- Oh, S.Y., Cho, K.A., Kang, J.L., Kim, K.H., & Woo, S.Y. 2014 Comparison of experimental mouse models of inflammatory bowel disease. *International Journal of Molecular Medicine*, **33**:333–340. <https://doi.org/10.3892/ijmm.2013.1569>
- Ohkawa, H., Ohishi, N., & Yagi, K. 1979 Assay for lipid peroxides in animal tissues thiobarbituric acid reaction. *Analytical Biochemistry*, **95**:351–358
- Orlando, F.A., Tan, D., Baltodano, J.D., Khoury, T., Gibbs, J.F., Hassid, V.J., Ahmed, B.H., & Alrawi, S.J. 2008 Aberrant crypt foci as precursors in colorectal cancer progression. *Journal of Surgical Oncology*, **98**:207–213. <https://doi.org/10.1002/jso.21106>
- Otoki, Y., Kato, S., Kimura, F., Furukawa, K., Yamashita, S., Arai, H., Miyazawa, T., & Nakagawa, K. 2017 Accurate quantitation of choline and ethanolamine plasmalogen molecular species in human plasma by liquid

- chromatography-tandem mass spectrometry. *Journal of Pharmaceutical and Biomedical Analysis*, **134**:77–85. <https://doi.org/10.1016/j.jpba.2016.11.019>
- Ozaki, T., & Nakagawara, A. 2011 Role of p53 in cell death and human cancers. *Cancers*, **3**:994–1013. <https://doi.org/10.3390/cancers3010994>
- Paul, S., Lancaster, G.I., & Meikle, P.J. 2019 Plasmalogens: A potential therapeutic target for neurodegenerative and cardiometabolic disease. *Progress in Lipid Research*, **74**:186–195. <https://doi.org/10.1016/j.plipres.2019.04.003>
- Perše, M., & Cerar, A. 2012 Dextran sodium sulphate colitis mouse model: traps and tricks. *Journal of Biomedicine and Biotechnology*, **2012**:1–13. <https://doi.org/10.1155/2012/718617>
- Perše, M., & Cerar, A. 2011 Morphological and molecular alterations in 1,2 dimethylhydrazine and azoxymethane induced colon carcinogenesis in rats. *Journal of Biomedicine and Biotechnology*, **2011**:1–14. <https://doi.org/10.1155/2011/473964>
- Raza, H., John, A., & Shafarin, J. 2016 Potentiation of LPS-induced apoptotic cell death in human hepatoma HepG2 cells by aspirin via ROS and mitochondrial dysfunction: Protection by N-acetyl cysteine. *PLoS ONE*, **11**:1–19. <https://doi.org/10.1371/journal.pone.0159750>
- Redza-dutordoir, M., & Averill-bates, D.A. 2016 Activation of apoptosis signalling pathways by reactive oxygen species. *BBA-Biochimica et Biophysica Acta*, **1863**:2977–2992. <https://doi.org/10.1016/j.bbamcr.2016.09.012>
- Reiss, D., Beyer, K., & Engelmann, B. 1997 Delayed oxidative degradation of polyunsaturated diacyl phospholipids in the presence of plasmalogen phospholipids in vitro. *Biochemical Journal*, **323**:807–814
- Rhee, S.H. 2014 Lipopolysaccharide: Basic biochemistry, intracellular signaling, and physiological impacts in the gut. *Intestinal Research*, **12**:90–95. <https://doi.org/10.5217/ir.2014.12.2.90>
- Richardson, J., Nelson, L., Curry, A., & Ralston, S. 2018 The increasing global incidences of Ulcerative Colitis; Implications for the economic burden of Ulcerative Colitis. *Value in Health*, **21**:1–268. <https://doi.org/https://doi.org/10.1016/j.jval.2018.04.556>
- Rodr, J., Belarbi, E., S, L.G., & Diego, L. 1998 J Rodriguez-Ruiz - Rapid simultaneous lipid extraction and transesterification for fatty acid analyses (1998).pdf **12**:689–691
- Rouser, G., Fleischer, S., & Yamamoto, A. 1970 Two dimensional thin layer chromatographic separation of polar lipids and determination of phospholipids by phosphorous analysis of spots. *Lipids*, **5**:445–500. <https://doi.org/10.4218/etrij.17.0116.0074>
- Rubio, J.M., Astudillo, A.M., Casas, J., Balboa, M.A., & Balsinde, J. 2018 Regulation of phagocytosis in macrophages by membrane ethanolamine plasmalogens. *Frontiers in Immunology*, **9**:1–14. <https://doi.org/10.3389/fimmu.2018.01723>
- Sakita, J.Y., Gasparotto, B., Garcia, S.B., Uyemura, S.A., & Kannen, V. 2017 A critical discussion on diet, genomic mutations and repair mechanisms in colon carcinogenesis. *Toxicology Letters*, **265**:106–116. <https://doi.org/10.1016/j.toxlet.2016.11.020>
- Sanchez-muñoz, F., Dominguez-lopez, A., Yamamoto-furusko, J.K., Sanchez-muñoz, F., & Dominguez-lopez, A. 2008 Role of cytokines in inflammatory bowel disease. *World Journal of Gastroenterology*, **14**:4280–4288. <https://doi.org/10.3748/wjg.14.4280>
- Sarotra, P., Kansal, S., Sandhir, R., & Agnihotri, N. 2012 Chemopreventive effect of different ratios of fish oil and corn oil on prognostic markers, DNA damage and cell cycle in colon carcinogenesis. *European Journal of Cancer Prevention*, **21**:147–154. <https://doi.org/10.1097/CEJ.0b013e32834c9bfb>
- Scaiola, E., Liverani, E., & Belluzzi, A. 2017 The imbalance between n-6/n-3 polyunsaturated fatty acids and inflammatory bowel disease: A comprehensive review and future therapeutic perspectives. *International*

- Seril, D.N., Liao, J., Yang, G.Y., & Yang, C.S. 2003 Oxidative stress and ulcerative colitis-associated carcinogenesis: studies in humans and animal models. *Carcinogenesis*, **24**:353–362. <https://doi.org/10.1093/carcin/24.3.353>
- Shi, L., Dai, Y., Jia, B., Han, Y., Guo, Y., Xie, T., Liu, J., Tan, X., Ding, P., & Li, J. 2019 The inhibitory effects of Qingchang Wenzhong granule on the interactive network of inflammation, oxidative stress, and apoptosis in rats with dextran sulfate sodium-induced colitis. *Journal of Cellular Biochemistry*, **120**:9979–9991. <https://doi.org/10.1002/jcb.28280>
- Steinberg, S.J., Dodt, G., Raymond, G. V., Braverman, N.E., Moser, A.B., & Moser, H.W. 2006 Peroxisome biogenesis disorders. *Biochimica et Biophysica Acta - Molecular Cell Research*, **1763**:1733–1748. <https://doi.org/10.1016/j.bbamcr.2006.09.010>
- Takahashi, T., Kamiyoshihara, R., Otoki, Y., Ito, J., Kato, S., Suzuki, T., Yamashita, S., Eitsuka, T., Ikeda, I., & Nakagawa, K. 2020 Structural changes of ethanolamine plasmalogen during intestinal absorption. *Food & function*, **11**:8068–8076. <https://doi.org/10.1039/d0fo01666g>
- Taylor, L.A., Pletschen, L., Arends, J., Unger, C., & Massing, U. 2010 Marine phospholipids - a promising new dietary approach to tumor-associated weight loss. *Supportive Care in Cancer*, **18**:159–170. <https://doi.org/10.1007/s00520-009-0640-4>
- Tlalkalova-Hogenova, H., Stepnkova, R., Kozakova, H., Hudcovic, T., Vannucci, L., Tuckova, L., Rossmann, P., Hrnecir, T., Kverka, M., Zakostelska, Z., Klimesova, K., Pribylova, J., Bartova, J., Sanchez, D., Fundova, P., Borovska, D., Srutkova, D., Zidek, Z., Schwarzer, M., Drastich, P., & Funda, D.P. 2011 The role of gut microbiota (commensal bacteria) and the mucosal barrier in the pathogenesis of inflammatory and autoimmune diseases and cancer: contribution of germ-free and gnotobiotic animal models of human diseases. *Cellular and Molecular Immunology*, **8**:110–120. <https://doi.org/10.1038/cmi.2010.67>
- Wall, R., Ross, R.P., Fitzgerald, G.F., & Stanton, C. 2010 Fatty acids from fish: the anti-inflammatory potential of long-chain omega-3 fatty acids. *Nutrition Reviews*, **68**:280–289. <https://doi.org/10.1111/j.1753-4887.2010.00287.x>
- Wallner, S., & Schmitz, G. 2011 Plasmalogens the neglected regulatory and scavenging lipid species. *Chemistry and Physics of Lipids*, **164**:573–589. <https://doi.org/10.1016/j.chemphyslip.2011.06.008>
- Woo, J.K., Choi, S., Kang, J.H., Kim, D.E., Hurh, B.S., Jeon, J.E., Kim, S.Y., & Oh, S.H. 2016 Fermented barley and soybean (BS) mixture enhances intestinal barrier function in dextran sulfate sodium (DSS)-induced colitis mouse model. *BMC Complementary and Alternative Medicine*, **16**:1–9. <https://doi.org/10.1186/s12906-016-1479-0>
- World Health Organization Fat and Oils in human Nutrition 1994 Report of a Joint Expert Consultation, Food and Agriculture Organization of the United Nations and the World Health Organization
- Yamashita, S., Abe, A., Nakagawa, K., Kinoshita, M., & Miyazawa, T. 2014a Separation and detection of plasmalogen in marine invertebrates by high-performance liquid chromatography with evaporative light-scattering detection. *Lipids*, **49**:1261–1273. <https://doi.org/10.1007/s11745-014-3957-9>
- Yamashita, S., Akada, K., Matsumoto, S., & Kinoshita, M. 2020a Effects of dietary ethanol extract from fruiting bodies of goldent oyster mushroom (*Pleurotus citrinopileatus*) on chronic colon inflammation in mice treated with dextran sulfate sodium salt. *Mushroom Science and Biotechnology*, **28**:7–14
- Yamashita, S., Fujisawa, K., Tominaga, Y., Nguma, E., Takahshi, T., Otoki, Y., Yamamoto, A., Higuchi, O., Nakagawa, K., Kinoshita, M., & Miyazawa, T. 2020b Absorption kinetics of ethanolamine plasmalogen and its hydrolysate in mice. *Journal of Oleo Science*, In press
- Yamashita, S., Hashimoto, M., Haque, A., Nakagawa, K., Kinoshita, M., Shido, O., & Miyazawa, T. 2017 Oral

- administration of ethanolamine glycerophospholipid containing a high level of plasmalogen improves memory impairment in amyloid β -infused rats. *Lipids*, **52**:575–585. <https://doi.org/10.1007/s11745-017-4260-3>
- Yamashita, S., Honjo, A., Aruga, M., Nakagawa, K., & Miyazawa, T. 2014b Preparation of marine plasmalogen and selective identification of molecular species by LC-MS/MS. *Journal of Oleo Science*, **63**:423–430. <https://doi.org/10.5650/jos.ess13188>
- Yamashita, S., Kanno, S., Honjo, A., Otoki, Y., Nakagawa, K., Kinoshita, M., & Miyazawa, T. 2016a Analysis of plasmalogen species in foodstuffs. *Lipids*, **15**:199–210. <https://doi.org/10.1007/s11745-015-4112-y>
- Yamashita, S., Kanno, S., Nakagawa, K., Kinoshita, M., & Miyazawa, T. 2015 Extrinsic plasmalogens suppress neuronal apoptosis in mouse neuroblastoma Neuro-2A cells: importance of plasmalogen molecular species. *RSC Advances*, **5**:61012–61020. <https://doi.org/10.1039/C5RA00632E>
- Yamashita, S., Kiko, T., Fujisawa, H., Hashimoto, M., Nakagawa, K., Kinoshita, M., Furukawa, K., Arai, H., & Miyazawa, T. 2016b Alteration in the levels of amyloid- β , phospholipid hydroperoxide, and plasmalogen in the blood of patients with Alzheimer's Disease: Possible interactions between amyloid- β and these lipids. *Journal of Alzheimer's Disease*, **50**:527–537. <https://doi.org/10.3233/JAD-150640>
- Yamashita, S., Sakurai, R., Hishiki, K., Aida, K., & Kinoshita, M. 2017 Effects of dietary plant-origin glucosylceramide on colon cytokine contents in DMH-treated mice. *Journal of Oleo Science*, **66**:157–160
- Yamashita, S., Seino, T., Aida, K., & Kinoshita, M. 2017 Effects of plant sphingolipids on inflammatory stress in differentiated Caco-2 cells. *Journal of Oleo Science*, **66**:1337–1342. <https://doi.org/10.5650/jos.ess17171>
- Yamashita, S., Shimada, K., Sakurai, R., Yasuda, N., Oikawa, N., Kamiyoshihara, R., Otoki, Y., Nakagawa, K., Miyazawa, T., & Kinoshita, M. 2019 Decrease in intramuscular levels of phosphatidylethanolamine bearing Arachidonic Acid during postmortem aging depends on meat cuts and breed. *European Journal of Lipid Science and Technology*, **121**:1800370. <https://doi.org/10.1002/ejlt.201800370>
- Yang, S.Y., Sales, K.M., Fuller, B., Seifalian, A.M., & Winslet, M.C. 2009 Apoptosis and colorectal cancer: implications for therapy. *Trends in Molecular Medicine*, **15**:225–233. <https://doi.org/10.1016/j.molmed.2009.03.003>
- Yang, Y., Tong, Q., Luo, H., Huang, R., & Li, Z. 2016 Chitoooligosaccharides attenuate lipopolysaccharide-induced inflammation and apoptosis of intestinal epithelial cells: Possible involvement of TLR4/NF- κ B pathway. *Indian Journal of Pharmaceutical Education and Research*, **50**:109–115. <https://doi.org/10.5530/ijper.50.1.14>
- Yavin, E., & Gatt, S. 1972 Oxygen-dependent cleavage of the vinyl-ether linkage of plasmalogen. *European Journal of Biochemistry*, **25**:431–436. <https://doi.org/10.1111/j.1432-1033.1972.tb01712.x>
- Yogosawa, S., & Yoshida, K. 2018 Tumor suppressive role for kinases phosphorylating p53 in DNA damage-induced apoptosis. *Cancer Science*, **109**:3376–3382. <https://doi.org/10.1111/cas.13792>
- Yusof, A.S., Isa, Z., & Shah, S.A. 2012 Dietary Patterns and Risk of Colorectal Cancer : A Systematic Review of Cohort Studies (2000-2011). *Asian Pacific Journal of Cancer Prevention*, **13**:4713–4717. <https://doi.org/http://dx.doi.org/10.7314/APJCP.2012.13.9.4713>
- Zhang, T., Xu, J., Wang, Y., & Xue, C. 2019 Health benefits of dietary marine DHA / EPA-enriched glycerophospholipids. *Progress in Lipid Research*, **75**:100997. <https://doi.org/10.1016/j.plipres.2019.100997>
- Zhu, W., Yu, J., Nie, Y., Shi, X., Liu, Y., Li, F., & Zhang, X.L. 2014 Disequilibrium of M1 and M2 macrophages correlates with the development of experimental inflammatory bowel diseases. *Immunological Investigations*, **43**:638–652. <https://doi.org/10.3109/08820139.2014.909456>

8. ABSTRACT (ENGLISH)

Introduction: Ethanolamine glycerophospholipid (EtnGpl) is a major subclass of glycerophospholipid in biological membranes and exists in three forms (alkenyl, alkyl, and acyl). The alkenyl form is referred to as ethanolamine plasmalogen (PlsEtn) and has a unique property of a vinyl ether linkage at the *sn*-1 position of the glycerol moiety. PlsEtn is critical for human health and has established roles such as reservoirs of second messengers, involved in membrane fusion, ion transport, cholesterol efflux, neuronal development, and acts as an endogenous antioxidant. Dysregulation of PlsEtn or low levels have been associated with several diseases such as Zellweger syndrome spectrum disorders, Alzheimer's disease, cardiovascular disease, and certain forms of cancer. In the recent past many researchers are interested in the health benefits of PlsEtn; however, despite of the above-mentioned functional roles, biological functions and the underlying mechanistic bases of dietary PlsEtn in colonic health are not well defined. Currently, the incidence of inflammatory bowel disease (IBD) and colon cancer are on the rise, globally. It is generally recognized that patients with IBD have significant increased risk of developing colon cancer primarily a result of chronic intestinal inflammation. Therefore, the main objective of my PhD study was to elucidate the functional role and metabolism of dietary PlsEtn during intestinal inflammation-related disorders using suitable *in vivo* and *in vitro* experimental models.

In the first study (Chapter 2), I used 1,2-dimethylhydrazine (DMH) carcinogen to induce aberrant crypt foci (ACF) formation in the colon of mice. In this study, I hypothesized that dietary PlsEtn may suppress colon inflammatory stress and subsequent formation of colon precancerous lesions (aberrant crypt foci – ACF) due to the abundance of vinyl ether linkages at the *sn*-1 position. Therefore, I investigated the effect of diets containing 0.1% purified EtnGpl from ascidian muscle with high PlsEtn (87.3 mol%) and from porcine liver with low PlsEtn (7.2 mol%) levels and consisting of relatively same n-3/n-6 ratio by supplementing with 1% fish oil on the formation of ACF using DMH-induced colon carcinogenesis mice model. **Results, discussion and conclusion:** Dietary EtnGpl suppressed DMH-induced aberrant crypt with one foci (AC1) and total ACF formation ($P < 0.05$). ACF suppression by dietary ascidian muscle EtnGpl was higher compared with dietary porcine liver EtnGpl. Additionally, dietary EtnGpl decreased DMH-induced oxidative damage, overproduction of TNF- α , and expression of apoptosis-related proteins in the colon mucosa. The effect of dietary ascidian muscle EtnGpl showed superiority compared with dietary porcine liver EtnGpl. Our results demonstrate the mechanisms by which dietary PlsEtn suppresses ACF formation and apoptosis. Dietary PlsEtn attained this suppression by reducing colon inflammation and oxidative stress hence a reduction in DMH-induced intestinal impairment. These findings provide new insights about the functional role of dietary PlsEtn during colon carcinogenesis.

In the second study (Chapter 3), I used lipopolysaccharide (LPS) to induced cell injury in differentiated Caco-2 cells. I hypothesized that extrinsic PlsEtn may inhibit apoptosis in human intestinal tract cells under LPS-

induced inflammatory stress. Here, I clarified that PlsEtn with abundant vinyl ether linkages has the potential to reduce the degree of LPS-induced apoptotic cells using differentiated Caco-2 cells as an *in vitro* model. **Results, discussion and conclusion:** Lipopolysaccharide (LPS) induced apoptosis of differentiated Caco-2 cells, which was suppressed by EtnGpl in a dose-dependent manner. Cells treated with ascidian muscle EtnGpl containing high levels of PlsEtn demonstrated a lower degree of apoptosis, and downregulated TNF- α and apoptosis-related proteins compared to those treated with porcine liver EtnGpl containing low PlsEtn. This indicates PlsEtn exerted the observed effects, which provided protection against induced inflammatory stress. Overall, our results suggest PlsEtn with abundant vinyl ether linkages is potentially beneficial in preventing the initiation of inflammatory bowel disease (IBD) and colon cancer.

In the third study, (Chapter 4), I used 1.5% dextran sulfate sodium (DSS) to induced colitis in mice colon. I hypothesized that dietary PlsEtn may suppress colon inflammatory mediators and histological damage due to the abundance of vinyl ether linkages at the *sn-1* position. In this study, I investigated the effect of diets containing 0.1% purified EtnGpl from ascidian muscle with high PlsEtn (86.2 mol%) and from porcine liver with low PlsEtn (7.7 mol%) levels and consisting of relatively similar n-3/n-6 ratio by supplementing with 1% fish oil on the impairment of colon lining using dextran sulfate sodium (DSS)-induced colitis in mice. **Results, discussion and conclusion:** Two groups of mice received AIN-93G diet with 1% fish oil (blank and control group) and another two groups received AIN-93G diet with 1% fish oil and either high PlsEtn level (ascidian muscle group) or low PlsEtn level (porcine liver group). After 38 days, DSS treatment shortened the colon length, decreased the body weight, and increased spleen weight compared to the blank group, which were improved by dietary EtnGpl, with ascidian muscle group showing superior effects. After 16 days (early/middle stage of inflammation), DSS treatment elevated MPO activity, TBARS, pro-inflammatory cytokines and proapoptosis-related proteins levels in the colon mucosa compared to the blank, which were lowered by dietary EtnGpl with ascidian muscle group showing higher suppression. Furthermore, ascidian muscle compared to porcine liver group led to higher levels of plasmalogens in the colon mucosa and plasma. Taken together, these results indicate that diets with abundant PlsEtn exert more anti-colitis effects by modulating apoptosis and inflammatory mediators in the colon mucosa.

Taken together, the three studies strongly correlate the metabolism and functional role of dietary PlsEtn with inhibition of chronic colon inflammation, hence the suppression of the associated IBD and colon cancer initiation. Moreover, the abundance of vinyl ether linkage showed enhanced suppression. Therefore, the findings of these studies indicate the potential of utilizing food sources rich in PlsEtn as dietary therapies for colon inflammation-related disorders such as IBD and colon cancer.

9. ABSTRACT (JAPANESE)

導入: エタノールアミングリセリン脂質 (EtnGpl) は、生体膜の主要構成成分であるグリセリン脂質の一種であり、3つの形態で存在する (アルケニル型、アルキル型、アシル型)。アルケニル型はエタノールアミンプラズマローゲン (PlsEtn) と呼ばれ、グリセロール部分の sn-1 位にビニルエーテル結合という特有の構造をもつ。PlsEtn はヒトの健康維持において重要である。セカンドメッセンジャーの貯蔵庫としての役割のほか、細胞膜融合やイオン輸送、コレステロール流出、神経発達、および内因性抗酸化作用に関与している。PlsEtn の調節不全や不足は、ツェルベガー症候群、自閉スペクトラム症候群、アルツハイマー病、循環器疾患やがんなどの様々な病気と関係しており、近年多くの研究者によって PlsEtn の健康に対する効果についての研究が行われるようになった。しかしながら上記で述べたような機能性があるにもかかわらず、大腸における食餌性 PlsEtn の生物学的な機能や根底の機序については未だ解明されていない。近年、炎症性腸疾患 (IBD) や大腸がんの患者数は世界的に増加しており、IBD 患者においては慢性の腸炎が引き金となり大腸がんに至るリスクが非常に高いことがよく知られている。本研究では、*in vivo*、*in vitro* 両観点から腸管炎症に対する食餌性 PlsEtn の機能性とその代謝機構について解明することを目的とした。

1つ目の研究 (第2章) においては、発がん物質である 1,2-ジメチルヒドラジン (DMH) を使用してマウスの大腸に異常腺窩巣 (ACF) を誘発させた。本研究では、食餌性 PlsEtn が大腸炎症ストレスとそれに伴う ACF 形成を抑制し、その効果は、PlsEtn には sn-1 位のビニルエーテル結合が富んでいるためではないかという仮説のもと、DMH によって誘発した大腸炎症モデルマウスを用いて、PlsEtn を高濃度 (87.3 mol%) で含むホヤの身由来の精製 EtnGpl を 0.1% 含有した食餌と、PlsEtn を低濃度 (7.2 mol%) で含むブタ肝臓由来 EtnGpl を含む食餌の効果並びに n-3/n-6 比が類似した 1% の魚油の ACF 形成に対する効果について検討した。

結果と結論: 食餌性 EtnGpl は DMH 誘発の異常クリプト (AC1) 形成、総 ACF 形成ともに抑制した ($P < 0.05$)。その抑制効果は、ブタ肝臓由来の食餌性 EtnGpl よりもホヤの身由来の食餌性 EtnGpl の方が高かった。また、食餌性 EtnGpl は DMH 誘発性の酸化障害、TNF- α の過剰な生産、結腸粘膜におけるアポトーシス関連タンパク質の発現を減少させた。ホヤの身由来 EtnGpl によるその効果は、ブタ肝臓由来のものよりも大きいことが示された。我々の研究結果は、食餌性 PlsEtn による ACF 形成抑制やアポトーシス抑制機構について明らかにした。食餌性 PlsEtn が大腸炎症と酸化ストレスを減少させることによって ACF 形成やアポトーシスが抑制され、それにより DMH 誘発腸障害が減少した。これらは大腸がん誘発における食餌性 PlsEtn の機能性についての新たな発見といえる。

2つ目の研究 (第3章) では、リポポリサッカライド (LPS) を用いて分化型 Caco-2 細胞における細胞障害との関係性を調べた。LPS 誘発性炎症ストレスのもと、ヒト腸管細胞における外因性 PlsEtn

はアポトーシスを抑制するのではないか、という仮説を立てた。ここでは、*in vitro* モデルの分化型 Caco-2 細胞を用いることによって、ビニルエーテル結合に富んだ PlsEtn は LPS 誘発アポトーシスを抑制させる可能性があるということを明確にした。

結果と結論: リポポリサッカライド (LPS) は分化型 Caco-2 細胞においてアポトーシスを誘導し、それは EtnGpl によって量依存的に抑制された。PlsEtn を多く含むホヤ由来の EtnGpl によって処理された細胞では、PlsEtn 含有量の少ないブタ肝臓由来の EtnGpl によって処理されたものと比較してアポトーシスレベルは低くなり、TNF- α 、アポトーシス関連タンパク質は下方制御された。このことは、PlsEtn が LPS 誘発性腸管炎症ストレスから保護したと考えられる。これらの結果より、ビニルエーテル結合に富んだ PlsEtn は、IBD や大腸がんの発生を防ぐ効果があることが示唆された。

3つ目の研究 (第4章) では、1.5% デキストラン硫酸ナトリウム (DSS) を用いマウスの結腸に大腸炎を誘発させた。sn-1 位にビニルエーテル結合が含まれる PlsEtn が、食餌により腸管炎症と組織障害を抑制するのではないか、という仮説を立て、デキストラン硫酸ナトリウム (DSS) を用いることによってマウスに誘発させた大腸炎の腸管内損傷に与える影響について調べた。サンプルとして PlsEtn を多く含む (86.2 mol%) ホヤ由来の精製 EtnGpl を 0.1% 含む食餌、PlsEtn 含有量の低い (7.7 mol%) ブタ肝臓由来の PlsGpl を 0.1 % 含む食餌、n-3/n-6 比を同様にした 1% 魚油を含む食餌を用いた。

結果と結論: 2群 (Blank 群 / Control 群) のマウスには 1% の魚油を含んだ AIN-93G 食が与えられ、他 2 群には 1% の魚油を含んだ AIN-93G と PlsEtn 高含有食 (ホヤ群) 並びに PlsEtn 低含有食 (ブタ肝臓群) が与えられた。38 日後、DSS 処理をした群では、Blank 群と比較して結腸が短くなり、体重が減少し、脾臓重量が増加した。これらの影響は EtnGpl の摂取により改善された。特にホヤ群においては顕著な改善が見られた。16 日後 (炎症初期/中期)、DSS 処理群は Blank 群と比較して、結腸粘膜における MPO 活性、TBARS、炎症性サイトカイン、プロアポトーシス関連タンパク質量が上昇したが、EtnGpl を摂取することによりそれらは低下した。特にホヤ群において顕著な抑制が見られた。さらに、ブタ肝臓群に比べてホヤ群では、結腸粘膜並びに血漿中におけるプラズマローゲンレベルが高くなった。これらの結果より、PlsEtn に富んだ食餌は、結腸粘液中のアポトーシス並びに炎症性メディエーターを調節することにより、大腸炎症抑制効果を示すことが示唆された。

これら 3 つの研究結果をまとめると、食餌性 PlsEtn は慢性の腸管炎症とそれに伴う IBD や大腸がんの誘発抑制と強く関係しているといえる。さらに、ビニルエーテル結合に富んだ EtnGpl においては高い抑制効果が見られた。本研究から得られた知見は、PlsEtn に富んだ食物摂取が、結腸炎症から生じる IBD や大腸がんに対する食事療法への活用の可能性を示した。